

A Framework for  
Screening Experiments and Modelling in Complex Systems

by

Abraham N. Aldaco Gastélum

A Dissertation Presented in Partial Fulfillment  
of the Requirement for the Degree  
Doctor of Philosophy

Approved April 2015 by the  
Graduate Supervisory Committee:

Dr. Violet R. Syrotiuk, Chair  
Dr. Charles J. Colbourn  
Dr. Arunabha Sen  
Dr. Douglas C. Montgomery

ARIZONA STATE UNIVERSITY

May 2015

## ABSTRACT

Complex systems are pervasive in science and engineering. Some examples include complex engineered networks such as the internet, the power grid, and transportation networks. The complexity of such systems arises not just from their size, but also from their structure, operation (including control and management), evolution over time, and that people are involved in their design and operation. Our understanding of such systems is limited because their behaviour cannot be characterized using traditional techniques of modelling and analysis.

As a step in model development, statistically designed screening experiments may be used to identify the main effects and interactions most significant on a response of a system. However, traditional approaches for screening are ineffective for complex systems because of the size of the experimental design. Consequently, the factors considered are often restricted, but this automatically restricts the interactions that may be identified as well. Alternatively, the designs are restricted to only identify main effects, but this then fails to consider any possible interactions of the factors.

To address this problem, a specific combinatorial design termed a *locating array* is proposed as a screening design for complex systems. Locating arrays exhibit logarithmic growth in the number of factors because their focus is on identification rather than on measurement. This makes practical the consideration of an order of magnitude more factors in experimentation than traditional screening designs.

As a proof-of-concept, a locating array is applied to screen for main effects and low-order interactions on the response of average *transport control protocol* (TCP) throughput in a simulation model of a *mobile ad hoc network* (MANET). A MANET is a collection of mobile wireless nodes that self-organize without the aid of any centralized control or fixed infrastructure. The full-factorial design for the MANET considered is infeasible (with over  $10^{43}$  design points) yet a locating array has only 421 design points.

In conjunction with the locating array, a “heavy hitters” algorithm is developed to identify the influential main effects and two-way interactions, correcting for the non-normal distribution of the average throughput, and uneven coverage of terms in the locating array. The significance of the identified main effects and interactions is validated independently using the statistical software JMP.

The statistical characteristics used to evaluate traditional screening designs are also applied to locating arrays. These include the matrix of covariance, fraction of design space, and aliasing, among others. The results lend additional support to the use of locating arrays as screening designs.

The use of locating arrays as screening designs for complex engineered systems is promising as they yield useful models. This facilitates quantitative evaluation of architectures and protocols and contributes to our understanding of complex engineered networks.

*To Araceli, my wife, constant companion, confidant and supporter  
and to my daughters Carolina, Paulina and Sofia Guadalupe,  
my beloved family.*

## ACKNOWLEDGEMENTS

This thesis would not have been possible without the support and guidance of my research advisor, Dr. Violet R. Syrotiuk. I am very grateful to Dr. Syrotiuk for helping me research in the areas of wireless networks, statistics, simulation and modelling. I learned from Dr. Syrotiuk not only scientific topics and research methods but also the attitude towards professional career and life.

I also want to thank my dissertation committee members, Dr. Charles Colbourn, Dr. Arunabha Sen and Dr. Douglas Montgomery for their support and advice. Special thanks to Dr. Colbourn for allowing me the honor of introduce a case study using locating arrays in networking; for his patience, wisdom and advice.

I want to thank for those who provided me financial support to accomplish my Ph.D. studies. Thanks to the Mexican Council of Science and Technology (CONACYT), the Tecnologico de Monterrey, the ASU TA work and fellowships, the Credito Educativo del Estado de Sonora and to my brothers, parents and extended family who always were aware of what I needed throughout my doctoral studies.

Thanks to Dr. Shelley Gray and Dr. Laila Restrepo who head a wonderful team in the Speech and Hearing Department of ASU, for trusting in me and giving me the opportunity to work in the LARRC lab in multiple projects and activities during my stay at ASU.

I want to express my gratitude to my friends in ASU who supported me and who made my life more pleasant. Special thanks to my lab members: Yuhan, Kahkashan, Chengmin Wang, Sai, Jeremy, Namrata, and my friends also Ph.D. students: Adrian, Billibaldo, Carlos, Gustavo, Javier, Helen, Salvador and Antonio.

Thanks to my beloved parents, Salvador and Eduviges, who taught me the importance of education, the values of love and work. Thanks to my parents in law, to my brothers and brothers in law because they always watched that nothing was missing to my family.

I thank God for allowing me to have such an experience that transformed my life for good.

And absolutely THANKS to my wife Araceli and my daughters Carolina, Paulina and Sofia Guadalupe for being a source of steadfast and unconditional love during these many years of study.

## TABLE OF CONTENTS

	Page
LIST OF TABLES .....	x
LIST OF FIGURES .....	xii
<b>CHAPTER</b>	
<b>1 INTRODUCTION</b> .....	<b>1</b>
1.1 Overview .....	7
<b>2 LITERATURE REVIEW</b> .....	<b>9</b>
2.1 Support for Voice over Wireless Networks .....	9
2.1.1 VoIP over Ad Hoc Networks and Wireless LANs .....	9
2.1.2 VoIP over Wireless Mesh Networks .....	11
2.2 Locating Arrays: A New Experimental Design for Screening Complex Engineered Systems .....	17
2.2.1 Locating Arrays as Screening Designs .....	20
2.3 Statistical Characteristics of Screening Designs .....	20
2.3.1 Correlation .....	21
2.3.2 Dummy coding .....	22
2.3.3 Variance Inflation Factor .....	23
2.3.4 Covariance .....	23
2.3.5 Fraction of Design Space .....	23
2.3.6 Aliasing .....	24
<b>3 CROSS-LAYER OPPORTUNISTIC ADAPTATION FOR VOICE OVER AD HOC NETWORKS</b> .....	<b>26</b>
3.1 Introduction .....	26
3.2 Factors Influencing Voice .....	28
3.3 Adaptation Architecture and Protocol .....	30

CHAPTER	Page
3.3.1 Packetization Delay, Packet Size, and Compression Level Calculations .....	33
3.4 Simulation Set-Up .....	35
3.4.1 Static Topologies .....	35
3.4.2 Mobile Scenarios .....	37
3.4.3 Wireless Channel Model .....	39
3.4.4 Simulation Parameters .....	39
3.4.5 Quantitative Degradation in Voice Quality (DVQ) Metric .....	41
3.4.6 Qualitative Mean Opinion Score (MOS) Metric .....	41
3.4.7 Non-Adaptive Protocols used for Comparison .....	42
3.5 Simulation Results .....	43
3.5.1 Results for Line and Line-Variant Topologies .....	43
3.5.2 Results for Grid and Irregular-Grid Topologies .....	47
3.5.3 Results for Mobile Scenarios .....	49
3.6 Performance Bounds .....	51
3.7 Conclusions .....	53
4 LOCATING ARRAYS: A NEW EXPERIMENTAL DESIGN FOR SCREENING COMPLEX ENGINEERED SYSTEMS .....	56
4.1 Introduction .....	56
4.2 Locating Arrays .....	59
4.2.1 A Small Example .....	62
4.3 Screening an Engineered System .....	64
4.3.1 Designing the Experiment .....	65
4.3.2 Screening Algorithm .....	66



CHAPTER	Page
4.3.3	Example of the Screening Algorithm ..... 68
4.3.4	Applying the Screening Algorithm ..... 69
4.4	Validation and Verification ..... 74
4.4.1	Full-Factorial Screening in JMP ..... 75
4.4.2	JMP Model vs. Analytical Models ..... 77
4.4.3	Predictive Accuracy of JMP Model ..... 79
4.4.4	Predictive Accuracy of Screening Model ..... 80
4.5	Conclusions ..... 80
5	STATISTICAL CHARACTERISTICS OF LOCATING ARRAYS ..... 83
5.1	Introduction ..... 83
5.2	Correlation ..... 83
5.3	Variance inflation factor (VIF) of the Locating Array ..... 86
5.4	Covariance ..... 86
5.5	Fraction of Design Space ..... 88
5.6	Statistical Properties based on Response ..... 89
5.6.1	Correlation between Main Effects and the Response ..... 89
5.6.2	Variability on the Response ..... 89
5.7	Aliasing ..... 91
5.8	Conclusions ..... 97
6	CONCLUSIONS AND FUTURE WORK ..... 98
	REFERENCES ..... 101
	APPENDIX ..... 113
A	LOCATING ARRAYS FOR SCREENING ENGINEERED SYSTEMS ..... 113
A.1	Factors and Levels used in the MANET Case Study ..... 114

CHAPTER	Page
A.2 Description of Factors and Levels used in the MANET Case Study . . . . .	118
A.3 The Locating Array . . . . .	121
A.4 Grouping of Factors . . . . .	135
A.5 The Screening Algorithm . . . . .	137
A.6 Predictive Model produced in JMP . . . . .	140
A.7 The $2^9$ full-factorial design utilized for JMP . . . . .	142

## LIST OF TABLES

Table	Page
2.1	Typical resolutions by type of aliasing. . . . . 18
2.2	Dummy coding of a categorical factor with 4 levels. . . . . 22
3.1	Characteristics of group applications and mobility model parameters. . . . . 38
3.2	Simulation and adaptive protocol parameters. . . . . 40
3.3	MOS listening-quality scale. . . . . 42
3.4	Standard audio/voice codec attributes. . . . . 43
3.5	Number of calls supported per flow with at least fair MOS (i.e., $MOS \geq 3$ ) by line and line-variant topologies for a 150 <i>ms</i> delay budget and no ROHC. Linear topologies establish one flow, while line-variant topologies establish two flows. The calls are multiplexed over the flows. . . . . 47
3.6	Number of calls supported per flow for grid topologies with at least fair MOS (i.e., $MOS \geq 3.0$ ) for a 150 <i>ms</i> delay budget and no ROHC. In the grid topology, the low interference (LI) and high interference (HI) traffic patterns each have two flows. In the irregular-grid topology, the LI traffic pattern has two flows while the HI traffic pattern has four flows. . . . . 50
3.7	Number of calls supported per flow for mobile scenarios with at least fair MOS (i.e., $MOS \geq 3.0$ ) for a 150 <i>ms</i> delay budget and no ROHC. The <i>event</i> , <i>march</i> , and <i>pursuit</i> applications use the <i>nomadic</i> , <i>column</i> , and <i>pursuit</i> mobility models, respectively. Two, four, and eight concurrent flows are considered in the event and march applications, while up to three concurrent flows are considered for the pursuit application. . . . . 51
3.8	Default parameter values per frame sent by IEEE 802.11b DCF. . . . . 53
4.1	Experimental design and response for each run. . . . . 63

Table	Page	
4.2	Locating faults due to main effects. ....	63
4.3	$\rho(T)$ for one-way interactions $T = \{(c, \nu)\}$ . ....	63
4.4	Locating faults due to two-way interactions. ....	64
4.5	Experimental design and average TCP throughput. ....	68
4.6	Screening model with twelve terms. ....	73
4.7	Summary statistics of the screening model in Table 4.6. ....	74
4.8	Unique factors from the screening model in Table 4.6. ....	75
4.9	Partial results of a $2^9$ full-factorial screening experiment using JMP 11.0 on the nine factors in Table 4.8. ....	76
5.1	Scale for the color map of the average percentage of alias relationships. ....	92
5.2	Average aliasing relationship (as a percentage) of two-factor interactions to main effects considering the number of levels in the factors involved. ....	94
5.3	Average aliasing relationships of two two-factor interactions considering the number of levels of the factors involved. ....	96
A.1	Factors and levels in the MANET ....	114
A.2	Description of the factors ....	118
A.3	The $(\bar{1}, \bar{2})$ -locating array used in experimentation. ....	121
A.4	Range [low, high] of coverage for groups of main effects. ....	135
A.5	Groups added to account for two-way interactions. ....	136
A.6	Unique factors from the screening model in Table 4.6. ....	140
A.7	Partial model of the $2^9$ full-factorial screening experiment using JMP 11.0 on the nine factors in Table A.6. ....	140
A.8	$2^9$ full-factorial design and TCP throughput ....	142

## LIST OF FIGURES

Figure	Page
1.1 Interaction graph, throughput response curve behaviour, histogram of observed TCP throughput. ....	5
3.1 System architecture: hop-by-hop and end-to-end adaptation. ....	31
3.2 The end-to-end protocol dynamics. ....	32
3.3 Variant of the line topology.....	36
3.4 Grid topology. ....	37
3.5 DVQ and MOS as a function of number of calls per flow for line topologies using the adaptive protocol (150 <i>ms</i> delay budget, no ROHC).....	44
3.6 DVQ and MOS as a function of number of calls per flow in line topologies using the adaptive protocol (300 <i>ms</i> delay budget, ROHC). ....	45
3.7 DVQ and MOS as a function of number of calls per flow in line topologies for the non-adaptive protocol using standard voice codecs (150 <i>ms</i> delay budget, no ROHC). ....	45
3.8 DVQ and MOS as a function of number of calls per flow in line-variant topologies using the adaptive protocol (150 <i>ms</i> delay budget, no ROHC). ..	46
3.9 Changes in compression over the call lifetime. ....	48
3.10 DVQ and MOS as a function of number of calls per flow in grid topologies using the adaptive protocol (150 <i>ms</i> delay budget, no ROHC).....	49
3.11 DVQ and MOS as a function of number of calls per flow in irregular-grid topologies using the adaptive protocol (150 <i>ms</i> delay budget, no ROHC). ..	50
3.12 Bounds on the number of calls supported as a function of compression rate.	54
4.1 Interaction of routing and MAC protocols on delay [132]. ....	58

Figure	Page
4.2 Distribution of the original observed average throughput, and corresponding normal probability plot. ....	70
4.3 Natural logarithm transformation of the original observed throughput, and corresponding normal probability plot. ....	70
4.4 Distribution of residuals after the first iteration of the screening algorithm, and corresponding normal probability plot. ....	72
4.5 TCP throughput as a function of packet size as predicted the by JMP model; all other factors are at their default levels. ....	77
4.6 JMP model vs. model proposed by [81]. ....	79
4.7 JMP model vs. model proposed by [100]. ....	79
4.8 Predictions by the JMP model and simulation results for random design points. ....	81
5.1 Correlation matrix of main effects and second order of main effects for the locating array used in Chapter 4 (see AppendixA.3). ....	85
5.2 Variance inflation factors (VIFs) of the locating array used in Chapter 4 (see Appendix A.3). ....	86
5.3 Covariance matrix for the main effects in the locating array used in Chapter 4 (see Appendix A.3). ....	87
5.4 Fraction of design space for the locating array used in Chapter 4 (see Appendix A.3). ....	88
5.5 Correlation between each of the main effects with the mean TCP throughput.	90
5.6 Variance in the TCP throughput caused per factor. ....	91
A.1 Coverage of main effects and groups constructed. ....	135
A.2 Set size of 2-way factor interactions and groups constructed. ....	136

## Chapter 1

### INTRODUCTION

Complex systems are pervasive in science and engineering. Some examples include complex engineered networks such as the internet, the power grid, and transportation networks. To quote from a recent report on complex engineered networks [92]:

The science of experiment design is widely used in science and engineering disciplines, but is often ignored in the study of complex engineered networks. This in turn has led to a shortage of simulations that we can believe in, of experiments driven by empirical data, and of results that are statistically illuminating and reproducible in this field.

Other works support this statement for both simulated and physical computer network systems [10, 12, 66, 70, 101]. Our objective in this dissertation is to contribute to the science of experimental design in the study of complex engineered networks.

The complex engineered network under consideration in this work is a *mobile ad hoc network* (MANET). A MANET is a collection of mobile wireless nodes that self-organize without centralized control or fixed infrastructure. MANETs add several interesting dimensions to the existing challenges of modelling complex engineered networks. Since MANETs possess no centralized control for data forwarding, there is no central infrastructure to model. Moreover, MANETs are wireless networks, introducing challenges in communication directly related to the characteristics of radio transceivers. Finally, MANETs are mobile networks — nodes in the network move, sometimes at high speed, causing conditions to change rapidly. These characteristics make MANETs challenging to model.

Some methods for modelling include polynomial regression models (a type of linear regression) [84], splines (which partition the region of interest into subregions and fit simple regression models to each) [121], and neural networks (a type of non-linear regression) [135]. In some form, each effectively applies *screening* to identify the most important among a set of factors in an experiment and to develop a model.

The first major contribution of this dissertation is to show that traditional designed experiments can be applied successfully to MANETs when domain experts help design the screening experiment. The support of voice communication is fundamental in the deployment of a MANET for the battlefield or emergency response. We use the QoS requirements of voice to screen for factors influencing its communication, and validate their significance through statistical analysis. Based on the results, we propose an opportunistic protocol within a cross-layer framework that adapts these factors at different time scales. Hop-by-hop adaptation exploits the PHY/MAC interaction to improve the use of the spectral resources through opportunistic rate-control and packet bursts, while end-to-end adaptation exploits the LLC/Application interaction to control the demand per call through voice coding and packet size selection. Our objective is to maximize the number of calls admitted while minimizing loss of quality. We evaluate the performance of the protocol in simulation with real audio traces using both quantitative and *mean opinion score* (MOS) audio quality metrics, comparing to several standard voice codecs. The results indicate that: (i) compression and packet-size selection play a critical role in supporting QoS over ad hoc networks; (ii) header compression is needed to limit the overhead per packet especially over longer paths; (iii) good voice quality is achieved even in strenuous network conditions.

However, there are various assumptions and limitations underlying many methods for screening and modelling. These include that:

1. the factors have only two levels;



2. the factors are not categorical;
3. the set of factors considered for experimentation is “not too large;”
4. the direction of response is known for specific factors; and
5. the data are normally distributed.

We consider each one in turn.

In most screening experiments, each factor takes on only two *levels* (or values): a minimum and maximum, or “low” and “high” value, often coded as  $-1$  and  $+1$  in *design of experiments* (DOE). The most common reason for this assumption is that it reduces the number of *design points* (scenarios or configurations for experimentation) in the experiment. For example, if there are  $k$  factors each with two levels, a full-factorial design [84] has  $2^k$  design points. If one factor instead has three levels then there are more points, namely  $2^{k-1}3^1$ , in the design. Restricting a factor to two levels also implies its effect is assumed to be linear. Clearly, the factors that are perceived as important depends on the region of interest explored in experimentation, *i.e.*, the range of the levels. In some cases the range and number of levels is clear, *e.g.*, the IEEE 802.11b protocol has a data rate per stream of 1, 2, 5.5, and 11 Mbps, whereas in other cases it is not, *e.g.*, the number of streams. Using only two levels for each factor is overly restrictive.

Factors are typically classified in two groups: *numerical* and *categorical*. Categorical factors are those whose values cannot be computed using arithmetic operations, even if the value is a number. They are utilized to separate information into categories and cannot be arranged in order of magnitude. One way to cope with a categorical factor in DOE is to introduce as many additional binary factors as it has levels to code the factor [84]. This increases the number of design points in the experiment. In engineered networks, categorical factors arise frequently since a factor may correspond to a protocol at a layer in the stack,

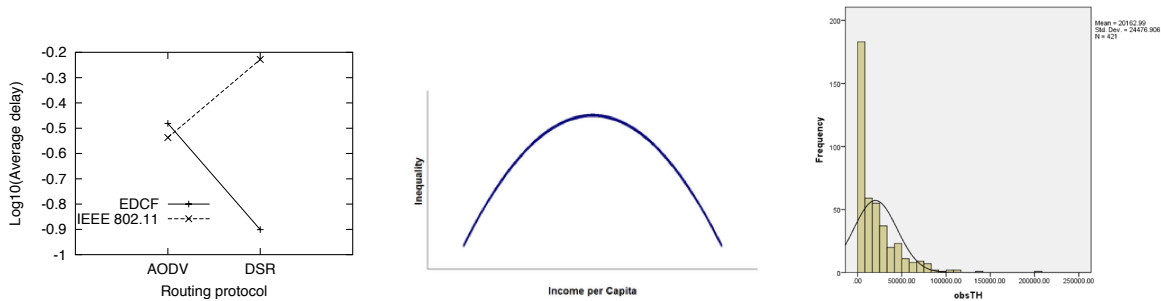
e.g., IEEE 802.11 or EDCF for *medium access control* (MAC), DSR or AODV for routing, and UDP or TCP for transport. Methods for direct and efficient consideration of categorical factors are needed.

It has been considered impractical to experiment with “many” factors; about 10 factors seems a suggested maximum [64, 84]. This is because the number of experiments in many experimental designs grows exponentially with the number of factors. Some grow linearly with the number of factors, e.g., supersaturated designs [37, 73, 84], but restrict the factors to two levels. Some designs aggregate the factors into groups, e.g., sequential bifurcation [65], to reduce the size of the design even more. But grouping requires care to ensure that factor effects do not cancel. This presents a “chicken and egg” problem: we need to know how to group in order to group. Often, DOE assumes a “domain expert” with the expertise to make decisions on factor restriction or grouping. Indeed we used this approach in our first contribution showing that traditional designed experiments can be applied to MANETs.

However, it is unlikely that a domain expert knows the importance of a particular factor or interaction in the system as a whole. For example, Figure 1.1a shows an *interaction graph*, i.e., how a change in the level of one factor affects the other factor with respect to the response, for the factors of routing and MAC protocol on average delay [132]. The MAC protocol has little impact on the average delay in AODV, while for DSR the impact is very large. If MAC protocols had been aggregated in this experiment then this important interaction would have been lost.

What makes an engineered network complex is not just its size, but also its structure (topology), its operation (protocols including control and management), its evolution over time, and that humans are involved in its design and operation [92]. It is unreasonable to expect that there is a single domain expert who knows and understands any complex engineered network. Even a group of experts is unlikely to anticipate all interactions among system components. Therefore, we argue that it is imperative not to eliminate factors from

experimentation a priori. Instead, an automatic and objective approach to screening is required.



(a) Interaction graph for routing and MAC protocol on average delay [132]. (b) Example inverted “U” curve. (c) Throughput distribution.

**Figure 1.1:** Interaction graph, throughput response curve behaviour, histogram of observed TCP throughput.

Kleijnen [64] states that, in his experience, users know the direction of the first-order effects of individual factors. At first glance, this seems an obvious statement. However, consider throughput in a wireless network as a function of the number of data streams. We expect throughput to increase with the number of streams, but not indefinitely. Indeed, by increasing the number of streams it may be possible to overload the network and see throughput decrease. Perhaps the throughput response curve is shaped similar to that in Figure 1.1b; such inverted “U” curve behaviour occurs in other fields, such as in economics [2], education [48], and psychology [112]. It is better not to assume the direction of the first-order effects of individual factors.

Many statistical techniques assume that data are normally distributed and have constant variance. Examples include the  $t$ -test used for hypothesis testing, and *ordinary least squares* (OLS) [84] used for estimating the unknown coefficients in a linear regression model. However Figure 1.1c, a histogram of observed throughput from simulation results, that we will see from our later experimentation, show that the data are not always normally distributed: we observe outliers, skew, and low kurtosis.

As we can see, many assumptions made in DOE are not well suited to planning and assessing experiments in complex engineered networks. To address these problems the definition of a *locating array* (LA) is formulated [18]. Locating arrays exhibit logarithmic growth in the number of factors because their focus is on identification rather than on measurement. This makes practical the consideration of an order of magnitude more factors in experimentation, removing the need for the elimination of factors by domain experts. As a result, LAs have the potential to transform experimentation in huge factor spaces such as those found in complex engineered networks. LAs allow factors to take on as many levels as is necessary, without the need to know the direction of response. Indeed, LAs treat all factors as categorical; the result of screening therefore is not just which factors are important, but the level at which each is important.

The second major contribution of this dissertation is to tackle head-on the goal of providing an automatic and objective approach to screening. We do so by applying an LA for screening the response of average TCP throughput in a simulation model of a MANET. The full-factorial design for this system is infeasible (over  $10^{43}$  design points!) yet an LA has only 421 design points. We validate the significance of the identified factors and interactions independently using the statistical software JMP. A “heavy hitters” approach, similar to that used in compressive sensing [19], is applied in developing a model using the LA; additional non-parametric techniques help mitigate the assumption of normality. Screening using locating arrays appears to be viable in complex engineered networks and to yield useful models.

The third and final major contribution of this dissertation is to take statistical characteristics commonly used to evaluate traditional screening designs and apply them to the evaluation of locating arrays. The low values in correlation, multicollinearity, and variance-covariance are good indicators that the locating array is an appropriate design to estimate the linear regression coefficients.

The fraction of design space plot shows uniform and small scaled prediction variance associated with the locating array. The locating array maximizes the experimental variance measured in the response caused by the factors; this is highly desired in a screening design.

The alias relationship of two-factor interactions to main effects is around 50% when the factors in the interaction and the main effects have 2 levels each. The aliasing decreases when the number of levels for the factors in the interaction and/or the main effects increases. On the other hand, the aliasing of two two-factors interaction is around 48% when the factors in both interactions have 2 levels each and increases up to around 69% when the factors in both interactions have 10 levels. All of these statistical results lend additional support to the use of locating arrays as screening designs.

In summary the three major contributions of this dissertation include:

1. Demonstrating the effectiveness of traditional DOE when a domain expert is used to help design the screening effort.
2. Tackling head-on the goal of providing an automatic and objective approach to screening through the use of a locating array.
3. Analyzing the statistical characteristics of the locating array comparing to more traditional screening designs.

## 1.1 Overview

The rest of this dissertation is organized as follows. Chapter 2 presents related work for subsequent chapters. It includes previous work on support of voice in MANETs, a summary of screening designs, and definitions of statistical measures commonly used for evaluating screening designs. Chapter 3 presents an opportunistic protocol within a cross-layer framework that adapts factors identified using a traditional screening approach at different time scales. The performance of the protocol is evaluated in simulation with real audio traces

using both quantitative and qualitative metrics, comparing to several standard voice codecs. Chapter 4 introduces locating arrays as new experimental designs for screening. The results demonstrate that locating arrays appear viable for screening complex engineered networks yielding models that are useful. Chapter 5 evaluates the statistical characteristics of locating arrays to support their use as a screening design. An analysis of correlation, multicollinearity, variance, and alias relationships of a locating array are provided. The statistics support that locating arrays are appropriate as screening designs. Finally Chapter 6 presents a summary of the conclusions as well as future research directions.

## Chapter 2

### LITERATURE REVIEW

#### 2.1 Support for Voice over Wireless Networks

##### 2.1.1 *VoIP over Ad Hoc Networks and Wireless LANs*

Specialized protocols that focus on voice support over ad hoc networks have been proposed. Wang et al. [134] proposes the combined use of multicasting and multiplexing of multiple voice packets into one packet as a way of reducing the per-packet overhead. As a result, the protocol shows an increase in the network capacity and a decrease in the delay experienced by voice calls. Priority queueing is employed as a way of preventing competing TCP traffic from starving voice traffic of resources. The analysis for ordinary VoIP capacity for ETSI Global System for Mobile (GSM) communications 06.10 Full Rate (FR) speech coder [27], ITU G.711, G.729, and G.723 voice codecs using IEEE 802.11b DCF access scheme at 11 *Mbps* shows voice capacities similar to our experimental and analytical results for the non-adaptive protocol presented in Chapter 3. The small difference between our results may be due to the use of a packet-loss rate below 1% compared to our 10%. The voice capacity of the multicast scheme, which improves the ordinary VoIP capacity by close to 100%, is less than that achieved by our adaptive protocol.

A modification of IEEE 802.11 is proposed in [22] in which the cyclic redundancy codes are computed only over those parts of the voice frame that have a high impact on the perceived quality rather than over the entire frame. In this way, less bandwidth is wasted in retransmission and less delay is introduced. In [23], the use of new speech coding techniques for supporting voice over ad hoc networks is proposed. One such technique is multiple description coding. It involves creating more than one bit stream from the source signal.

Each independent stream represents a coarse description of the transmitted signal. If more than one description is received, a refined signal is reconstructed. Another technique is scalable speech coding, which consists of sending a base stream at a minimum rate and one or more enhancement streams. Our work computes the frame check sequence (FCS) over the entire frame and does not make use of these speech coding techniques.

Obeidat et al. [95] studies the performance of adaptive voice communications over multi-hop wireless networks; the work in Chapter 3 extends that work significantly. In particular, a statistically designed experiment is used to quantify significant factors and their interactions on voice quality. This motivated the integration of end-to-end adaptation. In addition, the use of real audio traces allows the evaluation of audio quality metrics. We also consider more complex topologies and scenarios integrating mobility in studying the protocol to better understand how it performs in situations more representative of battlefield and emergency scenarios.

Fasolo et al. [28] presents a cloud of nodes that communicate with one gateway by means of multi-hop ad hoc connections to study the effect of multi-rate on voice capacity. They assessed their analysis through ns-2 simulations using IEEE 802.11b DCF access scheme at 11 *Mbps* and ETSI GSM 06.60 Enhanced Full Rate (EFR) voice codec [26]. Their results for a delay budget of 100 *ms* and less than 1% loss probability show a maximum of 6 and 3 concurrent voice connections for single-hop and multi-hop scenarios, respectively. As we will see, our adaptive protocol achieves higher voice capacity perhaps due to differences in the delay budget and loss probability. Moreover, our evaluation considers more extensive multi-hop and mobile scenarios.

A number of works consider voice capacity of WLANs. Adaptive modulation and adaptive compression have been applied separately in VoIP-based wireless and wired networks [4, 5, 116, 131]. Supporting packet voice over IEEE 802.11 has been investigated for both the DCF and PCF, however the performance is poor [133, 142].



Garg et al. [33] analyzes the number of simultaneous VoIP calls a single AP running the IEEE 802.11b DCF can support. Their experimentation uses an ITU G.711 a-Law codec with 10 *ms* of voice data. At 11 *Mbps*, 6 *calls* are supported by the AP with acceptable quality. An analytical model is developed for three standard codecs (ITU G.711 a-Law [51], G.723 [52], and G.729 [54]) considering DCF compliance and data transmission rates of the AP varying from 1 *Mbps* to 11 *Mbps* to validate the experimental results. Our model in §3.6 is similar and reports essentially the same number of VoIP calls supported for these standard codecs.

Hole et al. [45] quantifies the capacity of a wireless LAN using IEEE 802.11b at 11 *Mbps* carrying VoIP calls using analysis and simulation. The analytic upper bound matches the simulation results when channel quality is good. The capacity of the network is found to be highly dependent on the delay constraints of the carried voice. Given a delay budget constraint and non-ideal channel conditions they offer a means to select the voice data packet size (in *ms*) for the ITU G.711 and G.729 codecs. Our work on the non-adaptive protocols in Chapter 3 shows close results for the VoIP calls supported for the same standard codecs. We agree that the combined effects of delay and packet loss must be taken into consideration on the quality of the voice, hence we go beyond fixed codec attributes and offer a protocol that opportunistically adapts modulation, compression, and packet size to maximize call capacity and quality.

Along the same lines of research, Anjum et al. [3] investigate the capacity of wireless LANs for VoIP traffic and as a result suggest the use of controlled back-off and priority queueing at the AP when voice and data traffic co-exist.

### 2.1.2 VoIP over Wireless Mesh Networks

The advantage of using multiple radios on voice capacity has been investigated in [6, 63]. Kim et al. [63] proposes a model to accurately infer network capacity of VoIP calls

in *multi-channel multi-radio* (MCMR) WMNs. This is needed since accurate connection admission and control depend on accurate estimation of call capacity. Coordination of radios and channels is accomplished using the *hybrid multi-channel protocol* (HMCP). The model is validated through both test bed measurements and ns-2 simulations, accurately estimating capacity to within 6% of actual measurements and simulations. With speech compressed at 8 *Kbps*, up to 80 *calls* can be supported over a 5-hop line topology.

Bayer et al. [6] investigates the feasibility of VoIP over WMNs through measurements from a designed test bed. The use of dual radios is shown to provide significantly better performance than single radios. However, such improvements are seen only for large packet sizes. As a result, a hop-to-hop aggregation algorithm is proposed. Packets are held at intermediate nodes until there are enough packets to make a preset minimum size. However, the holding of packets is done as long as their delay has not reached a certain threshold. The network simulator is used to investigate the performance of the aggregation algorithm over an 802.11a with a basic rate of 6 *Mbps*, a data rate of 24 *Mbps* and a node separation of 45 *m*. With speech encoded using G.729a with voice activity detection, results show that around 350 *calls* can be supported with a MOS of 3.5.

While the use of multiple radios and the proper assignment of channels can result in an increase in network capacity, it still requires the use of such configurations with corresponding changes in the protocol stack. Our focus in the work in Chapter 3 is on the more common single-radio end systems.

Mansouri et al. [79] proposes a packet scheduling algorithm that takes into account wireless channel conditions, class of service of data carried, and whether a connection is new or handoff. A handoff occurs as the source of an ongoing multimedia session moves from the range of one wireless mesh router to that of another. The scheme favours handoff calls over new calls, and realtime traffic over non-realtime traffic. The algorithm successfully limits the delay of realtime traffic to 135 *ms*. The rate at which speech is compressed,

the protocol overhead is considered, and the mobility pattern considered is not described making it is hard to relate to their results. We plan to augment our work in Chapter 3 with scheduling and drop policies that take into account the nature of voice and possibly packet size. The channel-aware nature of this scheduling algorithm makes it a particularly good candidate as it gives a short-term prediction of network conditions.

van Geyn et al. [35] studies the performance of VoIP over a WMN running IEEE 802.11e for QoS provisioning. Both call quality and throughput are quantified. Using a static line topology, results show that over a single-hop up to 8 *calls* are supported, over 2-hops up to 6 *calls*, over 3-hops up to 4 *calls*, and over 4-hops up to 2 *calls*. A call is considered supported if it meets a MOS of 3.1. Fairness is also quantified to determine whether the network treats calls with identical QoS requirements fairly. Results show that a high degree of fairness is exhibited. Another aspect that is quantified is whether non-overlapping background traffic has an effect on call quality. A 3-hop call is separated from background traffic by 2-hops, 1-hop, and no-hops. The results show that the smaller the separation, the higher the impact on quality. The study does not consider the effect of mobility or frame bursting. While we do not investigate fairness or separation of background traffic, comparison with their results for line topologies reflects that our protocol in Chapter 3 shows superior performance.

Siddique et al. [118] estimates the VoIP call capacity of a single-hop WMN using analytic modelling. Network capacity is modelled as a maximization problem governed by quality constraints involving network parameters. The model can be expanded to multi-hop networks and to other types of realtime traffic. The main contribution is in the detailed modelling of delay and loss sources to capture impairment factors contributing to quality compromise. The model is solved numerically and its results are verified by simulations using ns-2. The results show that increasing the number of voice frames per packet results in an overall increase in network capacity but only to a certain degree beyond which

packetization delay results in call quality degradation. In addition, lower data rate coders, those more aggressive in compressing speech, result in a higher capacity, even though the coder's impairment factor can affect such a trend. The results also demonstrate the effect of increasing the data rate from 11 *Mbps* to 54 *Mbps*. The increase in network capacity is not matched by a comparable increase in call capacity. Further, higher data rate coders such as G.711 result in relatively higher gains in capacity than higher compression coders such as G.729a. This is because G.711 generates larger packets with less per-packet overhead. Lastly, employment of RTS/CTS is found to negatively affect the number of calls supported. Simulation results are solely of one-hop network with no mobility and are similar or inferior to the results of our protocol in Chapter 3.

Kulkarni et al. [69] proposes a cross-layer design for increasing the VoIP call capacity of a Wireless Mesh Networks (WMN). The study identifies parameters deemed crucial across three layers, MAC data rate, routing approach, and voice packetization interval. Four different MAC data rates are considered as provided by the IEEE 802.11b standard. Two routing approaches are investigated: hop-count and link-rate aware routing. Using G.711 for encoding speech, ten different packetization rates and corresponding packet sizes are considered. Simulations in  $ns-2$  are used to generate responses to variations of the parameters. An  $n$ -factorial analysis and linear regression fitting are used to derive algebraic equations for the call capacity. Fitting equations are found using the SAS GLM procedure. In plotting these functions, parameter-combinations that provide the highest capacity are found. As for the goodness of fit, an *analysis of variance* (ANOVA)  $R^2$  greater than 70 is considered an indicator of acceptable call quality. Results show the positive effect of using link rate-aware routing. Packetization has an effect on capacity but only to a certain degree beyond which it becomes negligible. We only consider hop-count as a link metric in our routing protocol. However, link-rate aware routing is shown to give a substantial improvement and appears to be worthwhile to consider.

Packet aggregation is proposed by many studies as a way of mitigating the per-packet overhead of inherently small voice packets [43, 62, 97]. Hasegawa et al. [43] proposes the use of bidirectional packet aggregation and network coding for the support of VoIP over WMN. The proposed protocol is implemented in a test bed and is also verified through simulations. Using a line topology, bidirectional traffic is aggregated then network-coded using an XOR operation. Aggregation opportunities are increased by having intermediate routers hold packets for a time period equal to their queueing delay share of the total delay budget. With node separation of 100 m and a number of hops varying between 2 and 7, the protocol is shown to support around 23 *calls* of speech compressed using G.711 over a 7-hop connection. A call is considered supported if its network delay is limited to 150 ms and its loss rate is within 5%.

Okech et al. [97] proposes a dynamic approach to packet aggregation to increase VoIP call capacity in WMNs. Aggregation is performed only on packets going to the same next hop. The optimal aggregation size is chosen based on the *signal-to-noise and interference ratio* (SNIR) of the outgoing link. Knowledge of the receiving MAC of the SNIR is used to compute *bit error rate* (BER) for the employed modulation technique. BER is then used to compute the *frame error rate* (FER). The algorithm then chooses an aggregation size that limits FER to less than 0.1%. This value is chosen so that the end-to-end error rate is small. Nodes maintain a queue for each outgoing link. Aggregation takes place whenever a queue grows past certain threshold or when oldest packet has crossed certain delay threshold. Performance is investigated using the network simulator ns-2 and is compared against non-dynamic aggregation and plain 802.11. Using a static line topology, the approach is shown to have superior performance in terms of all network parameters and in call capacity. However, it is not obvious what is considered acceptable call quality.

Kim et al. [62] proposes a scheme integrating packet aggregation and header compression to limit overhead and maximize VoIP capacity of a WMN. Aggregation takes place

both end-to-end and hop-to-hop with the first contributing to the end-to-end delay and the latter working within the MAC delay. End-to-end aggregation is applied intra-flow, to packets coming from the same flow, while hop-to-hop aggregation is applied between flows. Since end-to-end aggregation is applied intra-flow, the scheme is augmented with header elimination of the second to the last packets of an aggregated packet. Simulations using the network simulator show that using G.729a speech, the scheme can result in supporting more than 10 *calls* over 4 to 8 hops of a line topology. While our results in Chapter 3 using the same coder show a call capacity of 10 *calls* over one hop, the use of aggregation and header elimination enables their scheme to support 7 times as much (a line topology provides an ideal scenario for aggregation). Many studies reach to the same conclusion regarding the merit of aggregation and we intend to incorporate it into our future work.

Aggregation-aware routing is investigated in [77, 108]. Liwlompaisan et al. [77] proposes a routing scheme that combines packet aggregation, multi-path routing, utilization awareness, and event-triggered rerouting. A link that can be part of many paths allows for higher chances of aggregation, and hence is more attractive in route discovery. This, however, may result in hot spot routing behaviour. As a result, the saturated utilization is taken into account in the cost so that routes go around such spots. As an additional measure to limit the hot spot effect, backward traffic is sent on a path different from forward traffic. Also, an intermediate hot spot node sensing high medium utilization may request certain source nodes to reroute their traffic. Simulations are conducted using the network simulator ns-3 of 802.11a WMN with speech encoded at a rate of 64 *kbps*. Quality constraints are 300 *ms* of delay budget and loss rate of 10%. The results show an increase in the number of supported calls over longer paths (4-9 hops). The delay behaviour is not improved but is not aggravated in comparison with similar protocols.

Along the same lines, Ramprashad et al. [108] uses a theoretical framework to investigate the joint effect of routing and admission with packet aggregation, bursting and rate

adaptation of multiple packets in a single transmission opportunity on VoIP call capacity of a multi-hop 802.11 network. Analytic results are verified through simulation of a 2-hop scenario using the ns-2 network simulator. Results show that the analytical framework provides a tight upper-bound when compared with simulation. In the presence of channel errors, around 22 calls can be supported. As for rate adaptation, the results show that joint optimization of other factors is only of interest in a 2 to 3 dB SNR region between rate switches. Our cross-layer framework in Chapter 3 does not include the routing layer. Incorporating more layers involves a trade-off between performance and protocol complexity.

## 2.2 Locating Arrays: A New Experimental Design for Screening Complex Engineered Systems

*Full factorial* designs are sets of all possible combinations of all factors and all value levels per factor [84, 91]. Therefore, the size of full factorial designs, i.e., the number of rows (tests) in the design, grows exponentially with the number of factors. A full factorial design is the most costly in experimental resources. The designs are *multilevel* if the number of levels per factor are different. Most common, however, are two-level designs. In this case, a design for  $k$  factors is denoted by  $2^k$ .

Full factorial designs are arrays of *balanced* columns. That is, each level of each factor appears an equal number of times across the tests. Also, they are orthogonal designs. An *analysis of variance* (ANOVA) is readily calculated for the results of full factorial experiments. From this, the significant main effects and interactions may be identified.

*Fractional factorial* designs (FFDs) are balanced designs that are fractions of full factorial designs. Fractional factorial designs for screening are *regular* designs commonly of two-levels per factor; denoted  $2_R^{k-p}$ . Here,  $k$  is the number of factors and  $p$  is the number of generators. Also,  $p$  describes the size of the fraction  $\frac{1}{2^p}$ ;  $R$  is the resolution of the design [91]. The *generators* are expressions of factors confounded (indistinguishable from one

another) and they determine the alias structure. *Resolution* is a property of the fractional factorial design used for grouping in different types of aliasing main effects and low-order interactions.

Although only a fraction the size of a full factorial design, fractional factorial designs are relatively large even for a modest number of factors. The size of fractional factorial designs is still exponential in the number of factors.

Regular FFD designs have a simple aliasing structure and can be identified as Resolution III, IV, or V according with the type of aliasing between main effects and two- or higher-order interactions [8].

Typical resolutions by type of aliasing are shown in Table 2.1.

**Table 2.1:** Typical resolutions by type of aliasing.

<b>Resolution</b>	<b>Type of aliasing</b>
III	Main effects can be confounded by two-factor interactions. Estimate main effects, but these may be confounded with two-factor interactions.
IV	Main effects are aliased by three-factor interactions and two-factor interactions are aliased by two-factor interactions.
V	Main effects are aliased by four-factor interactions and two-factor interactions are aliased by three-factor interactions.

Non-regular fractional factorial designs are widely used in various screening experiments for their run size economy and flexibility in accommodating various combinations of factors with different numbers of levels [137]. Unlike regular FFDs, non-regular FFDs may exhibit a complex aliasing structure and analyzing their resolution is difficult; see, e.g., [76] for generating the alias relationships for the two-level Plackett and Burman designs.

A fractional factorial design is *saturated* when it investigates  $k = N - 1$  factors in  $N$  tests (rows) [84]. There are only  $k$  degrees of freedom to represent the number of terms of the model. That reduces the number terms forming the models describing the system. Supersaturated designs contain more factors than tests ( $k > N - 1$ ). They are not large enough to estimate all the main effects (let alone interactions) because the number of de-



degrees of freedom is not large enough, [37, 74, 84]. While supersaturated designs are cost effective in terms of the size of the design, when building a supersaturated design it is inevitable that orthogonality is abandoned in favour of small size designs [75]. The designs lose efficiency and, there is multicollinearity among the regressors and biased estimation of regression coefficients.

*Definitive screening designs* are designs of quantitative factors of three levels (-1, 0 and +1) for continuous or categorical variables in the presence of active first- and second-order effects [60]. Each test is accompanied by its mirror test. That is, for each test  $i$  containing -1 and +1 values in the factors, there is another test  $j$  which contains exactly a +1 value where test  $i$  has a -1 and it has a -1 where test  $i$  has a +1. Also, each pair of tests contains the 0 value level in each different factor. Those characteristics make it a self-foldover design. One test is at the center of the design region with all the factors at their 0 setting. If  $k$  be the number of factors, definitive screening designs have  $k \times 2 + 1$  tests. Main effects are independent of two-factor interactions and two-factor interactions are not completely confounded with other two-factor interactions. Definitive screening designs are limited to factors with three levels.

A *D-optimal* design is one of the most popular experimental designs among those using optimality criteria. A model to fit, and a bound on the number of tests ( $N$ ), must be specified a priori; that is, it restricts the factors to be analyzed to those forming the model specified. Let  $X$  be the matrix of all possible combinations of the factors and interactions included in the model to fit. The optimality criterion for building D-optimal designs selects  $N$  tests that attempt to maximize  $|X'X|$ , the determinant of  $X'X$  of the pre-specified model [84, 85, 87, 91]. A candidate design consists of  $N$  tests taken from  $X$  with maximum determinant. Because the factors to be analyzed are restricted only to those forming the model defined a priori, the  $X$  matrix is usually non-orthogonal and the effects estimates are correlated. Hence, the variance of the estimated regression coefficients is usually high. Moreover, the

estimated regression coefficient of any factor depends on which other predictor factors are included in the model.

### 2.2.1 Locating Arrays as Screening Designs

Colbourn et al. [18] introduces the definition of a *locating array* (LA). Locating arrays are special cases of covering arrays (CAs) which have been studied extensively [15, 16, 42, 90]. CAs have been used for testing software [20, 24, 67, 68], hardware [114, 127], composite materials [13], biological networks [110, 115], and others. Their use to facilitate location of interactions is examined in [80, 139], and measurement in [46, 47]. Algorithms for generating covering arrays range from greedy (e.g., [9, 31]) through heuristic search (e.g., [94, 130]). In [16] provides the only available deterministic means of producing covering arrays with more than a few hundred factors.

For the case study MANET with 75 factors a standard product construction [17] is utilized and a post-optimization method [89] to reduce the number of levels for each factor. A locating array with 421 rows results.

In Chapter 4 locating arrays (LAs) are introduced for screening a complex engineered network.

## 2.3 Statistical Characteristics of Screening Designs

Here we overview statistical characteristics of screening designs that will be used in Chapter 5 to evaluate the locating array.

Montgomery et al. [85] introduces the formulation of the  $X$  matrix which is constructed from the factors (*i.e.*, the independent regressors). The estimate of linear regression coefficients  $\hat{\beta} = (X'X)^{-1}X'y$  is shown. The  $X$  matrix is used to compute the correlation matrix, the variance inflation factor (VIF) and, the variance-covariance matrix. Here, the  $X$  matrix is computed using unit length scaling because the difference of units from factors [85].

Because variance is a measure of design quality, maximizing the experimental variance and minimizing the within-group variability are main goals for experimental design [140]. The overall variance properties over the entire design space is plotted using a fraction of design space (FDS) [87, 88]. Commercial software can be utilized to obtain the FDS [59].

The aliasing relationships show the confounding between factors or interactions. Lin et al. [76] shows a mathematical procedure to show the alias relationships for the two-levels Plackett and Burman designs.

### 2.3.1 Correlation

Correlation indicates if a value of one variable changes in response to changes in the value of the other variable. The *correlation coefficients* are the off-diagonal values of the  $(\mathbf{X}'\mathbf{X})$  matrix and the values in the  $(\mathbf{X}'\mathbf{y})$  matrix. The correlation coefficients of the  $p \times p$  correlation matrix  $(\mathbf{X}'\mathbf{X})$  between regressors and the  $p \times 1$  correlation matrix  $(\mathbf{X}'\mathbf{y})$  between regressors and the response, in standardized form, can range from  $-1.0$  to  $+1.0$ .

A correlation coefficient of  $0.0$  means that there is no association between the variables. The presence of values close to  $-1.0$  or  $+1.0$  is an indicator of near-linear dependency between two regressors. That is, the correlation is present.

Generally the different regressors of a model and also the response are measured in different units. The regressors and response can be scaled using unit length scaling [85] for producing dimensionless regression coefficients, the standardized form of regression coefficients.

$$w_{ij} = \frac{x_{ij} - \bar{x}_j}{\sqrt{S_{jj}}} \quad (2.1)$$

where  $i = 1, 2, \dots, N$  the number of design points and  $j = 1, 2, \dots, k$  is the number of factors in the design,  $x_{ij}$  is each value  $ij$  in the design,  $\bar{x}_j$  is the average of the values in

column  $j$ , and  $\sqrt{S_{jj}}$  is the corrected sum of squares for the regressor  $x_j$  (i.e.,  $\sqrt{S_{jj}} = \sqrt{\sum_{i=1}^N (x_{ij} - \bar{x}_j)^2}$ ).

The presence of correlation has serious effects on the least squares estimates of the regression coefficients. Therefore, a strong correlation between two regressors results in large values and large variances and covariances of the least squares estimators of the regression coefficients  $\hat{\beta}_j$  corresponding. That is, a poor estimate of the regression coefficients is obtained.

In modeling, if there exists a strong correlation between two factors included in the model, the elimination of one of them is recommended.

### 2.3.2 Dummy coding

Dummy coding is used to create from one categorical factor of  $k$  levels,  $k - 1$  categorical factor of two-levels, basically holding only ones and zeroes [41]. If the original factor is binary, there is no need to code it. Table 2.2 shows the dummy coding of one categorical factor, Factor A, of 4 levels. Column Factor A contains the 4 levels of the Factor A. Then columns from A1 to A3 shows the 3 categorical factors of two-levels constructed using dummy coding. As shown, there is an implicit factor dummy coded corresponding to the value level when Factor A is 1 which does not generate a coded factor to avoid redundancy.

**Table 2.2:** Dummy coding of a categorical factor with 4 levels.

<b>Factor A</b>	<b>A1</b>	<b>A2</b>	<b>A3</b>
1	0	0	0
2	1	0	0
3	0	1	0
3	0	1	0
4	0	0	1

### 2.3.3 Variance Inflation Factor

The elements on the main diagonal of an  $(X'X)^{-1}$  matrix are called the *variance inflation factors* (VIFs) [85]. The VIFs are an indicator of multicollinearity, or the correlation of one factor with the rest of the factors in the design. High VIF values (exceeding 5 or 10) indicate serious problems with multicollinearity and result in poor estimates of the associated regression coefficients [85].

### 2.3.4 Covariance

Covariance is a measure of the strength of the correlation between two or more sets of random variates. The covariance for two random variates  $X$  and  $Y$ , each with sample size  $N$ , is defined by the expectation value  $cov(X, Y) = \sum_{i=1}^N \frac{(x_i - \mu_x)(y_i - \mu_y)}{N}$ , where  $\mu_x$  and  $\mu_y$  are the respective means of  $X$  and  $Y$  [85].

### 2.3.5 Fraction of Design Space

In general, it is not known in advance what part of a design space is of most interest. Therefore, it is desirable for the variance of a predicted value to be as uniform as possible throughout the design space. A *variance dispersion graph* (VDG) evaluates the performance of a design in terms of its prediction variance [88]. The scaled version of a VDG, a *standardized prediction variance* (SPV) allows for fair comparisons among designs with different numbers of runs. The SPV for a design point  $x_0$  does not depend on the response, but only on the design  $X$ . It is defined as  $v(x_0) = Nx_0'(X'X)^{-1}x_0$  where  $N$  is the number of rows in the design,  $x_0$  is the design point for which the prediction variance is evaluated, and  $X$  is the design.

A *fraction of design space* (FDS) plot shows the cumulative fraction of the design space on the  $x$ -axis (from 0 to 1) versus the scaled prediction variance on the  $y$ -axis. The more

the fraction of the design space for a SPV is close to the minimum, the better is the design [87]. Also, the flatter the curve, the more stable the SPV distribution is for that design (*i.e.*, it is more uniform). An FDS is a precise tool to compare designs [87].

### 2.3.6 Aliasing

When it is not possible or not desired to run all tests of the runs of a full factorial design (*e.g.*,  $2^k$ ), *confounding* is a design method to arrange a complete factorial experiment in blocks or fractions. Then certain effects (main or interactions) are indistinguishable from one another. That is, some effects are estimated by the same linear combination of the experimental observations as some blocking effects [84, 91].

For example, the full factorial design of 5 binary factors A, B, C, D and E has 32 design points. The fractional factorial design  $2^{5-2}_{III}$  (resolution III) confounding  $D=+AB$  and  $E=+AC$  is:

Test	A	B	C	D	E
1	0	0	0	1	1
2	1	0	0	0	0
3	0	1	0	0	1
4	1	1	0	1	0
5	0	0	1	1	0
6	1	0	1	0	1
7	0	1	1	0	0
8	1	1	1	1	1

The defining relation is  $I=ABD=ACE=BCDE$ . Assuming non significant higher-order interactions, the aliasing relationships are:

<b>Effect</b>	<b>Alias</b>
A	BD CE
B	AD
C	AE
D	AB
E	AC
BC	DE
BE	CD

That is, the columns in the  $2_{III}^{5-2}$  corresponding to some main effects or interactions are indistinguishable. For example, the Factor A is indistinguishable or completely aliased with the interaction of the two factors Factor B and Factor D.

## Chapter 3

# CROSS-LAYER OPPORTUNISTIC ADAPTATION FOR VOICE OVER AD HOC NETWORKS

### 3.1 Introduction

*Voice over IP* (VoIP) is one of the fastest growing applications in networking [134]. The rate at which wireless access points are spreading only increases the importance of VoIP over wireless [71]. Supporting voice over ad hoc networks is part of realizing an all-IP goal.

The wireless channel introduces many challenges for supporting voice. These include the inherent broadcast nature of the channel, temporal response variability due to fading and absorption, and sensitivity to noise and interference. Ad hoc networks also suffer from a scarcity of resources and a lack of centralized control. When combined, these challenges make supporting voice in these networks a formidable task. Our interest is in supporting voice in the battlefield, or in emergency situations; therefore, our focus is on call admittance and survival with acceptable quality as opposed to providing the quality we have come to expect in wire-line telephony.

Experience in cellular networks has shown that adaptive applications are resilient and robust [38, 39, 72]. In addition, cross-layer design, where performance gains are accomplished through exploiting the dependence between protocol layers, gives better performance compared to traditional approaches [107]. However, increasing the number of layers involved in a cross-layer design does not always translate into better performance. If not used carefully, unintended cross-layer interactions may have undesirable consequences on overall system performance [61].



Combining the merits of both adaptation and cross-layer design, while cognizant of the care required, we propose an opportunistic adaptive protocol within a cross-layer framework for supporting VoIP over ad hoc networks. We incorporate three of the seven approaches to cross-layer design identified by [125]: explicit notification from one layer to another, directly setting a parameter of a different layer, and vertical calibration across different layers of the protocol stack.

We tackle the time-variant channel quality and capacity by introducing adaptive modulation to maximize channel utilization. We also minimize the amount of real-time traffic introduced in the network by using adaptive voice compression. A side effect of using adaptive compression is to also vary the audio packet size used.

Adaptation of three factors, namely modulation, compression, and packet size, requires collaboration of three layers of the protocol stack: the physical, link, and application layers. In terms of time scale, adaptation of modulation occurs on a hop-by-hop basis as channel quality varies from one hop to another and occurs at a fast pace. Adaptation of compression and packet size, on the other hand, occur on an end-to-end basis as this depends on the path quality and therefore occurs on a longer time scale. Having the protocol work at two different time scales combines the benefits of having an accurate picture of both local and end-to-end conditions, and reduces protocol overhead.

This research makes the following contributions:

- A cross-layer architecture for voice over ad hoc networks is presented that combines the use of modulation, compression, and packet size spanning three layers of the protocol stack: physical, link, and application.
- An adaptive protocol is proposed that operates at two time scales, on a hop-by-hop basis and an end-to-end basis, capturing local channel quality and end-to-end network statistics, respectively.

- A high fidelity simulation model is used that includes the simulation of packetization delay and physical layer details, play-out buffers, among others.
- Both quantitative and *mean opinion score* (MOS) audio quality metrics are evaluated using real audio traces, with comparisons to several standard voice codecs.

The rest of this chapter is organized as follows. The factors whose adaptation is important in providing acceptable voice quality in §3.2 are identified. Using the selected factors, an opportunistic adaptive protocol in §3.3 is proposed. In §3.4 we describe the simulation set-up, and define the quantitative *degradation in voice quality* (DVQ) and the qualitative subjective *mean opinion score* (MOS) performance metrics. Through simulation with real audio traces the performance of our protocol is evaluated for both static topologies and mobile scenarios in §3.5 comparing to non-adaptive protocols using standard voice codecs. An analysis bounding the maximum voice capacity for our protocol is presented in §3.6. Finally, conclusions are shown and future work is proposed in §3.7.

### 3.2 Factors Influencing Voice

The *quality-of-service* (QoS) requirements of voice are:

1. A 0 to 150 *ms* end-to-end delay is acceptable for most applications [50].
2. Voice can tolerate a packet loss on the order of  $10^{-2}$  to  $10^{-4}$  [123].
3. Delay variations of less than 75 *ms* give good quality [83].

*End-to-end delay* is the time from when a frame is generated at the caller until it is played at the callee. There are five components to end-to-end delay: (1) *Packetization delay* is the delay at the caller to collect all bits that compose a packet. (2) *Queueing delay* is the time a packet spends waiting to be forwarded. (3) *Transmission delay* is the time it takes to first transmit a packet, while (4) *propagation delay* is the time for it to propagate through

a link. Finally, (5) *play-out delay* is the time a packet spends in the buffer of the callee for smooth play out. The *delay budget* refers to the total end-to-end delay beyond which packets are considered stale.

For one-way transmission time the [50] recommendation is that a 0 to 150 *ms* delay is acceptable for most applications but a delay above 400 *ms* is unacceptable. For highly interactive tasks, quality may suffer at a delay of 100 *ms*.

Voice can tolerate a small amount of packet discard. Either the decoder uses sequence numbers to interpolate for lost packets, or the encoder adds redundancy in the sent packets [82]. These techniques work well when the losses are isolated. For compressed voice, *packet loss concealment* is used by most codecs and involves the callee producing a replacement for a lost packet. This is possible because of the short-term self-similarity in audio data [103]. If bursty losses take place then gaps occur and the quality of voice suffers.

*Delay variation* (or jitter) is the difference between the minimum and the maximum delay that packets encounter in a single session, and it results from variable queueing delays. It is important for voice traffic to be played at the callee at a rate matching the rate generated at the caller [126]. Buffering is used to overcome jitter. Once the callee starts receiving packets, it buffers them for a time equal to the delay variation, and then starts playing them out. When packets arrive late some packets in the buffer are consumed, while early arrival results in the buffer growing.

From these QoS requirements, delay variation is the key quality impairment for voice. In [32] is shown that the availability of bandwidth can limit the impact of delay. This suggests that we should choose factors that control the ratio of offered load to the available bandwidth in this study. One way to increase the available bandwidth is by introducing adaptive modulation where the spectral efficiency changes depending on the current channel conditions. Another is to control the real-time traffic within the network. Adaptive voice

compression compresses a real-time stream in light of the current channel and network conditions.

In VoIP over wireless, a packet has substantial overhead consisting of headers from four protocols: the *real-time protocol* (RTP), the *user datagram protocol* (UDP), the *internet protocol* (IP), and the *medium access control* (MAC) protocol. While it is important to maximize the payload per packet, a large payload results in high packetization delay which may impact the perceived quality at the callee. This suggests that for adaptive compression to be beneficial, the level of compression has to be selected jointly with packet size.

Together, these motivate our selection of three factors for our study: modulation, compression, and packet size. There are many trade-offs to consider in their adaptation. We have used statistically designed screening experiments to validate that these factors and interactions among them are influential on delay. See [96] for a complete description of the experiments and the associated results.

### 3.3 Adaptation Architecture and Protocol

Reinforced by the results of the statistical analysis, we design a cross-layer opportunistic protocol; Figure 3.1 shows the architecture of the adaptive protocol. The protocol combines hop-by-hop and end-to-end adaptation each working at a different time scale. Cross communication between the *physical* (PHY) and *medium access control* (MAC) layers takes place at every hop along the path from the caller to the callee and enables adaptive modulation. While we use the *opportunistic auto rate* (OAR) protocol over IEEE 802.11b to make use of the multi-rate capability of the PHY layer [111], the architecture we propose is generic and can work with any multi-rate PHY/MAC. Cross communication between the *logical link control* and *application* (LLC/APP) layers, on the other hand, takes place only at the caller and enables adaptive selection of compression rate and packet size.

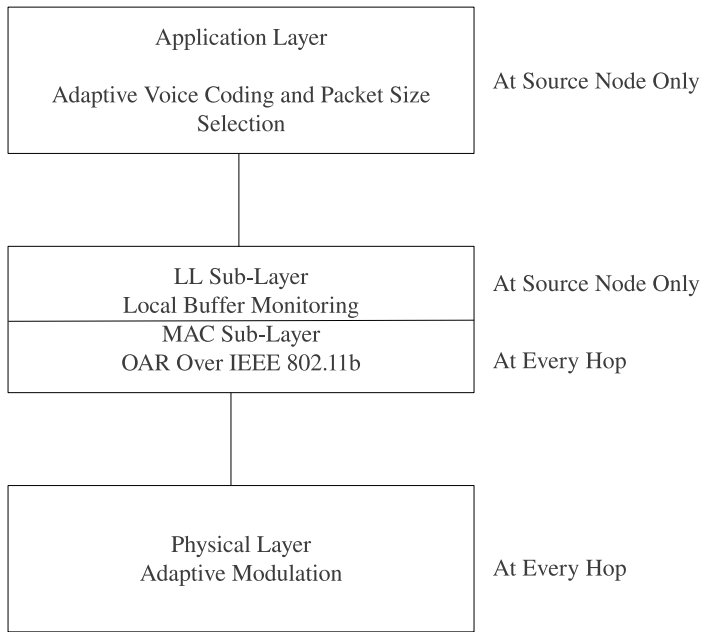


**Figure 3.1:** System architecture: hop-by-hop and end-to-end adaptation.

The dynamics of the cross-layer communication between the PHY/MAC layers is as follows: At every hop, when a node receives a *request-to-send* (RTS) packet, it analyzes the signal quality and extracts the *signal-to-noise ratio* (SNR) information to select the transmission rate. The decision involves determining the highest achievable transmission rate from the current channel conditions; higher transmission rates require a stronger received signal [111]. Once the receiver chooses the most suitable modulation for the packet transmission, it piggybacks its decision in the *clear-to-send* (CTS) packet. Upon receiving the CTS, this information is extracted and communicated to the PHY layer.

Compression and packet size selection depend on the end-to-end feedback regarding the network conditions expressed in terms of the packet loss ratio and average packet delay. Figure 3.2 shows the end-to-end protocol dynamics at a high level. An *epoch-length* is the duration of time the callee waits before sending feedback to the caller. Whenever it receives a packet, the callee updates its statistics for packet loss and average packet delay for the current epoch. Average delay is first calculated by subtracting the time stamp of every arriving packet from its arrival time. The total delay of all packets arriving within an

epoch is then divided by their number. Packet loss is calculated by monitoring the packet identifiers and logging the number missing.

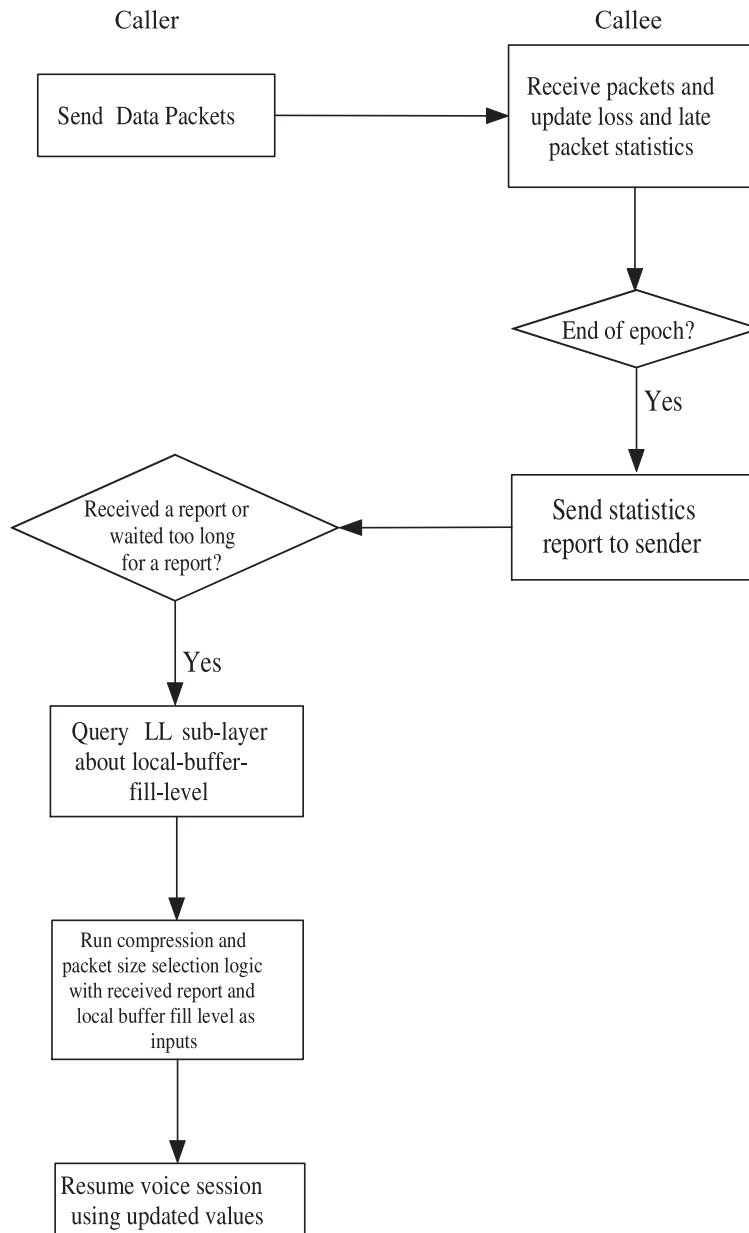


**Figure 3.2:** The end-to-end protocol dynamics.

At the end of every epoch the callee sends a 12 *byte* statistics report, containing 6 *byte* fields of loss and delay statistics, to the caller. On receipt of the statistics report, the caller invokes the adaptive protocol to calculate both the packet size and the compression level.

### 3.3.1 Packetization Delay, Packet Size, and Compression Level Calculations

The adaptive protocol selects the packet size to maximize the payload per packet and limit the overhead per packet, and minimize the contribution of packetization delay to the total end-to-end delay to improve the voice quality experienced.

When the network is lightly loaded and end-to-end delay is low, most of the delay budget is directed to the packetization delay component maximizing packet size without compromising quality experienced by the user. When load conditions are high, the maximum packetization delay that can be allocated without contributing to end-to-end delay is equal to the time the packet has to wait in the local LLC buffer before getting transmitted over the channel. A pipelining opportunity is created where packet size is maximized without contributing to end-to-end delay.

The protocol starts by querying the LLC layer regarding the average delay in the local buffer. Using both the local buffer delay and the end-to-end delay and loss statistics, the protocol starts by calculating the packetization budget. This is the greater of the local delay, and the delay budget minus the end-to-end delay. This way, the contribution of packetization delay to the accrued end-to-end delay is minimized.

For example, consider a network experiencing light load conditions with a network delay of  $70\text{ ms}$ . If the delay budget for our application is  $150\text{ ms}$  then there is up to  $150 - 70 = 80\text{ ms}$  that can be used toward packetization. This way, with high likelihood, the packet reaches the callee on time while the payload is maximized. However, since the network delay is an average value, a *safety-margin* is used. In our experiments, we assume a fixed value of  $20\text{ ms}$  for the safety-margin.

On the other hand, consider a network experiencing heavy load conditions with an average delay of  $140\text{ ms}$ . If the delay budget is  $150\text{ ms}$  then the remainder of the delay budget is too small to use for packetization. However, if the average delay of the local buffer is

30 *ms* then we can use this value for packetization as producing a packet any earlier than 30 *ms* does not reduce the end-to-end delay. This is because the packet must wait 30 *ms* in the local buffer. This way, the protocol does not add to the total delay while, at the same time, the packet size is maximized.

One more factor that contributes to the packetization delay, and hence the packet size to select, is the current loss ratio. If the loss ratio crosses a maximum threshold, the protocol cuts the packetization budget by a predefined percentage. The reason is to avoid sending packets with a large payload because losing large packets has a great impact on quality.

Following the approach of [14], in our experiments we assume that half of the losses are due to channel errors, since there is currently no way to differentiate loss due to congestion from one due to channel noise in wireless networks.

The protocol then calculates the compression rate to use. If the loss ratio is higher than a maximum threshold, the compression rate is cut to half of the current value. If the current average delay crossed a maximum threshold, the protocol again cuts the compression rate by half. If neither of these two conditions is true and both the loss ratio and average delay are less than some predefined minimum thresholds, the protocol increases the compression rate to the next rate within the available set of compression rates. In this approach, the protocol reacts quickly to "bad news" and conservatively to "good news."

Next, the protocol makes sure that the compression rate and the packetization delay calculated do not fall outside the allowed ranges. The protocol also ensures that packetization delay is within the limits of the minimum and maximum thresholds to prevent sending very small or very large payloads. As a last step, the protocol calculates the packet size based on the packetization budget and the chosen compression rate. It then ensures that the calculated packet size is an integer multiple of the frame size of the given compression rate.

In cases where the caller fails to receive a statistics report for a number of epochs equal to *feedback-timer-length*, the protocol reacts as follows. To start, the protocol cuts the com-



pression rate in half as a way of mitigating any network congestion that may be preventing the arrival of feedback from the callee. Next, the protocol queries the LLC layer for the local buffer delay and uses this value as the packetization delay. As before, the protocol makes sure that the compression rate and the packetization delay calculated do not fall outside the allowed ranges, calculates the packet size based on the packetization budget and the chosen compression rate, and makes sure the calculated packet size is an integer multiple of the frame size of the given compression rate.

The thresholds that the protocol uses depend on the application. If the application requires stringent quality requirements, the thresholds may be adjusted to produce high quality. Likewise, if the main goal is to communicate even if quality is reduced, thresholds may be relaxed to produce acceptable quality.

### 3.4 Simulation Set-Up

We use the `ns-2` network simulator [93] release `2.1b7a` to evaluate the performance of our opportunistic adaptive protocol. We move from simple to more sophisticated static topologies in order to attribute cause to observations, and then consider mobile scenarios.

#### 3.4.1 Static Topologies

We start with a line topology with  $i$  hops,  $1 \leq i \leq 5$ , where node 1 is the caller and node  $i + 1$  is the callee. This topology minimizes MAC-layer contention and physical-layer co-channel interference and thus gives an idea about the upper-bound performance of our protocol. The distance between nodes is set to  $150\text{ m}$  for two reasons. The first is to allow the different modulation schemes to be used whenever channel conditions allow. The second is that when nodes are closer the interference effect on one another is higher.

To consider the impact of MAC layer contention, we next use a variant of the line topology shown in Figure 3.3. The total load generated is divided between callers 1 and 2 and

is communicated to the callee. In addition to the added contention, node 3 is a bottleneck as both nodes 1 and 2 need to pass their traffic through 3 to the rest of the network; this is ensured by placing nodes 1 and 2 a distance of  $200\text{ m}$  away from node 3.

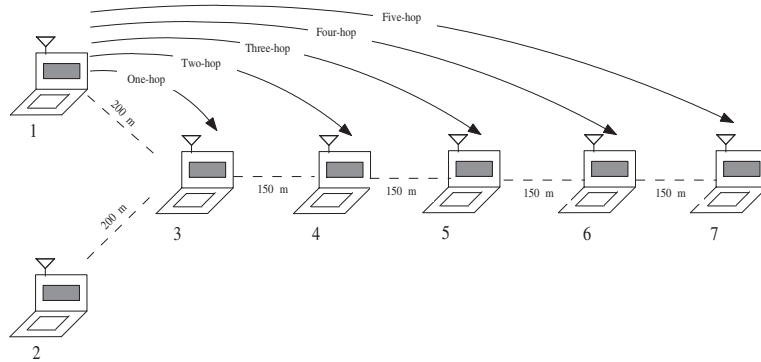


**Figure 3.3:** Variant of the line topology.

We then consider a  $5 \times 5$  grid topology shown in Figure 3.4. The distance between a node and each of its horizontal and vertical neighbors is  $150\text{ m}$ . We consider two concurrent flows to introduce co-channel interference. We vary the intensity of interference by varying the distance between the two flows. We start with a *low-interference traffic pattern* with  $flow_1$  from caller node 3 to callee node 11 and  $flow_2$  from caller node 15 to callee 23. For the *high-interference traffic pattern*, we move the caller of  $flow_2$  to node 8 and its callee to node 16. The distance between the two flows results in co-channel interference and may cause packets not to be routed on the direct 2-hop path (we observed many different 3-hop paths taken).

Following the approach of [120], we then introduce irregularity in the grid topology by uniformly varying the placement of each node within a square of side  $40\text{ m}$  centered at the grid point. This way, the network remains connected while at the same time link quality depends on the distance between nodes. We vary the placement of nodes from one simulation run to another. For the irregular-grid, the low-interference traffic pattern consists of two concurrent flows, while the high-interference traffic pattern selects four concurrent

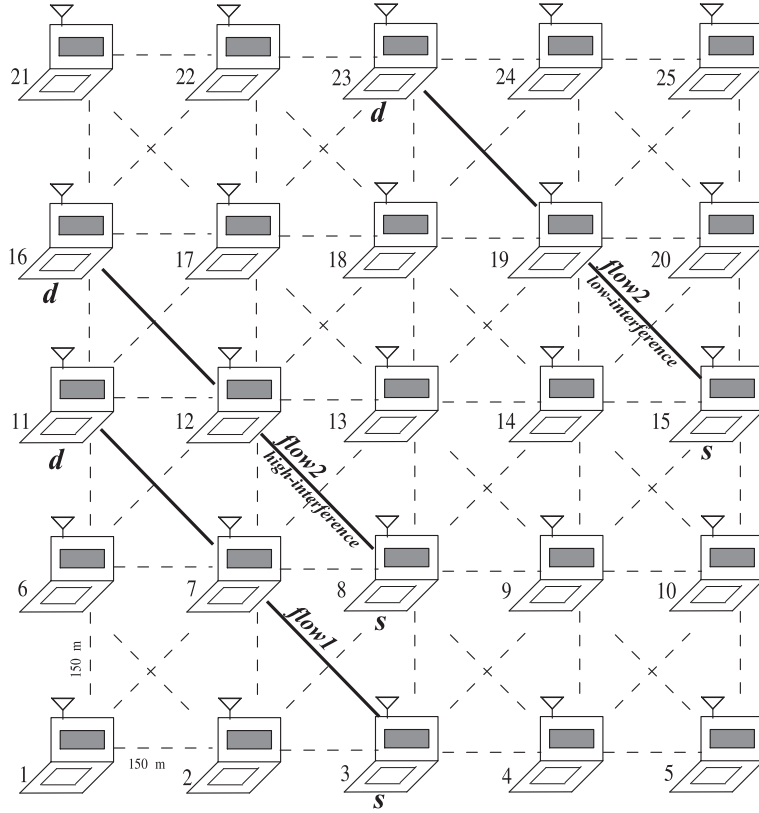


**Figure 3.4:** Grid topology.

flows, with caller-callee pairs selected at random. Similar to the grid, a route in the irregular-grid may use a variable number of hops.

Even though the topologies described so far are static, we use the Ad hoc On-demand Distance Vector (AODV) routing protocol [103] to establish the caller-callee paths because routes may vary over time due to interference and other physical layer effects.

### 3.4.2 Mobile Scenarios

We also study the impact of mobility on the performance of our protocol. The scenarios where we envision our protocol to be employed involve team work where a group is coordinating its actions in the battlefield or an emergency situation. Therefore, we focus on three group applications: an event, a march, and a pursuit modelled by a *nomadic*, a *column*,

and a *pursuit* mobility model, respectively. Table 3.1 summarizes these applications, their characteristics, and the parameters used to model them.  $\bar{s}$  refers to the average speed of a node,  $\Delta s$  is the range in which speed changes,  $\bar{p}$  refers to the average pause time of a node, and  $\Delta p$  is the range in which pause time changes.

**Table 3.1:** Characteristics of group applications and mobility model parameters.

Application & Model	Characteristics	N	$\bar{s}$ (m/s)	$\Delta s$ (m/s)	$\bar{p}$ (s)	$\Delta p$ (s)	$r$ (m)	$\Delta r$ (m)
Event, Nomadic	Walking speed Long pauses	40	0.5	0.5	60	60	0	10
March, Column	Walking speed No pauses	50	1.0	1.0	0	0	10	5
Pursuit, Pursuit	Vehicle high speed No pauses	10	20.0	10.0	0	0	0	5

A nomadic mobility model captures the collective movement of a group of nodes from one point to another. Nodes within a group follow a reference point around which they move freely. When the reference point moves, all nodes move to the new location where they move freely again. In a column mobility model nodes move around a certain line which is moving ahead. A pursuit mobility model captures the movement of a group of nodes chasing a target.

To derive the movement pattern for each of these mobility models, we use the implementation of the *reference point group mobility* (RPGM) generic model [11]. The three mobility models can be derived from this model by varying two parameters:  $r$ , the reference point separation, and  $\Delta r$ , the node separation from the reference point. The *reference point separation* refers to the pace at which the group center moves while *node separation from the reference point* defines the coupling of the group, i.e., how far nodes are from their reference point. For these parameters, we use the values summarized in Table 3.1 which are taken from [25] and are chosen because the movement traces they represent are appropriate for our applications.  $N$  is the number of nodes in the group.

We consider two, four, and eight concurrent flows for event and march applications, and up to three concurrent flows for the pursuit application.

### 3.4.3 Wireless Channel Model

We use a Ricean fading model of the wireless channel. The ns-2 wireless extensions of fading [129] are based on a simple and efficient approach first proposed by [106]. Even though the channel modelling extensions accurately simulate the wireless channel for each individual flow, fading components of channels for different flows are identical, which is unrealistic. A way to solve this problem was suggested in [111]. We use the modified model in our simulations.

### 3.4.4 Simulation Parameters

Table 3.2 summarizes the simulation parameters. We consider two delay budgets to account for a spectrum of applications. For applications that require a high level of interaction, we use a delay budget of 150 *ms*. For more elastic applications, we use a delay budget of 300 *ms*. Any packet arriving at the callee past its delay budget is considered late and is counted as stale.

Each packet consists of headers, and a payload segment consisting of an integral number of audio frames. The headers total 56 *bytes*. Thus if the payload is 100 *bytes*, what is transmitted is a 156 *byte* packet. To make sure that there is a reasonable number of voice frames in a packet, we do not transmit a packet with less than 50 *ms* of voice.

As a way of mitigating the high overhead per packet, we use the *robust header compression* (ROHC) protocol [7]. [109] show that communicating GSM speech with the optimistic variant of ROHC results in an average header size of 6 *bytes*. If the UDP checksum is turned off, the average header size is reduced further to 4 *bytes*. In a separate study, Seeling et al. show similar performance results when communicating high quality video with optimistic

**Table 3.2:** Simulation and adaptative protocol parameters.

<b>Simulation Parameter</b>	<b>Value</b>
Simulator	ns-2.1b7a
Simulation hardware	Intel Core 2 Quad CPU Q9550 at 2.83 GHz, 8 GB RAM
Simulation time	1000 s
Simulation warm-up time	500 s
Audio stream	audio book in mono, WAVE format 8000 <i>samples/s</i> , quantized at 16 <i>bits</i>
Audio stream compression	Speex [122]
Static topologies	Line, line-variant, grid, and irregular-grid
Mobile scenarios	See Table 3.1
Transmission Range	250 <i>m</i>
Channel rates	2, 5.5, and 11 <i>Mbps</i>
Fading model	Ricean with $K = 10$ dB with flow dependent fading [111]
<b>Protocol Parameter</b>	<b>Value</b>
Routing protocol	AODV [103]
MAC protocol	OAR over IEEE 802.11b [111]
Compression levels	3, 5, 7, 8, 12, 16, 24, and 32 <i>Kbps</i>
ROHC	enabled and disabled
Overhead per packet	56 <i>bytes</i> (ROHC disabled), 32 <i>bytes</i> (ROHC enabled)
Buffer size	100 <i>packets</i> , drop-tail queueing policy
Delay budget	150 <i>ms</i> and 300 <i>ms</i>
<i>epoch-length</i>	1 <i>s</i>
<i>feedback-timer-length</i>	3 <i>s</i>
<i>min-loss-thresh</i>	1%
<i>max-loss-thresh</i>	10%
<i>perc-chnl-contrib</i>	50%
<i>min-pack-delay</i>	50 <i>ms</i>
<i>max-pack-delay</i>	100 <i>ms</i>
<i>min-delay-budget</i>	50 <i>ms</i>
<i>max-delay-budget</i>	130 <i>ms</i>
Safety margin	20 <i>ms</i>
Statistics report size	12 <i>bytes</i>

ROHC enabled [113]. We adopt these results compressing the UDP/IP header from 28 to 4 bytes. Each experiment is run with ROHC disabled and then enabled.

In all cases, we run at least 50 replicates of each experiment.

### 3.4.5 Quantitative Degradation in Voice Quality (DVQ) Metric

We gather both quantitative and qualitative metrics of voice quality. The *degradation in voice quality* (DVQ) is a quantitative metric [58] defined as:

$$DVQ = \frac{p_{lost} + p_{late}}{p_{total}}$$

where  $p_{lost}$  is the number of packets lost,  $p_{late}$  is the number of packets arriving after their delay budget, and  $p_{total}$  is the total number of packets sent. As a result,  $0 \leq DVQ \leq 1$  and gives the percentage of lost and late packets.

Since adaptive compression and packet size selection are used, measuring the amount of speech by *counting the number of packets is inaccurate because the amount of speech per packet depends on the compression level*. This is because packets that are the same size may carry different amounts of voice payload. Therefore, in the computation of DVQ, rather than counting packets, we extract the amount of speech per packet.

### 3.4.6 Qualitative Mean Opinion Score (MOS) Metric

While the smaller the DVQ the better, how DVQ correlates to perceived voice quality is unclear. To this end we use a subjective metric, the *mean opinion score* (MOS) [55]. MOS is expressed by the scale shown in Table 3.3 with range from 1 (bad) to 5 (excellent), providing a numerical indication of the listening quality of the received audio stream.

All our simulations use real voice traces as input to the simulation. Raw recorded speech, in the form of audio books stored in mono, WAVE-format, serves as input to the simulation.

**Table 3.3:** MOS listening-quality scale.

Quality of speech	Score
Excellent	5
Good	4
Fair	3
Poor	2
Bad	1

The audio book consists of 8000 *samples/s* with each sample quantized at 16 *bits*. This stream is then modified according to the dynamics of the adaptive protocol.

The audio stream compression is achieved using the *Speex* open source audio compression format [122]. *Speex* is part of the GNU project and is based on *code excited linear prediction* (CELP). It has the capability to compress voice at bit rates ranging from 2 to 44 *Kbps*. The coder has many functionalities including voice activity detection, packet loss concealment, echo cancellation, and noise suppression.

The received stream is compared with the original audio stream of the same duration (no larger than 2 *mins*) using the methodology in [57]. The *perceptual evaluation of speech quality* (PESQ) [53] algorithm measures speech quality comparing an original speech reference with the callee's version, which has a known correlation to MOS.

### 3.4.7 Non-Adaptive Protocols used for Comparison

We compare our adaptive protocol to non-adaptive versions of the protocol in which the modulation and packet size are fixed to standard settings of voice codecs, and the MAC protocol is IEEE 802.11b DCF used at fixed data rate of 2 *Mbps*. We also experimented with a data rate of 11 *Mbps* but because all of the results show a similar trend to the results at 2 *Mbps* we do not present them here. Table 3.4 shows the codecs, and their ITU-T or ETSI standard settings.



**Table 3.4:** Standard audio/voice codec attributes.

<b>Codec</b>	<b>Bit Rate (Kbps)</b>	<b>Payload (bytes)</b>	<b>Framing Interval (ms)</b>
G.711	64	80	10
		160	20
		240	30
G.729	8	10	10
		20	20
		30	30
G.723	6.3	8	10
		16	20
		24	30
GSM-EFR 6.60	12.4	31	20
GSM-FR 6.10	13.2	33	20

### 3.5 Simulation Results

We first present simulation results for the static topologies and then for the mobile scenarios. We plot the DVQ and the MOS as a function of the number of calls per flow, however when we tabulate the number of calls supported per flow we only count calls in which the listening quality is at least fair, i.e., the  $MOS \geq 3$ . If  $MOS < 3$ , we consider the quality of the voice to be too poor for our applications of interest, i.e., voice communication in the battlefield or for emergency response.

#### 3.5.1 Results for Line and Line-Variant Topologies

Figure 3.5 shows the DVQ and MOS for our adaptive protocol as a function of number of calls for line topologies with  $1 \leq i \leq 5$  hops, with a delay budget of  $150\text{ ms}$ , and no header compression employed; all results are summarized in Table 3.5. The DVQ and MOS almost appear as mirror images of each other. Overall, longer line topologies support fewer voice calls with fair listening quality. This is expected as longer paths result in longer delay due to more queueing at intermediate hops, resulting in more lost and late packets. The delay also increases because a node cannot both send and receive at the same time with a

half-duplex transceiver. For example, in a four-hop path, node 3 cannot receive from node 2 and send to node 4 concurrently.

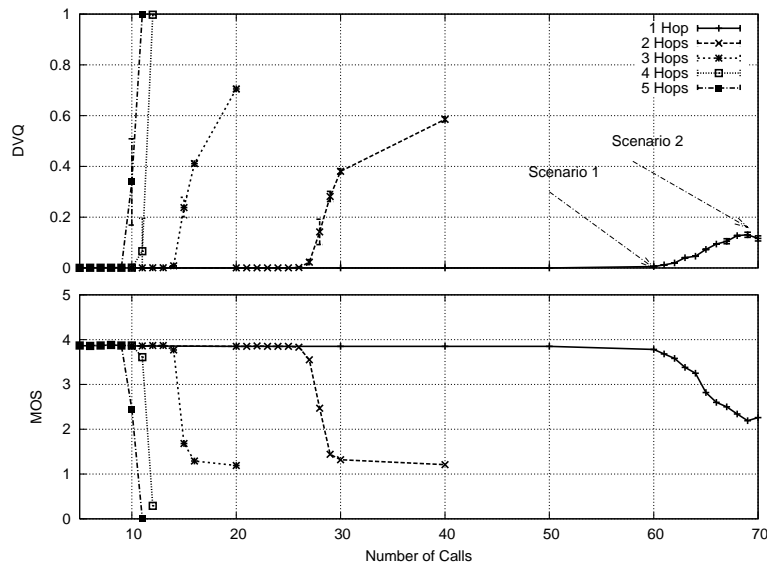


**Figure 3.5:** DVQ and MOS as a function of number of calls per flow for line topologies using the adaptive protocol (150 ms delay budget, no ROHC).

We repeat the experiment with a relaxed delay budget of 300 ms and with header compression enabled. These results are given in Figure 3.6. Not surprisingly, more calls with fair quality can be supported with a less stringent delay budget. Since this is true for all topologies we considered, henceforth we only present our results for the stricter delay budget of 150 ms.

Now, we repeat the experiments for the line topologies using the non-adaptive protocol with standard voice codecs; all of these results are included in Table 3.5. Figure 3.7 shows the DVQ and MOS as a function of the number of calls per flow for the settings yielding the highest performance; this occurs when the framing interval is the longest. Interestingly, when the DVQ is zero the corresponding MOS for each codec is different; this confirms prior observations [56]. The highest MOS of 4.19 is achieved by the G.711 codec with a framing interval of 30 ms while the G.723 obtains the lowest MOS of 3.27 with the same framing interval. The highest MOS does not correspond to the highest voice capacity

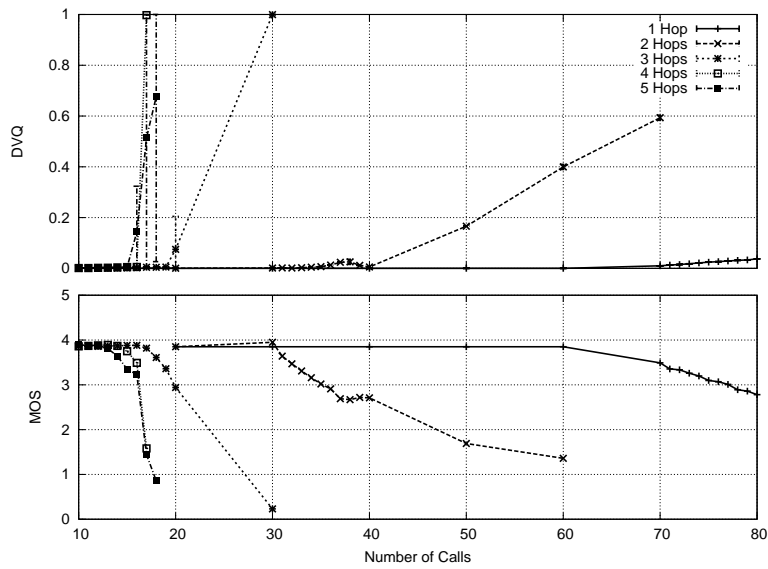


**Figure 3.6:** DVQ and MOS as a function of number of calls per flow in line topologies using the adaptive protocol (300 *ms* delay budget, ROHC).

of 16 *calls*; this is achieved by the G.723 with a 20 *ms* framing interval. In all cases, the adaptive protocol outperforms the non-adaptive protocol, often supporting at least five times the number of calls.

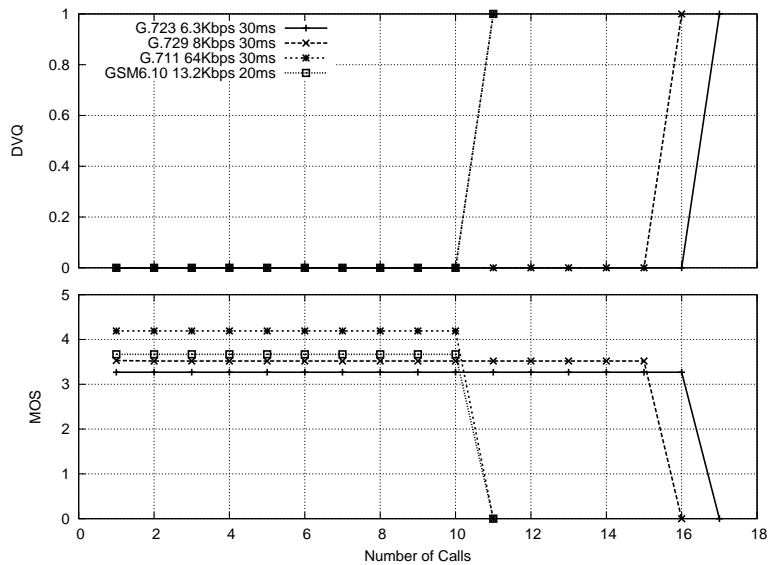


**Figure 3.7:** DVQ and MOS as a function of number of calls per flow in line topologies for the non-adaptive protocol using standard voice codecs (150 *ms* delay budget, no ROHC).

The line variant topologies introduce MAC layer contention between the two callers. Figure 3.8 shows the DVQ and MOS as a function of the number of calls per flow achieved by the adaptive protocol in the line-variant topologies using a  $150\text{ ms}$  delay budget and no ROHC. The results are tabulated in Table 3.5 on a per flow basis. Because each caller establishes a flow, the total number of calls is twice that tabulated. Hence, between the channel contention and the bottleneck node, the number of calls are supported in the line-variant topologies ranges from about 59% to 80% that compared to the corresponding line topologies. The non-adaptive protocol, using the settings yielding the highest performance per codec, supports approximately 20% to 50% of voice capacity of the adaptive protocol.

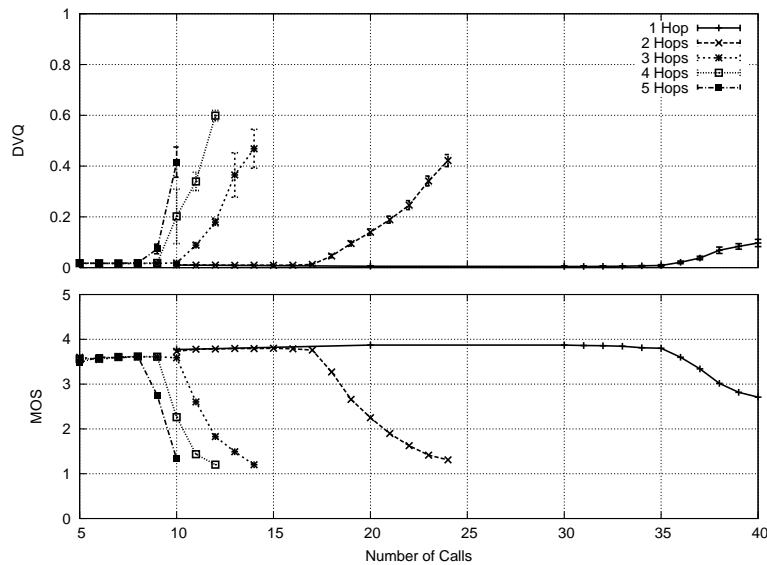


**Figure 3.8:** DVQ and MOS as a function of number of calls per flow in line-variant topologies using the adaptive protocol ( $150\text{ ms}$  delay budget, no ROHC).

### 3.5.1.1 Changes in Compression over Call Lifetime

In order to better understand the behaviour of the adaptive protocol in terms of the speed of adaptation and the quality experienced over the lifetime of a call we show the changes in compression rate of a call for two different scenarios in Figure 3.9. We select scenarios 1 and 2 of Figure 3.5 to focus on the details of a call's behaviour. Scenario 2 is one call out

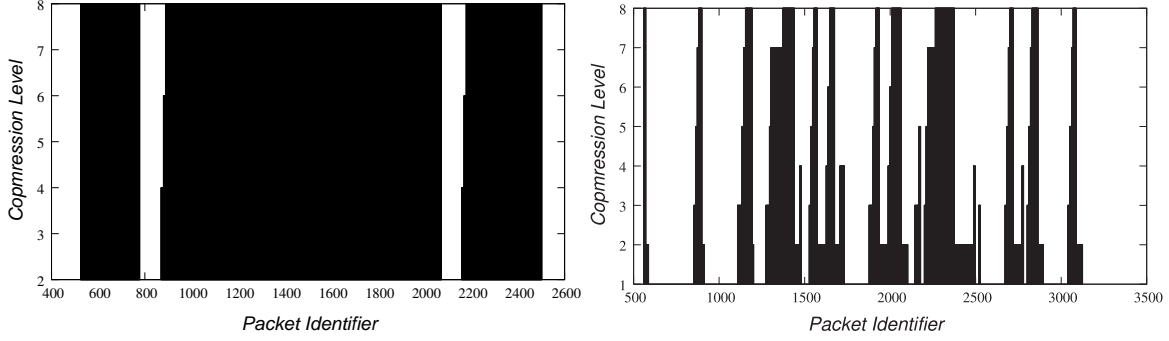
**Table 3.5:** Number of calls supported per flow with at least fair MOS (i.e.,  $MOS \geq 3$ ) by line and line-variant topologies for a 150 ms delay budget and no ROHC. Linear topologies establish one flow, while line-variant topologies establish two flows. The calls are multiplexed over the flows.

<b>Line:</b>		<b>Number of Calls per Flow</b>				
		<b>1-Hop</b>	<b>2-Hops</b>	<b>3-Hops</b>	<b>4-Hops</b>	<b>5-Hops</b>
Adaptive protocol		64	27	14	11	10
Non-adaptive G.711	10 ms	4	2	1	1	1
	20 ms	8	4	2	2	2
	30 ms	10	5	3	2	2
Non-adaptive G.729	10 ms	5	2	1	1	1
	20 ms	10	5	3	3	2
	30 ms	15	8	5	4	4
Non-adaptive G.723	10 ms	5	3	1	1	1
	20 ms	10	5	3	3	2
	20 ms	16	8	5	4	4
Non-adaptive GSM-EFR 6.60	20 ms	10	5	3	2	2
Non-adaptive GSM-FR 6.10	20 ms	10	5	3	2	2
<b>Line-Variant:</b>		<b>1-Hop</b>	<b>2-Hops</b>	<b>3-Hops</b>	<b>4-Hops</b>	<b>5-Hops</b>
Adaptive protocol		19	9	5	4	4
Non-adaptive G.711	30 ms	5	2	1	1	1
Non-adaptive G.729	30 ms	5	4	2	1	1
Non-adaptive G.723	30 ms	7	4	2	2	2
Non-adaptive GSM-FR 6.10	20 ms	5	2	1	1	1

of 69 multiplexed calls over a one-hop path and has a  $MOS = 2.19$ . Scenario 1 is a better situation of one call out of 60 multiplexed calls; this call has a  $MOS = 3.78$ . As Figure 3.9 shows, scenario 2 experiences more frequent fluctuations in compression as it keeps adjusting its rate in response to the changes in network load and channel conditions. Scenario 1 only adjusts its rate a few times. When conditions are stable and fewer calls are multiplexed in a flow, callers experience good listening quality. When trying to support more calls and conditions fluctuate, the protocol keeps looking for the current best achievable quality which may result in poor listening quality.

### 3.5.2 Results for Grid and Irregular-Grid Topologies

We next study the performance of our adaptive protocol for the grid topologies. This topology introduces co-channel interference in the *low-interference traffic pattern*, and



(a) One call from Scenario 1 of Figure 3.5      (b) One call from Scenario 2 of Figure 3.5  
**Figure 3.9:** Changes in compression over the call lifetime.

heavy contention in the *high-interference traffic pattern* because the caller, intermediate, and callee nodes are within the transmission range of their counterparts in the other flow.

Using a  $150\text{ ms}$  delay budget and no header compression, we plot the DVQ and MOS for grid topologies in Figure 3.10 as a function of the number of calls per flow. Unlike the linear topologies, there is some oscillation in the DVQ (and hence MOS) in the grid topologies. Therefore, when we tabulate the results in Table 3.6, we find the number of calls supported by the first MOS value below 3, and then find the number of calls supported for last MOS value above 3. This gives us a range on the number of calls supported. Using this method, our adaptive protocol supports from [0-10] calls per flow in the low-interference traffic pattern and from [0-5] calls per flow in the high-interference traffic pattern with fair listening quality.

We compare the performance of grid topologies and the line-variant topologies with two and three-hop paths as both of these topologies have two competing flows. The number of calls per flow supported in each topology is comparable; see Tables 3.5 and 3.6.

The final static scenarios that we consider are the irregular-grid topologies. Using a delay budget of  $150\text{ ms}$  and no header compression, we present the number of calls supported per flow in a low-interference traffic pattern (two flows), and in a high-interference traffic pattern (four flows) in Figure 3.11. The variance of the results is high because in the

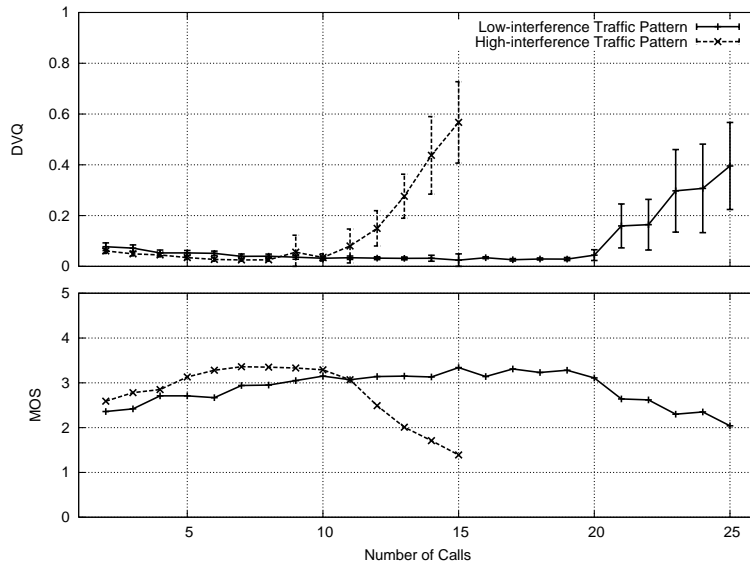


**Figure 3.10:** DVQ and MOS as a function of number of calls per flow in grid topologies using the adaptive protocol (150 ms delay budget, no ROHC).

irregular-grid topologies the caller-callee pairs are selected at random. Table 3.6 shows that from [0-3] calls per flow are supported in the low-interference traffic pattern, but no calls of fair listening quality are supported in the high-interference traffic pattern.

Our adaptive protocol supports roughly twice the number of calls for each interference pattern in grid topologies compared to any of the non-adaptive protocols. The same is true for irregular-grid topologies, but only for the low-interference pattern. For the high interference pattern, the adaptive protocol does not support any calls with  $MOS \geq 3$  while the G.729 and GSM-FR 6.10 occasionally support one call.

### 3.5.3 Results for Mobile Scenarios

Table 3.7 tabulates the number of calls per flow supported by the adaptive protocol for the *event*, *march*, and *pursuit* applications using the *nomadic*, *column*, and *pursuit* mobility models, respectively. In these mobile scenarios, the node separation is very small ( $\leq 10 m$ ) compared to the node separation in the static topologies ( $\geq 150 m$ ). As a result, the signal power is very strong and the flows are able to tolerate more interference and are conse-

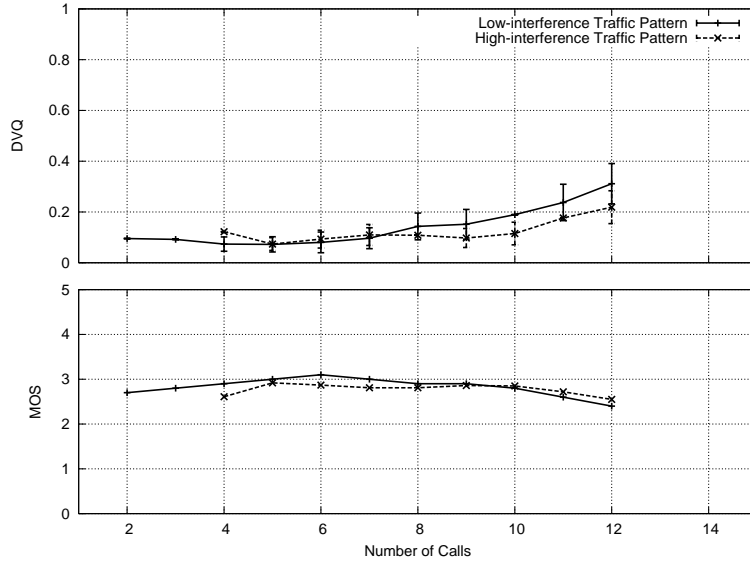


**Figure 3.11:** DVQ and MOS as a function of number of calls per flow in irregular-grid topologies using the adaptive protocol (150 ms delay budget, no ROHC).

**Table 3.6:** Number of calls supported per flow for grid topologies with at least fair MOS (i.e.,  $MOS \geq 3.0$ ) for a 150 ms delay budget and no ROHC. In the grid topology, the low interference (LI) and high interference (HI) traffic patterns each have two flows. In the irregular-grid topology, the LI traffic pattern has two flows while the HI traffic pattern has four flows.

<b>Grid:</b>	<b>Number of Calls per Flow</b>	
	<b>LI Pattern</b>	<b>HI Pattern</b>
Adaptive protocol	[0-10]	[0-5]
Non-adaptive G.711 (30 ms)	[0-3]	[0-2]
Non-adaptive G.729 (30 ms)	[0-4]	[0-3]
Non-adaptive G.723 (30 ms)	[0-4]	[0-3]
Non-adaptive GSM-FR 6.10 (20 ms)	[0-3]	[0-2]
<b>Irregular-Grid:</b>	<b>LI Pattern</b>	<b>HI Pattern</b>
Adaptive protocol	[0-3]	0
Non-adaptive G.711 (30 ms)	[0-1]	0
Non-adaptive G.729 (30 ms)	0	[0-1]
Non-adaptive G.723 (30 ms)	0	0
Non-adaptive GSM-FR 6.10 (20 ms)	[0-1]	[0-1]



quently able to support a higher number of calls per flow in the adaptive protocol. Even though the presence of mobility affects performance, since the nodes are moving as a group and are relatively close to each other, high performance is achieved. The results depend on the traffic pattern (reflected by large error bars in each of the figures). The adaptive protocol supports at least five times more calls when compared to any non-adaptive approach.

**Table 3.7:** Number of calls supported per flow for mobile scenarios with at least fair MOS (i.e.,  $MOS \geq 3.0$ ) for a 150 ms delay budget and no ROHC. The *event*, *march*, and *pursuit* applications use the *nomadic*, *column*, and *pursuit* mobility models, respectively. Two, four, and eight concurrent flows are considered in the event and march applications, while up to three concurrent flows are considered for the pursuit application.

<b>Event Application:</b>	<b>Number of Calls per Flow</b>		
	<b>2-Flows</b>	<b>4-Flows</b>	<b>8-Flows</b>
Adaptive protocol	46	21	9
Non-adaptive G.711 (30 ms)	5	2	1
Non-adaptive G.729 (30 ms)	8	4	2
Non-adaptive G.723 (30 ms)	8	4	2
Non-adaptive GSM-FR 6.10 (20 ms)	5	2	1
<b>March Application:</b>	<b>2-Flows</b>	<b>4-Flows</b>	<b>8-Flows</b>
Adaptive protocol	46	21	8
Non-adaptive G.711 (30 ms)	5	2	1
Non-adaptive G.729 (30 ms)	8	4	2
Non-adaptive G.723 (30 ms)	8	4	2
Non-adaptive GSM-FR 6.10 (20 ms)	5	2	1
<b>Pursuit Application:</b>	<b>1-Flow</b>	<b>2-Flows</b>	<b>3-Flows</b>
Adaptive protocol	96	46	29
Non-adaptive G.711 (30 ms)	10	5	3
Non-adaptive G.729 (30 ms)	15	8	5
Non-adaptive G.723 (30 ms)	16	8	5
Non-adaptive GSM-FR 6.10 (20 ms)	10	5	3

### 3.6 Performance Bounds

To gain an understanding of how the performance of our protocol compares to an upper bound, we quantify the theoretical maximum number of concurrent calls that can be supported on a single-hop IEEE 802.11b access point (AP) for the compression rates and

packet sizes we have used in our simulations. We assume that the traffic is saturated and that no time is wasted in contention.

The transmission of a voice packet over an IEEE 802.11b network triggers the following steps. RTP, UDP, and IP headers totalling 40 *bytes* are added to the voice packet. As well, a 6 *byte* LLC *sub-network access protocol* (SNAP) header is included to reflect the transported network-layer protocol [34]. A 24 *byte* MAC header is required, together with a 4 *byte* *Frame Check Sequence* (FCS) calculated over the entire frame. The channel is sensed to see if it is clear for a *distributed inter-frame space* (DIFS) duration. If so, a *physical layer convergence protocol* (PLCP) preamble is added. The short frame format requires 72 *bits* of the PLCP preamble to be transmitted at a required rate of 1 *Mbps* and 48 *bits* of the PLCP header to be transmitted at a required rate of 2 *Mbps*. The frame is then transmitted by the caller at the IEEE 802.11 data rate in use (one of 2, 5.5, or 11 *Mbps*). After waiting a *short inter-frame space* (SIFS) duration, the callee creates a 14 *byte* *acknowledgment* (ACK) frame, and adds a PLCP preamble and header to be transmitted at the required rates of 1 and 2 *Mbps*, respectively. The callee transmits an ACK at the IEEE 802.11b data rate.

Since IEEE 802.11b supports three transmission rates, the time needed to transmit a packet depends on the rate used. However, regardless of the data rate in use by the adaptive protocol, some fields are transmitted at a fixed rate as specified by the standard [49]. The default parameter values for IEEE 80211b DCF are shown in Table 3.8.

The *packet transmission time* (PTT), in  $\mu s$ , of a voice packet is calculated as:

$$\begin{aligned} \text{PTT} &= \text{DIFS} + \text{SIFS} + 2 \times (\text{PLCP Preamble} + \text{PLCP Header}) \\ &+ \frac{(\text{RTP/UDP/IP/LLC/MAC Headers} + \text{Payload} + \text{ACK}) \times 8}{\text{data rate}} \end{aligned}$$

The number of *packets per a voice call* (PPVC) per second is equal to:

$$\text{PPVC} = \left\lceil \frac{\text{Compression Rate (bps)}}{\text{Payload} \times 8} \right\rceil \times 2.$$

The multiplication by two is to account for the bidirectional nature of a call. Given the equations for PTT and PPVC, the maximum number of concurrent calls that are supported is given by:

$$\text{Maximum Number of Calls} = \left\lfloor \frac{10^6}{\text{PTT} \times \text{PPVC}} \right\rfloor.$$

**Table 3.8:** Default parameter values per frame sent by IEEE 802.11b DCF.

Parameter	Value
Distributed Inter-Frame Space (DIFS)	50 $\mu s$
Short Inter-Frame Space (SIFS)	10 $\mu s$
RTP/UDP/IP headers	40 <i>bytes</i>
LLC/MAC headers	34 <i>bytes</i>
Payload	codec dependent
Long PLCP(preamble and header), 192 bits	192 $\mu s$
Frame Check Sequence (FCS)	4 <i>bytes</i>
Aknowlegement (ACK) at 2 <i>Mbps</i>	14 <i>bytes</i>
SlotTime	20 $\mu s$
$CW_{min}, CW_{max}$	32 <i>slots</i> , 1024 <i>slots</i>

Figure 3.12 uses these equations to plot the maximum number of calls supported as a function of the compression rate for data rates of 2 *Mbps* and 11 *Mbps* with the minimum and maximum payload, respectively. Since the analysis is done for a single-hop IEEE 802.11b access point, it bounds the results for the single-hop line topology most closely. The adaptive protocol supports 64 *calls* in this case, which lies between the two bounds. The analysis does not take into account that the adaptive protocol varies the modulation, compression, and packet size, over the call lifetime and is therefore a only a loose bound on performance.

### 3.7 Conclusions

Adaptation and cross-layer design are two approaches to address the challenges of supporting voice over ad hoc networks. We identified the factors of compression, modulation, and packet size to adapt based on the QoS requirements of voice. Our resulting oppor-

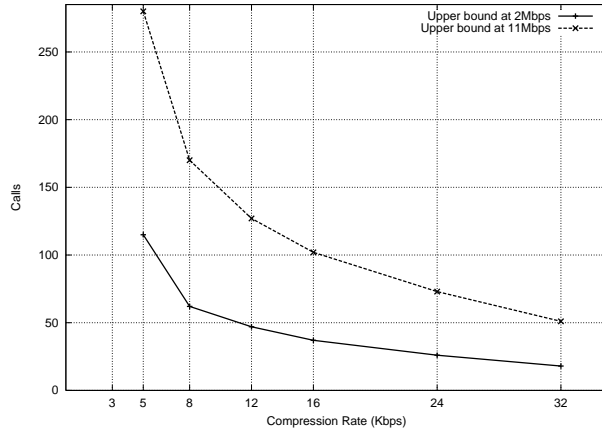


**Figure 3.12:** Bounds on the number of calls supported as a function of compression rate.

tunistic protocol combines adaptation on two time scales: hop-by-hop and end-to-end. The performance of our protocol was evaluated through simulations in static and mobile scenarios, carrying real-time audio traffic using both quantitative (DVQ) and qualitative (MOS) audio metrics.

Our work may be extended in several ways. The protocol may be combined with a multi-path diversity approach where multiple paths are used between a caller-callee pair. Different paths may carry voice packetized, compressed, and modulated differently to optimize network performance and call quality. In general, QoS-aware routing, which takes interference of the flows into account, rather than following the shortest hop-count path may be useful.

The use of *forward error correction* (FEC) is another avenue of work. Even though the use of FEC introduces extra overhead, it can curb the rate of lost and late packets. A node can decide whether to use no compression and experience a high loss rate or consider aggressive compression while applying FEC.

The impact of traffic heterogeneity, where voice, data, and video are supported concurrently, is another important study. Unlike real-time applications which are particular about delay but more resilient to losses, data applications are bandwidth-greedy, delay-elastic, and

intolerant to loss. Employing special measures, such as the use of priority queueing, may be needed to ensure appropriate support for voice applications.

Finally, experiments using human subjects to obtain MOS results in battlefield or emergency situations would be useful for future work on supporting voice in these types of scenarios.

## Chapter 4

# LOCATING ARRAYS: A NEW EXPERIMENTAL DESIGN FOR SCREENING COMPLEX ENGINEERED SYSTEMS

### 4.1 Introduction

Computer and networked systems are examples of *complex engineered systems* (CESs). In [92], the complexity of an engineered system is not just due to its size, but also arises from its structure, operation (including control and management), evolution over time, and that people are involved in its design and operation .

Experimentation is often used to study the performance of CESs. At its most basic, a system may be viewed as transforming some input variables, or *factors*, into one or more observable output variables, or *responses*. Some factors of a system are *controllable*, whereas others are not.

Objectives of experimentation include:

**Screening:** Which factors and interactions are most influential on a response?

**Confirmation:** Is the system currently performing in the same way as it did in the past?

**Discovery:** What happens when new operating conditions, materials, factors, *etc.*, are explored?

**Robustness:** Under what conditions does a response degrade?

**Stability:** How can variability in a response be reduced?

Our focus is on screening using techniques from statistical *design of experiments* (DoE). DoE refers to the process of planning an experiment so that appropriate data are collected and analyzed by statistical methods, in order to result in valid and objective conclusions. Hence any experimental problem includes both the design of the experiment and the statistical analysis of the data.

Suppose that there are  $k$  factors,  $F_1, \dots, F_k$ , and that each factor  $F_j$  has a set  $L_j = \{v_{j,1}, \dots, v_{j,\ell_j}\}$ , of  $\ell_j$  possible *levels* (or values). A *design point* is an assignment of a level from  $L_j$  to  $F_j$ , for each factor  $j = 1, \dots, k$ . An *experimental design* is a collection of design points. When a design has  $N$  design points, it can be represented by an  $N \times k$  array  $A = (a_{i,j})$  in which each row  $i$  corresponds to a design point and each column  $j$  to a factor; the entry  $a_{i,j}$  gives the level assigned to factor  $j$  in the  $i$ th design point. When run, a design point results in one or more observable responses.

A *t-way interaction* (or interaction of *strength t*) in  $A$  is a choice of  $t$  columns  $i_1, \dots, i_t$ , and the selection of a level  $\nu_{i_j} \in L_{i_j}$  for  $1 \leq j \leq t$ , represented as  $T = \{(i_j, \nu_{i_j}) : 1 \leq j \leq t\}$ . Every design point in  $A$  *covers*  $\binom{k}{t}$  interactions of strength  $t$ .

When the objective of experimentation is screening, it is often recommended to keep the number of factors low. It has been considered impractical to experiment with “many” factors; about ten factors is a suggested maximum [64, 84]. Generally, two levels for each factor is considered to work well in screening experiments.

Methods for screening seek to reduce the number of design points required because the exhaustive *full-factorial design* [84, 91] is too large. For  $k$  factors each with two levels it has  $2^k$  design points. An *analysis of variance* (ANOVA) allows the significant factors and interactions on the response to be identified.

A *fractional factorial design*  $2_R^{k-p}$  is a  $\frac{1}{2^p}$  fraction of a full factorial design with  $k$  two-level factors. The design is described by  $p$  *generators*, expressions of factors that are confounded; the generators determine the alias structure. A design is of *resolution R* if no  $m$ -factor effect is aliased with another effect containing fewer than  $R - m$  factors.

A *D-optimal* design is a popular experimental design among those using optimality criteria. A model to fit, and a bound  $N$  on the number of design points, must be specified *a priori*; this restricts the factors to be analyzed to those in the model. The size of a D-optimal design is bounded by the size of a full-factorial design.

Some designs aggregate the factors into groups, e.g., sequential bifurcation, a sequential method to improve design efficiency [65]. Grouping requires care to ensure that factor effects do not cancel. This presents a “chicken and egg” problem: we need to know how to group in order to group. Often, a domain expert is expected to make such grouping decisions. While such experts may have considerable knowledge, it is doubtful whether an expert knows the importance of a specific factor or interaction in a CES.

An *interaction graph* depicts how a change in the level of one factor affects the other factor with respect to a response. Figure 4.1 shows an interaction graph for the factors of routing and *medium access control* (MAC) protocol on average delay in a network. The choice of MAC protocol (EDCF or IEEE 802.11) has little impact on the average delay in the AODV routing protocol, while for the DSR routing protocol the impact is very large; see [132]. If MAC protocols were aggregated, this significant interaction would be lost.

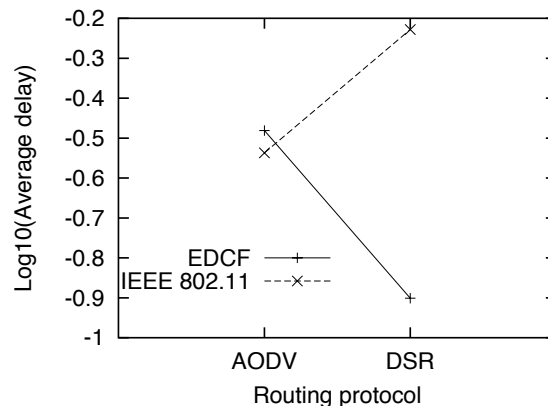


**Figure 4.1:** Interaction of routing and MAC protocols on delay [132].

A fractional factorial design is *saturated* when it investigates  $k = N - 1$  factors in  $N$  design points [84]. It has only  $k$  degrees of freedom to represent the terms of the model. In a *supersaturated design*, the number of factors  $k > N - 1$ ; such designs contain more factors than design points. These designs are only able to estimate a main effects model [73, 84]. Thus they cannot consider possible interactions at all.



Even with substantial and detailed domain knowledge, it is imperative not to eliminate or aggregate factors *a priori*. Our goal, therefore, is an automatic and objective approach to screening. To address this problem we have formulated the definition of a *locating array* (LA) [18]. Locating arrays exhibit logarithmic growth in the number of factors because their focus is on identification rather than on measurement. This makes practical the consideration of an order of magnitude more factors in experimentation, removing the need for the elimination of factors. As a result, LAs have the potential to transform experimentation in huge factor spaces such as those found in CESs.

The rest of this chapter is organized as follows. §4.2 defines a locating array, and gives an example of how a design is used for location. §4.3 presents preliminary results applying an LA for screening the response of TCP throughput in a simulation model of a mobile wireless network. The full-factorial design for this system is infeasible — it has over  $10^{43}$  design points! Yet there is an LA with only 421 design points. We develop an algorithm using the LA to identify the significant factors and interactions from the data collected, providing a small example. In §4.4 we validate the significance of the identified factors and interactions independently using the statistical software JMP. Finally, in §4.5 we summarize, discuss potential threats to our approach, directions for this research, and conclude.

## 4.2 Locating Arrays

Reducing the number of design points required relies on a *sparsity of effects* assumption, that interactions of interest involve at most a small, known number  $t$  of interacting factors. As one means of reduction, we define *locating arrays* (LAs) [18]. For a set of factors each taking on a number of levels, an LA permits the identification of a small number of significant interactions among small sets of (factor, level) combinations.

LAs differ from standard designed experiments, which are used to *measure* interactions and to develop a model for the response as a function of these [84]. “Search designs” [36,

117, 124] also attempt to locate interactions of higher strength, but their focus remains on measurement and hence on balanced designs. Rao [44] shows that the number of design points in a balanced design must be at least as large as the number of interactions considered. Thus if  $t$ -way interactions among  $k$  factors each having  $v$  levels are to be examined, balanced designs only reduce the  $v^k$  exhaustive design points to  $O(k^t)$ . The selection of few factors from hundreds of candidates by this reduction is not viable. By lessening the requirement from measurement to identification, LAs are not subject to the Rao bound.

Fortunately LAs behave more like *covering arrays*, experimental designs in which every  $t$ -way interaction among factors appears in at least one design point. Unlike designed experiments, the number of design points in a covering array for  $k$  factors grows as a *logarithmic* function of  $k$  (see [105], for example). In [18], a construction of LAs using covering arrays of higher strength is given, and hence LAs also exhibit this logarithmic growth, making them asymptotically much more efficient than balanced designs. This motivates the consideration of covering arrays, which have been the subject of extensive study [15, 16, 42, 90]. They are used in testing software [20, 24, 67, 68], hardware [114, 127], composite materials [13], biological networks [110, 115], and others. Their use to facilitate location of interactions is examined in [80, 139], and measurement in [46, 47]. Covering arrays form the basis for combinatorial methods to learn an unknown classification function using few evaluations — these arise in computational learning and classification, and hinge on locating the relevant attributes (factors) [21]. Algorithms for generating covering arrays range from greedy (e.g., [9, 31]) through heuristic search (e.g., [94, 130]). However, combinatorial constructions (see [16]) provide the only available deterministic means of producing covering arrays with more than a few hundred factors.

A design point, when run, yields one or more responses. For ease of exposition, we classify the responses in two groups, those that exceed a specified threshold and those that do not. So we suppose that the outcome of a run of a design point is a single binary response

(“pass” or “fail”). A *fault* is caused by one or more  $t$ -way interactions, and is evidenced by a run failing.

Given an experimental design and the set of interactions that cause faults, the outcomes can be easily calculated: A run fails exactly when it contains one or more of the faulty interactions, and does not fail otherwise. In order to observe a fault, the interaction must be covered by at least one design point. With no restriction on the interactions that can cause faults, every interaction must be covered. Then the best one can do is to form all  $\prod_{j=1}^k \ell_j$  possible design points, the exhaustive design. Using sparsity of effects, an upper bound  $t$  is placed on the strength of interactions that may be faulty. Then we require that every  $t$ -way interaction be covered; in other words, the design is a covering array of strength  $t$ .

Let  $A = (a_{i,j})$  be an experimental design, an  $N \times k$  array where in each row  $i$ , levels in the  $j$ th column are chosen from a set  $L_j$  of size  $\ell_j$ . For array  $A$  and  $t$ -way interaction  $T = \{(i_j, \nu_{i_j}) : 1 \leq j \leq t\}$ , define  $\rho(A, T) = \{r : a_{r,i_j} = \nu_{i_j}, 1 \leq j \leq t\}$  as the set of rows of  $A$  in which  $T$  is covered. For a set  $\mathcal{T}$  of interactions,  $\rho(A, \mathcal{T}) = \cup_{T \in \mathcal{T}} \rho(A, T)$ . Locating faults requires that  $\mathcal{T}$  be recovered from  $\rho(A, \mathcal{T})$ , whenever  $\mathcal{T}$  is a possible set of faults.

Let  $\mathcal{I}_t$  be the set of all  $t$ -way interactions for an array, and let  $\overline{\mathcal{I}}_t$  be the set of all interactions of strength *at most*  $t$ . Consider an interaction  $T \in \overline{\mathcal{I}}_t$  of strength less than  $t$ . Any interaction  $T'$  of strength  $t$  that contains  $T$  necessarily has  $\rho(A, T') \subseteq \rho(A, T)$ . In this case, when  $T$  is faulty we are unable to determine whether or not  $T'$  is also faulty. Call a subset  $\mathcal{T}'$  of interactions in  $\mathcal{I}_t$  *independent* if there do not exist  $T, T' \in \mathcal{T}'$  with  $T \subseteq T'$ . In general, some interactions in  $\mathcal{I}_t$  (or perhaps  $\overline{\mathcal{I}}_t$ ) are believed to be faulty, but their number and identity are unknown. The faulty interactions cannot be identified precisely from the outcomes, *even if the full factorial design is employed*, without some restriction on their number. (Consider the situation in which every design point run fails.) We therefore suppose that a maximum number  $d$  of faulty interactions is specified.

**Definition 4.2.1 ([18])** An array  $A$  is  $(\bar{d}, \bar{t})$ -locating if whenever  $\mathcal{T}_1, \mathcal{T}_2 \subseteq \overline{\mathcal{T}_t}$  and  $\mathcal{T}_1 \cup \mathcal{T}_2$  is independent,  $|\mathcal{T}_1| \leq d$ , and  $|\mathcal{T}_2| \leq d$ , it holds that  $\rho(A, \mathcal{T}_1) = \rho(A, \mathcal{T}_2) \Leftrightarrow \mathcal{T}_1 = \mathcal{T}_2$ .

If there is any set of  $d$  interactions of strength  $t$  that produce exactly the outcomes obtained when using a  $(d, t)$ -locating array  $A$  to conduct experiments, then there is exactly one such set of interactions. To avoid enumeration of all sets of  $d$  interactions of strength  $t$ , one can employ a stronger condition that for every interaction  $T$  of strength at most  $T$  and every set  $\mathcal{T}_1 \subseteq \overline{\mathcal{T}_t}$  that does not contain  $T$  and for which  $\mathcal{T}_1 \cup \{T\}$  is independent, it holds that  $\rho(A, T) = \rho(A, \mathcal{T}_1) \Leftrightarrow T \in \mathcal{T}_1$ . A locating array meeting this stronger condition is termed a *detecting array* in [18]. When using a detecting array, if there are at most  $d$  independent faulty interactions each of strength at most  $t$ , they are characterized precisely as the interactions that appear in no run that passes. We typically employ the term locating array to refer to both, but for reasons of computational efficiency the locating arrays that we use are, in fact, detecting arrays.

In practice, one does not know *a priori* how many interactions are faulty, or their strengths. Nevertheless, when responses are continuous, we can select a threshold on the responses so as to limit the number of design points yielding a “fail” outcome to locate those that make the most substantial contribution to the response. We exploit this fact later in §4.3.2.

#### 4.2.1 A Small Example

An example is provided to demonstrate fault location, and show the limitations of covering arrays for this purpose. Suppose that we use the experimental design for five binary factors in Table 4.1. It is a *covering array* in which each of the  $2^2 \binom{5}{2} = 40$  two-way interactions is covered. A response for each design point run is listed in the adjacent column.

First, let us locate faults due to main effects (*i.e.*, the individual factors or one-way interactions). The second design point run passes, so all (factor, level) pairs in it are known not to be faulty. Therefore in Table 4.2(a), that considers only the second design point, when

**Table 4.1:** Experimental design and response for each run.

Design Points	Factors					Response
	1	2	3	4	5	
1	0	1	1	1	1	Fail
2	1	0	1	0	0	Pass
3	0	1	0	0	0	Fail
4	1	0	0	1	1	Pass
5	0	0	0	0	1	Pass
6	1	1	0	1	0	Pass

factor 1 is set to one, the run is not faulty. Similarly, for factors 2, 3, 4, and 5 set to zero, one, zero, and zero, respectively. This is indicated by a check-mark ( $\checkmark$ ) in the table. Repeating to check coverage of each one-way interaction for each successful run, no single (factor, level) error accounts for the faults; see Table 4.2(b).

**Table 4.2:** Locating faults due to main effects.

(a) Run 2			(b) All Runs		
Factors	0	1	Factors	0	1
1		$\checkmark$	1	$\checkmark$	$\checkmark$
2	$\checkmark$		2	$\checkmark$	$\checkmark$
3		$\checkmark$	3	$\checkmark$	$\checkmark$
4	$\checkmark$		4	$\checkmark$	$\checkmark$
5	$\checkmark$		5	$\checkmark$	$\checkmark$

Computing  $\rho(T)$  for every one-way interaction, we obtain the sets in Table 4.3. Because no two sets are equal, the array is  $(\bar{1}, \bar{1})$ -locating and when there is a single faulty one-way interaction it can be located. However, because  $\{1, 3, 5\} \cup \{2, 3, 5\} = \{1, 3, 5\} \cup \{1, 2\}$ , when rows 1, 3, and 5 fail and 2, 4, and 6 pass, we cannot determine the two faulty interactions — the array is *not*  $(\bar{2}, \bar{1})$ -locating.

**Table 4.3:**  $\rho(T)$  for one-way interactions  $T = \{(c, \nu)\}$ .

$\nu \downarrow c \rightarrow$	1	2	3	4	5
0	{1,3,5}	{2,4,5}	{3,4,5,6}	{2,3,5}	{2,3,6}
1	{2,4,6}	{1,3,6}	{1,2}	{1,4,6}	{1,4,6}

Now, let us try to locate faults due to two-way interactions. Because the second design point run passes, all two-way interactions in it are known not to be faulty; Table 4.4(a) records the results. Repeating to check for coverage of each two-way interaction for each

**Table 4.4:** Locating faults due to two-way interactions.

(a) Run 2					(b) All Runs				
Factors	00	01	10	11	Factors	00	01	10	11
1, 2			✓		1, 2	✓		✓	✓
1, 3				✓	1, 3	✓		✓	✓
1, 4			✓		1, 4	✓		✓	✓
1, 5			✓		1, 5		✓	✓	✓
2, 3		✓			2, 3	✓	✓	✓	
2, 4	✓				2, 4	✓	✓		✓
2, 5	✓				2, 5	✓	✓	✓	
3, 4			✓		3, 4	✓	✓	✓	
3, 5			✓		3, 5	✓	✓	✓	
4, 5	✓				4, 5	✓	✓	✓	✓

successful run, those interactions not found to pass in this way in Table 4.4(b) form a set of *candidate faults*. In this example, there are nine interactions in the set of candidate faults. Now for the two-way interaction  $\{(1, 0), (2, 1)\}$ ,  $\rho(\{(1, 0), (2, 1)\}) = \{1, 3\}$ , and it is the only two-way interaction for which this holds; and, no one-way interaction  $T$  has  $\rho(T) = \{1, 3\}$ . Hence if there is a single fault, it must be  $\{(1, 0), (2, 1)\}$ , and we have located the fault.

Our success for one response is not sufficient, however. Because  $\rho(\{(1, 0), (2, 1)\}) = \{1\} = \rho(\{(2, 1), (3, 1)\})$ , if only run 1 fails, there are at least two equally plausible explanations using only a single two-way interaction. Indeed  $A$  is *not*  $(\bar{1}, \bar{2})$ -locating. Thus the ability to locate is more than simply coverage!

### 4.3 Screening an Engineered System

We now apply locating arrays for screening in a complex engineered system. One example of a CES for which it has been particularly difficult to develop models is a *mobile ad hoc network* (MANET). A MANET is a collection of mobile wireless nodes that self-organize without the use of any fixed infrastructure or centralized control. We seek to use a locating array to screen for the influential factors and interactions on average *transport control protocol* (TCP) throughput in a simulation model of a MANET.

### 4.3.1 Designing the Experiment

We use the `ns-2` simulator [93], version 2.34, for our experimentation. Since our response of interest is average TCP throughput, we select the *file transfer protocol* (FTP) as our application because it uses TCP for reliability. We select the *internet protocol* (IP), the *Ad hoc On-demand Distance Vector* routing protocol (AODV) [104], and IEEE 802.11b *direct sequence spread spectrum* (DSSS) as protocols at the network, data link, and physical layers of the protocol stack. We also use the mobility, energy, error, and propagation models in `ns-2`. From these protocols and models we identify 75 *controllable* factors. The region of interest for each factor, *i.e.*, the range over which the factor is varied, ranges from two to ten levels, with some set according to recommendations in [86]. See Appendix A for a pointer to details of the factors and their levels.

The full-factorial design for this factor space is infeasible; it has over  $10^{43}$  design points! In contrast, the locating array *constructed and checked manually* has only 421 design points. Except for small locating arrays [128], no general construction methods have been published. We adopted a heuristic approach to construct the LA.

Initially we selected a covering array with 75 factors and 10 levels per factor, constructed using a standard product construction [17]. We applied a post-optimization method [89] to reduce the number of levels for each factor to the desired number, eliminating rows in the process and forming an array  $C$  with 143 design points. The resulting array provides coverage of two-way interactions but does not support location. When  $T$  and  $T'$  are interactions, to distinguish them we require that  $\rho(T) \neq \rho(T')$ , but we ask for more, namely that  $|\rho(T) \setminus \rho(T')| \geq 2$  and  $|\rho(T') \setminus \rho(T)| \geq 2$ ; this ensures that for every two interactions of interest, there are at least two design points containing one but not the other. To accomplish this, we formed three copies of  $C$ , randomly permuted their symbols within each column, and formed their union (so that every two-way interaction is covered at least three times).

The resulting array  $B$  with 429 rows turned out to be  $(\bar{1}, \bar{2})$ -detecting. Three rows were selected by a greedy method to ensure the stronger condition that  $|\rho(T) \setminus \rho(T')| \geq 2$  for every pair  $T, T'$  of interactions; then eleven rows were deleted by a greedy algorithm to remove redundant rows, ultimately producing a design with 421 rows. Appendix A gives a pointer to the locating array used as the experimental design. Our objective was not to find the smallest possible array, because a fair evaluation of the efficacy of locating arrays should not rely on substantial additional structure being present.

Ten replicates of each design point in the LA are run in `ns-2`; for each a response of TCP throughput is measured. These are averaged for each design point resulting in a vector with 421 entries of observed average TCP throughput  $obsTh$ .

#### 4.3.2 Screening Algorithm

We describe an algorithm for screening at a high level to facilitate understanding. In each iteration of the algorithm the most significant main effect or two-way interaction is identified. These terms are accumulated in a *screening model* of average TCP throughput. However, this screening model is *not* intended as a predictive model; the quality of its current estimate allows the algorithm to select the next most significant term. The screening model is used only to identify influential main effects and two-way interactions. With its output, a predictive model can be built; see §4.4.

Initially, the screening model has no terms. With no other information, it should estimate the average TCP throughput to be the average of the vector of observed average throughput. This is unlikely to be a very good estimation!

Our strategy to identify the most significant factor or interaction as the term to add to the screening model is as follows. Suppose that factor  $F_j$ ,  $1 \leq k \leq 75$ , has  $\ell_j$  levels  $L_j = \{v_{j,1}, \dots, v_{j,\ell_j}\}$ . For each level  $\ell$ ,  $1 \leq \ell \leq \ell_j$ , of factor  $F_j$  iterate through each of the 421 design points of the locating array  $A$ . For each design point  $i$ ,  $1 \leq i \leq 421$ , partition



the contribution of the (factor  $F_j$ , level  $v_{j,\ell}$ ) combination into one of two sets:  $S$  or  $\bar{S}$ . If the design point has the factor  $F_j$  set to level  $\ell$ , *i.e.*,  $a_{i,j} = v_{j,\ell}$ , then add the throughput measured for design point  $i$ ,  $obsTh[i]$ , to  $S$ ; otherwise add  $obsTh[i]$  to  $\bar{S}$ . Then, compute the (absolute) difference of the average of sets  $S$  and  $\bar{S}$ . (Of course, metrics other than the difference of averages could be used.) Either the difference is zero (*i.e.*, the average TCP throughput collected in the sets  $S$  and  $\bar{S}$  is the same), or it is non-zero. If the difference is non-zero, then one possible explanation is that the (factor  $F_j$ , level  $v_{j,\ell}$ ) combination is responsible for the difference.

Our hypothesis is that the (factor  $F_j$ , level  $v_{j,\ell}$ ) combination over all combinations for which the difference between the sets is the greatest is the most significant one. If this is correct, then a term of the form  $c \cdot (F_j, v_{j,\ell})$  is added to the screening model. The coefficient  $c$  is equal to the difference in average TCP throughput of each set. When this term is added to the screening model, it makes the same estimation for average TCP throughput for sets  $S$  and  $\bar{S}$ .

In the first iteration of this algorithm, the estimate (*i.e.*, the average of the vector of observed average TCP throughput) is used to determine deviations from each entry in the vector  $obsTh$ . We now have a screening model that apparently includes the most significant factor. It is now used to produce a new estimate of average TCP throughput and update the vector of residual throughput. The algorithm can be applied repeatedly to the residuals to identify the next most important factor or interaction.

While this algorithm is described for (factor, level) combinations, we actually iterate over all one-way (*i.e.*, all (factor, level) combinations) *and* all two-way interactions (*i.e.*, all pairs of (factor, level) combinations) to identify the main effect or two-way interaction of highest significance. Any number of stopping conditions may be used to decide when to terminate the model development. We use the  $R^2$ , the coefficient of determination, indicating how well data fits a line or curve; when it shows marginal improvement, we stop.

The locating array constructed for our CES is a  $(\bar{d} = 1, \bar{t} = 2)$ -locating array, meaning it only guarantees to be able to locate (identify) at most one  $(\bar{d} = 1)$  main effect or two-way (i.e., up to  $\bar{t} = 2$ -way) interaction. It is interesting that the LA may be used iteratively to identify subsequent significant main effects or interactions. In this sense, the algorithm uses a “heavy-hitters” approach as in compressive sensing [19].

### 4.3.3 Example of the Screening Algorithm

A small example is provided to step through one iteration of the screening algorithm. Suppose that we use the experimental design for four binary factors in Table 4.5. It is a covering array of strength three and therefore also a  $(2, 1)$ -detecting array. Factor 1 corresponds to the distribution function used for introducing errors (uniformly or exponentially distributed), factor 2 to the error rate ( $10^{-7}$  or  $10^{-5}$ ), factor 3 to the number of flows at the application layer (1 or 18), and factor 4 to the TCP packet size (64 or 2048); the levels are taken as “binary” for this example. All remaining factors are set to their default levels for experimentation. A response of observed TCP throughput for each design point, averaged over ten replicates, is listed in the column *obsTh*. (All measures are truncated to integers for simplicity.)

**Table 4.5:** Experimental design and average TCP throughput.

	Factors				<i>obsTh</i>	<i>resTh</i>
	1	2	3	4		
1	0	0	0	0	63339	-14699
2	0	0	1	1	29860	-48178
3	0	1	0	1	80801	2764
4	0	1	1	0	3804	-74234
5	1	0	0	1	373866	295828
6	1	0	1	0	3879	-74159
7	1	1	0	0	56656	-21382
8	1	1	1	1	12095	-65943

The overall mean of the *obsTh* is 78038. Therefore, the screening model initially estimates this value for average TCP throughput, i.e.,  $T = 78038$ . The residuals (*resTh*) are

computed in Table 4.5 by taking the difference of the observed average throughput for each design point with this initial fitted value.

Now, we iterate over each (factor,level) combination. Factor 1 is set to its low level in design points 1–4. Therefore  $S = \frac{1}{4} \sum_1^4 resTh[i] = \frac{-134347}{4} = -33586$  and  $\bar{S} = \frac{1}{4} \sum_5^8 resTh[i] = \frac{134344}{4} = 33586$ . The absolute difference,  $|S - \bar{S}| = |-33586 - 33586| = 67172$ .

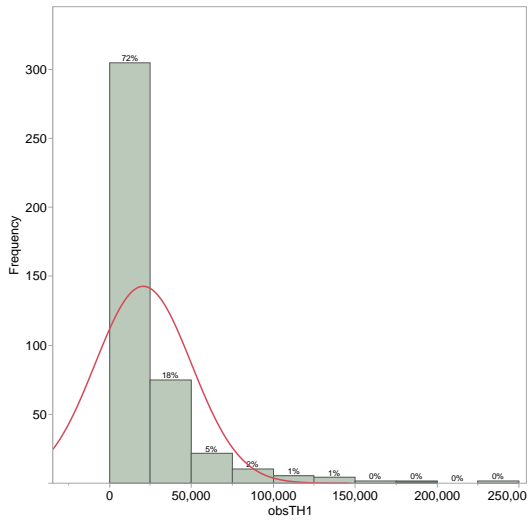
Repeating for each (factor, level) combination, as well as all two-way interactions, we find that it is a main effect that has highest absolute difference with a value of 131255. It occurs when factor 3 is set to its lowest level, namely when the number of flows at the application layer is only one. Hence we attribute this as the explanation for the largest difference and add the term  $c \cdot (F_3, v_{3,0})$  to the model. The method of *ordinary least squares* (OLS) is used to fit the intercept and coefficient  $c$  of the new term. This results in an updated model of  $T = 12410 + 131255 \cdot (F_3, v_{3,0})$ . Its coefficient of determination is  $R^2 = 0.33$ .

Using this updated model, the residuals can be recomputed as input to the next iteration of the algorithm.

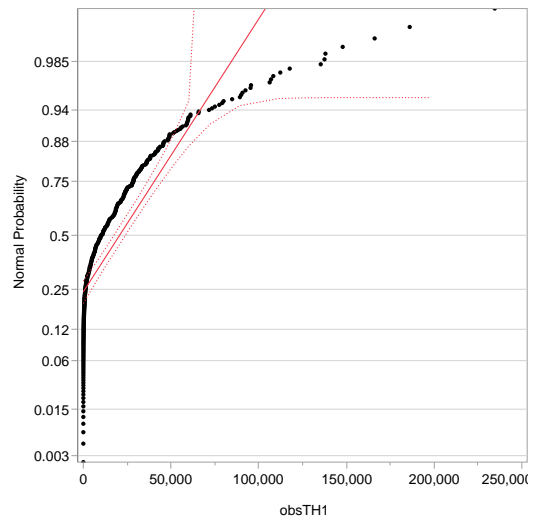
Next, we describe some of the obstacles arising in the practical application of the screening algorithm.

#### 4.3.4 Applying the Screening Algorithm

In applying the screening algorithm to our CES, several obstacles arose. The first is that the measured average TCP throughput is not normally distributed, as Figure 4.2 shows; this is not uncommon in systems experimentation [98]. The best transformation of the data is a natural logarithm (Figure 4.3a). From the normal probability plot (Figure 4.3b), we find that the transformed data are still not normally distributed; nevertheless, we work with this transformation of the data.

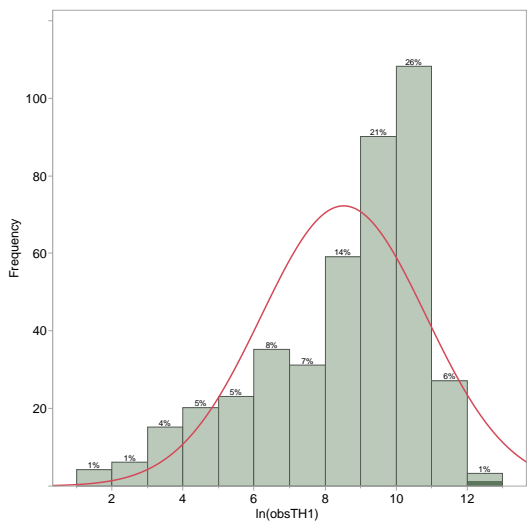


(a) Throughput distribution.

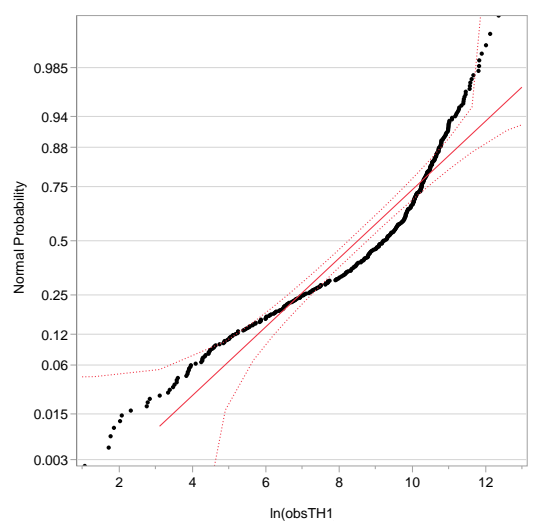


(b) Normal probability plot.

**Figure 4.2:** Distribution of the original observed average throughput, and corresponding normal probability plot.



(a) ln transformation.



(b) Normal probability plot.

**Figure 4.3:** Natural logarithm transformation of the original observed throughput, and corresponding normal probability plot.

A much larger problem arises from the fact that the LA does not cover each main effect and two-way interaction the same number of times. Indeed, binary factors are covered much more frequently (some as many as two hundred times in the 421 row LA) compared to two-way interactions of factors with ten levels (only a handful of times). This is unavoidable when one-way and two-way interactions are compared, and when factors have a different numbers of levels.

Consider the behaviour of the screening algorithm. For a binary factor the sets  $S$  and  $\bar{S}$  have the same or nearly the same size and, as a result, the average of each set has small variance. In the example in §4.3.3, each (factor, level) combination is covered four times (each column of the array has four zeros and four ones). However in general, as the number of levels for a factor increases, the size of the sets  $S$  and  $\bar{S}$  may become markedly different, and the variance of the average of each set may increase greatly. Returning to the example in §4.3.3, the two-way interactions are not covered equally. Consider the two-way interaction  $\{(1, 0), (2, 0)\}$ . It is covered in only two rows of the array, namely  $|\rho(\{(1, 0), (2, 0)\})| = |\{1, 2\}| = 2$  (this is true for all two-way interactions in this example). Even in this small array, the coverage of two-way interactions is unbalanced resulting in  $S$  accumulating two values and  $\bar{S}$  accumulating six values. This makes any direct comparison among (factor, level) combinations and/or two-way interactions impossible.

To address this problem, factors are grouped according to the number of times each level is covered in the LA; see Appendix A.4 for a pointer to the details on how groups are formed. Now, in each iteration of the screening algorithm, the first step is to select the most significant factor or interaction from each group. Then from these candidates, the most significant factor or interaction overall is selected.

The Figure 4.4 shows the graphical tests for normality of the residuals after the first iteration of the screening algorithm. (Similar behaviour of the residuals is observed after each iteration.) While the figures indicate that the residuals are close to normally distributed,

we check using the non-parametric Shapiro-Wilk test. This test indicates that the residuals are still not normally distributed. Hence, we use the Wilcoxon rank sum test and the Mann-Whitney  $U$ -test [29, 78, 136] to select the most significant factor or two-way interaction within each group. Then, to select the most significant factor or interaction over all groups, the Akaike information criterion ( $AIC_C$ ) [1] is used.

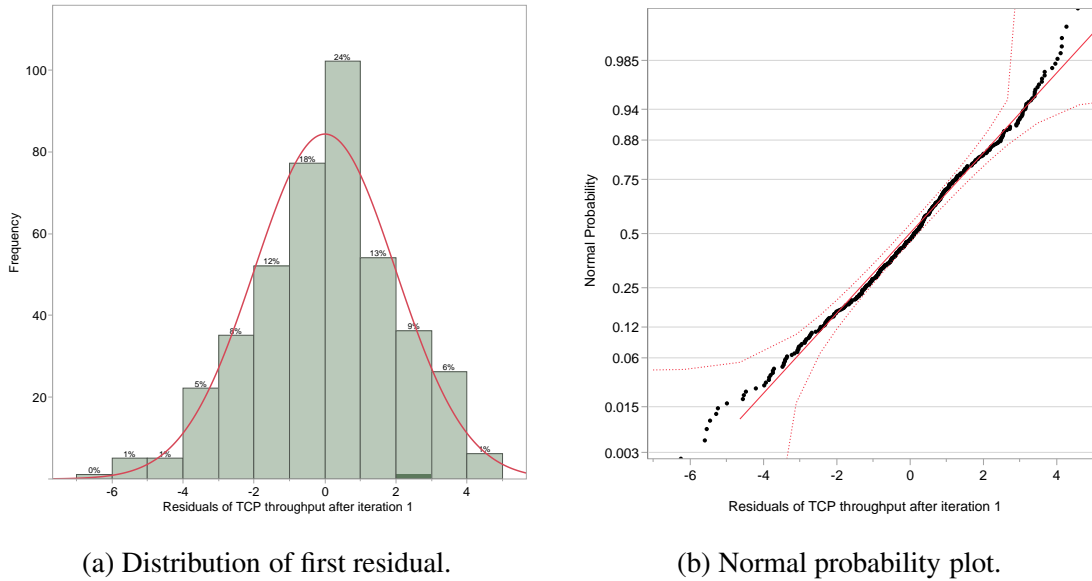


**Figure 4.4:** Distribution of residuals after the first iteration of the screening algorithm, and corresponding normal probability plot.

We still need to fit the intercept and the coefficients of the terms. For a linear model with the assumptions of expected error of zero and expected variance in the error to be equal, the method of ordinary least squares (OLS) is used. However, if the expected variance in the error is unequal, OLS is no longer appropriate [85]. In this case, the method of *weighted least squares* (WLS) is used to fit the intercept and coefficients of the terms in the screening model.

The screening algorithm, see Appendix A.5, adds one term to the model on each iteration. In this case, the algorithm terminates when  $maxTerms$  terms have been added to the model. Optionally, any additional criterion as a stopping condition can be added; for

example the coefficient of determination ( $R^2$ ) which explains how well the model fits the observed data.

#### 4.3.4.1 The Resulting Screening Model

Table 4.6 gives the screening model for average TCP throughput developed in twelve iterations of the screening algorithm; Table 4.8 lists its unique factors. A Student's  $t$ -test was run on each term in the screening model and each was found to be significant;  $\beta_0$  is the intercept and  $\beta_i$  is the coefficient of term  $i$ ,  $1 \leq i \leq 12$ .

**Table 4.6:** Screening model with twelve terms.

t-Test	$\beta_i$	Factor or interaction, and level(s)
52.6	5.6	
34.5	4.4	ErrorModel_ranvar_Uniform
32.8	4.0	ErrorModel_unit_pkt)
-29.1	-4.7	(ErrorModel_ranvar_Uniform) * (ErrorModel_unit_pkt)
-11.8	-1.6	TCP_packetSize_64
-12.1	-1.5	MAC_RTSThreshold_0
-9.3	-1.2	TCP_packetSize_128
6.5	0.9	(TCP_RTTvar_exp_2) * (TCP_min_max_RTO_0.1)
6.6	0.7	TCP_min_max_RTO_0.2
8.4	1.1	(ErrorModel_unit_pkt) * (ErrorModel_rate_1.0E-07)
6.3	1.1	(ErrorModel_ranvar_Uniform) * (MAC_RTSThreshold_0)
5.5	0.7	APP_flows_1
5.2	0.5	RWP_Area_8

The first notable observation about this screening model is that it contains both main effects and two-way interactions. Moreover, it contains factors from across the layers of the protocol stack (application, transport, and MAC) and not just the transport layer; in addition, it includes factors from the error model and the mobility model. Aside from these differences with other models of TCP throughput (such as [30, 40, 81, 99, 100, 102, 138, 141, 143]), the screening model includes not just which factors or two-way interactions are significant, but the level at which each is significant.

From the statistical point of view, Table 4.7 shows a strong correlation among the regressors and the response of average TCP throughput. The F statistic indicates that the model is significant to the response.

**Table 4.7:** Summary statistics of the screening model in Table 4.6.

$R^2$  and Adjusted  $R^2$ : 0.84

Standard deviation: 0.92

F statistic: 180.6 on 12 and 408 *df*, p-value < 7.89e-155

We are encouraged by the factors and interactions identified. This includes how and into what unit errors are introduced (using a uniform distribution into packets rather than bit errors), and their interaction. Smaller sized packets (64 and 128 bytes) tend to reduce throughput. When RTS/CTS is always on (*i.e.*, the threshold is zero bytes), there is a negative impact on throughput compared to when it is configured to 1500 or 3000 bytes (always off). The retransmission timeout (RTO) and round trip time (RTT) are part of TCP's congestion control mechanism; the RTO infers packet loss by observing duplicate acknowledgements and the RTT is related to the propagation delay. The RTO is significant by itself, and in its interaction with the RTT as they work to correct and prevent network congestion. The synthetic error model of the simulator drops packets comparing them with data from an uniform distribution at a steady-state loss event rate of  $1.0E-07$ ; this is the lowest error rate used and naturally it corresponds with higher throughput. Smaller simulation areas also result in higher throughput; a larger area has longer average shortest-hop path lengths and average higher network partition rates both of which negatively affect throughput. The throughput response is higher with fewer flows because increasing the number of flows not only may overload the network but more flows are more challenging to route in a MANET.

#### 4.4 Validation and Verification

From the 75 controllable factors used in experimentation, nine unique factors are present in the twelve terms in the screening model in Table 4.6; these are listed in Table 4.8.



**Table 4.8:** Unique factors from the screening model in Table 4.6.

Factor	Level	
	Minimum	Maximum
TCP_RTTvar_exp_	2	4
ErrorModel_ranvar_	<i>Uniform</i>	<i>Exponential</i>
ErrorModel_unit_	<i>pkt</i>	<i>bit</i>
MAC_RTSThreshold_	0	3000
ErrorModel_rate_	1.0E-07	1.0E-05
RWP_Area_	8	40
TCP_min_max_RTO_	0.1	40
APP_flows_	1	18
TCP_packetSize_	64	2048

In order to validate the factors and interactions identified, we first conduct a full-factorial experiment for these nine factors using the extremes of their region of interest, using the statistical software JMP to analyze the results. From this, we produce a predictive model of average TCP throughput. We then examine the quality of this predictive model by comparing how it performs on random design points (*i.e.*, a design point in which the level of each factor is selected at random).

We present our validation results next.

#### 4.4.1 Full-Factorial Screening in JMP

We conduct an independent  $2^9$  full-factorial experiment on the nine factors in Table 4.8. All remaining  $75 - 9 = 66$  factors are fixed to their default levels. Ten replicates of each of the  $2^9$  design points is run, and TCP throughput measured. The results of the experimentation are input to the JMP statistical software, version 11.0 [59].

The results from the full-factorial screening experiment are given in Table 4.9. It includes only the main effects and two-way interactions sorted in increasing order by the  $p$ -value. The results indicate high commonality with the main effects and two-factor interactions selected by the screening algorithm that formed the screening model in Table 4.6. Indeed, both models have the same four most significant terms (though in a different order),

and all factors and interactions in Table 4.6 are a subset of the terms in Table 4.9. Appendix A gives a pointer to the details of the predictive model for average TCP throughput that was fit using a subset of the significant terms in Table 4.9.

**Table 4.9:** Partial results of a  $2^9$  full-factorial screening experiment using JMP 11.0 on the nine factors in Table 4.8.

Term	p-Value
ErrorModel_ranvar_*ErrorModel_unit_	< .0001*
ErrorModel_ranvar_	< .0001*
ErrorModel_unit_	< .0001*
TCP_packetSize_	< .0001*
APP_flows_	< .0001*
TCP_min_max_RTO_	< .0001*
RWP_Area_	< .0001*
MAC_RTSThreshold_	< .0001*
ErrorModel_unit_*TCP_packetSize_	< .0001*
ErrorModel_rate_	< .0001*
ErrorModel_ranvar_*MAC_RTSThreshold_	< .0001*
APP_flows_*RWP_Area_	< .0001*
ErrorModel_unit_*ErrorModel_rate_	< .0001*
TCP_packetSize_*ErrorModel_rate_	< .0001*
ErrorModel_unit_*MAC_RTSThreshold_	< .0001*
ErrorModel_ranvar_*APP_flows_	< .0001*
APP_flows_*TCP_min_max_RTO_	< .0001*
ErrorModel_unit_*APP_flows_	< .0001*
ErrorModel_ranvar_*TCP_min_max_RTO_	< .0001*
ErrorModel_ranvar_*TCP_packetSize_	< .0001*
TCP_packetSize_*APP_flows_	< .0001*
TCP_min_max_RTO_*RWP_Area_	< .0001*
ErrorModel_ranvar_*RWP_Area_	< .0001*
MAC_RTSThreshold_*ErrorModel_rate_	< .0001*
TCP_min_max_RTO_*ErrorModel_rate_	< .0001*
TCP_min_max_RTO_*TCP_rttvar_exp_	0.0001
ErrorModel_unit_*TCP_min_max_RTO_	0.0001
APP_flows_*ErrorModel_rate_	0.0003
RWP_Area_*MAC_RTSThreshold_	0.0006
ErrorModel_unit_*RWP_Area_	0.001
TCP_rttvar_exp_	0.0012
TCP_packetSize_*RWP_Area_	0.002
APP_flows_*MAC_RTSThreshold_	0.0116
RWP_Area_*ErrorModel_rate_	0.0444
ErrorModel_ranvar_*TCP_rttvar_exp_	0.0515

Figure 4.5 shows the results of evaluating the JMP predictive model as a function of the TCP packet size, for the three levels of error rate. As in the experimentation, all remaining factors are fixed at their default levels. As expected, the results show that the highest TCP throughput is achieved when the error rate is at the lowest level ( $1.0E-07$ ). For a given error rate the TCP throughput increases as a function of packet size, after which it decreases. An exception is for packet size 1024. Aside from this exception, these results also confirm our intuition of TCP throughput behaviour. The reason for this exception deserves further study but may be related to the default settings used for the other 66 factors not varied in this screening experiment.

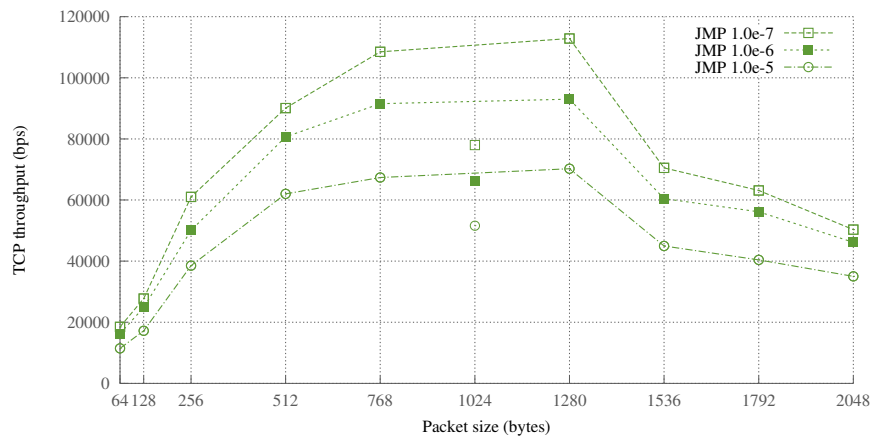


**Figure 4.5:** TCP throughput as a function of packet size as predicted by the JMP model; all other factors are at their default levels.

We now examine the predictive accuracy of the JMP model for random design points.

#### 4.4.2 JMP Model vs. Analytical Models

Many analytical models of TCP throughput have been developed (not all for MANETs). Most include factors from the transport layer only. Some even restrict the factors to those involved in TCP's congestion control mechanism [30, 40, 81, 99, 100, 102, 138, 141, 143], such as the round trip time (RTT), retransmission timeout (RTO), advertised window, congestion window, slow start threshold, and fast retransmit and fast recovery mechanisms.

Some models also include the packet size and loss rate. There is some agreement among the factors identified by the locating array (Table 4.8) and those found in existing models of TCP throughput. Interestingly, none of the models include interactions among factors yet there are known cross-layer interactions with TCP in wireless networks (see, as one example [119]).

We compare our predictive model of TCP throughput produced by JMP to two models frequently referenced in the literature. [81] propose the following model of TCP throughput,  $T$ :

$$T = \frac{MSS \times C}{RTT \times \sqrt{p}},$$

where  $C = \sqrt{3/2}$ , MSS is the maximum segment size in bytes, the RTT is in seconds, and  $p$  is the loss rate as a percentage. [100] propose a related model including the RTO and the packet size  $s$  instead of the MSS.

$$T = \frac{s}{RTT \sqrt{\frac{2p}{3}} + RTO(3\sqrt{\frac{3p}{8}})p(1 + 32p^2)}.$$

To facilitate comparison of the model produced by JMP to these models, the bit error rate was converted to a packet error rate. The RTT utilized for evaluating the model in [81] is set constant to 300 ms. The RTT and the RTO utilized for evaluating the model in [100] are the average of the values RTT and RTO from 24 data sets. Figure 4.6 shows that the TCP throughput predicted by [81] is much higher (by an order of magnitude) than our JMP model for all loss rates; the throughput also does not appear to have reached a maximum.

Figure 4.7 shows that the TCP throughput predicted by [100] is comparable to that of [81] for the loss rates of  $1.0E-06$  and  $1.0E-07$ . However, for the loss rate of  $1.0E-05$ , the throughput predicted is comparable to that of our JMP model, except for the two smallest packet sizes (64 and 128 bytes). Padhye et al. also shows a very slight decrease in throughput for this case.

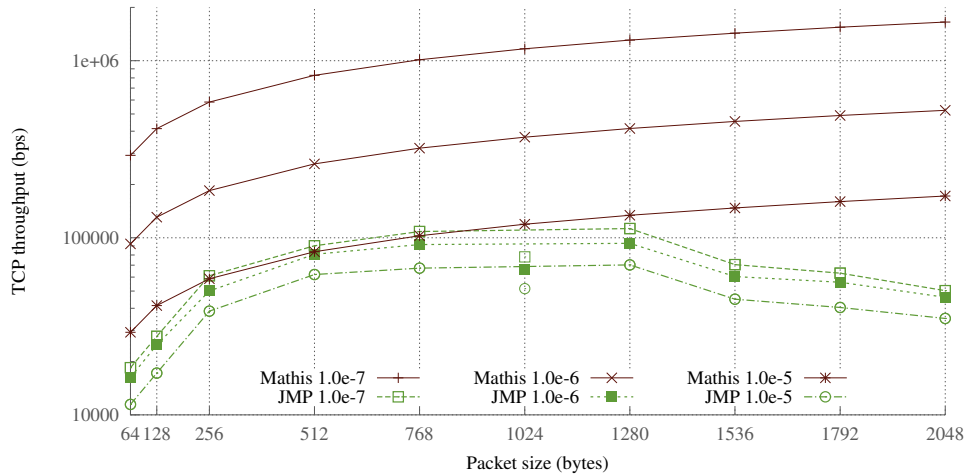


Figure 4.6: JMP model vs. model proposed by [81].

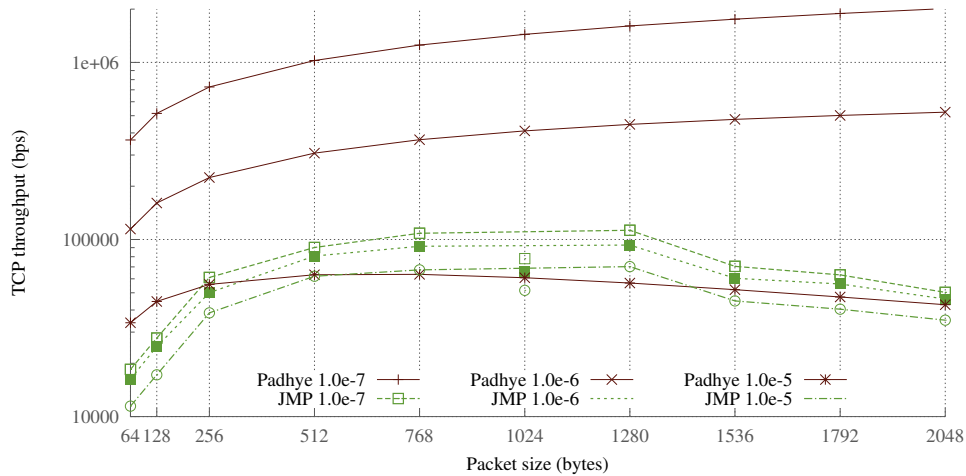


Figure 4.7: JMP model vs. model proposed by [100].

Except for the highest error rate in Padhye et al., the models in [81] and in [100] greatly overestimate TCP throughput compared to our JMP model. Perhaps it is because they do not consider other factors from across layers of the protocol stack, or two-way interactions among factors that are significant for TCP throughput.

#### 4.4.3 Predictive Accuracy of JMP Model

In order to test the predictive accuracy of the JMP model, a new experimental design of one hundred random design points is constructed. In constructing each design point, for

each of factor  $F_j$ ,  $1 \leq j \leq 75$ , a random level from  $L_j$  is selected. New mobility scenarios are also generated. Ten replicates of each of the random design points are run in the ns-2 simulator, and the TCP throughput measured. In addition, for each experiment in the design, the JMP model is evaluated generating a new data set of fitted TCP throughput.

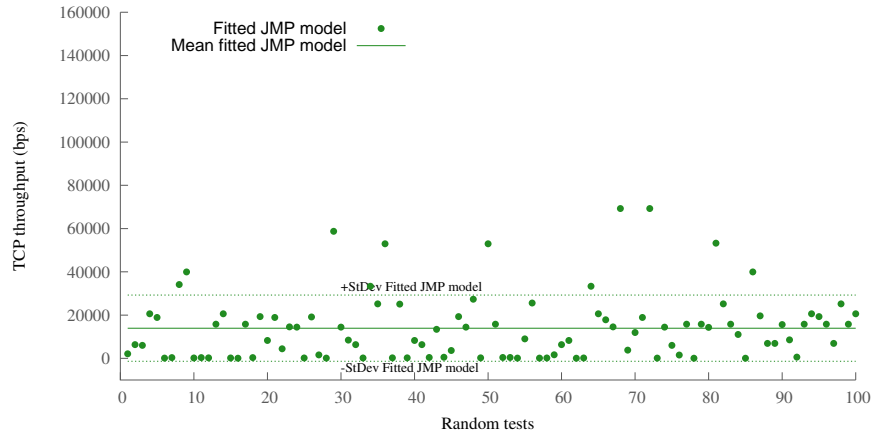
Figure 4.8 shows the average TCP throughput from simulation, and the fitted throughput from the JMP model corresponding to this random design. The mean TCP throughput from the simulations is 20,892 bps whereas the mean from the JMP model is lower, only 13,946 bps. However, the standard deviation of the results from the JMP model is smaller than the standard deviation from the simulations. Both models exhibit a few outliers. Approximately 94% of the results predicted for TCP throughput from the JMP model are in one standard deviation of the simulation results. Considering the size of the factor space, we conclude that the predicted average TCP throughput of the JMP model is similar to the average TCP throughput measured in simulation.

#### 4.4.4 *Predictive Accuracy of Screening Model*

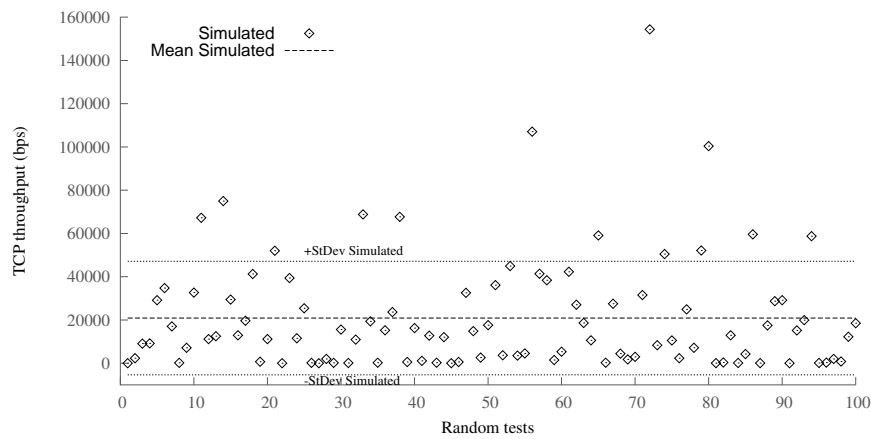
While the model developed in applying the screening algorithm based on the LA (Table 4.6) is not intended to be used as a predictive model, we were curious about its predictive accuracy. Appendix A gives a pointer to a summary of results similar to those in this section for the screening model. To our surprise, the predictive accuracy of the screening model is reasonably good. The screening model does appear to have more variability than the model developed in JMP.

### 4.5 Conclusions

Locating arrays capture the intuition that in order to see the effect of a main effect or interaction, some design point must cover it; and in order to distinguish it, the responses for the set of design points that cover it must not be equally explained by another small set of



(a) Predictions by JMP.



(b) Simulation results.

**Figure 4.8:** Predictions by the JMP model and simulation results for random design points.

main effects or interactions. In a complex engineered system, many main effects and interactions may be significant, but our method identifies them one at a time, iteratively improving a screening model. In this way, an experimental design must be able to repeatedly locate a single “most significant” main effect or interaction. Our results show that using locating arrays for screening appears promising. Indeed while the screening targeted the identification of significant factors and two-way interactions, the screening model developed also reflects the actual behaviour well.

Despite this, the method aims only to deal with many factors and their interactions to identify the significant ones. We advocate that further experimentation is necessary after

the screening is completed, both to confirm the screening results and to build a predictive model. One must be cautious not to over-fit the experimental results and claim unwarranted confidence; confirmation is needed. This is particularly a concern if the stopping criterion chosen locates too many or too few significant interactions; while our choice of  $R^2$  appears to have worked well, future effort should address the impact of different stopping criteria. A second concern is the selection criterion for the next factor or interaction to include. Subsequent selections depend upon selections already made, so our method could in principle be misdirected by a bad selection. Our criterion of using the differences between responses for  $S$  and those for  $\bar{S}$  has also worked well, but we cannot be certain that such a simple selection suffices in general. Finally, we have employed only a few locating arrays; while they have worked well in our analyses, constructing a suitable locating array remains a challenging problem that merits further research.

Certainly further experimentation is needed to assess the merit of screening using LAs, in particular on physical not just simulated complex engineered systems, and draw firm conclusions. What we can conclude is that in a challenging CES arising from a MANET, screening using locating arrays is viable and yields useful models.



## Chapter 5

### STATISTICAL CHARACTERISTICS OF LOCATING ARRAYS

#### 5.1 Introduction

In this chapter, several statistical metrics are considered in an attempt to evaluate the quality of locating arrays when they are used as screening designs. Specifically, the metrics of correlation, variance inflation factors, covariance, fraction of design space, as well as statistical properties based on the response, and aliasing are evaluated for the locating array used in Chapter 4. As we will see, all metrics indicate that the locating array appears to share statistical properties with “good” screening designs.

#### 5.2 Correlation

The method of least squares [84, 85] is used to estimate the coefficients of a linear regression model while minimizing the error between the observed data and its corresponding fit given by the regression equation. A multiple linear regression model with  $k$  regressors is  $y = \beta_0 + \beta_1 x_1 + \beta_2 x_2 + \dots + \beta_k x_k + \epsilon$ , where  $x_1, x_2, \dots, x_k$  are the variables,  $\beta_0, \dots, \beta_k$  are the coefficients to estimate, and  $\epsilon$  is the error. It is assumed that the error  $\epsilon$  has an expected value  $E(\epsilon) = 0$  and  $\text{Var}(\epsilon) = \sigma^2$ , i.e., it is normally distributed  $N(0, \sigma^2)$ .

The representation of a linear regression model in matrix notation is  $\mathbf{y} = \mathbf{X}\hat{\boldsymbol{\beta}} + \boldsymbol{\epsilon}$ , where the  $\hat{\boldsymbol{\beta}} = (\mathbf{X}'\mathbf{X})^{-1}\mathbf{X}'\mathbf{y}$  is the array of the estimated linear regression coefficients.

The product  $(\mathbf{X}'\mathbf{X})$  is the *correlation matrix* of the regressors and  $\mathbf{X}'\mathbf{y}$  is the correlation between the regressors and the response. Correlation indicates whether a value of one variable changes in response to changes in the value of another variable. While it is desired

for the factors in  $X$  to be independent, it is common for there to be some correlation among them. Therefore, the smaller the correlation, the better the statistical properties of  $X$ .

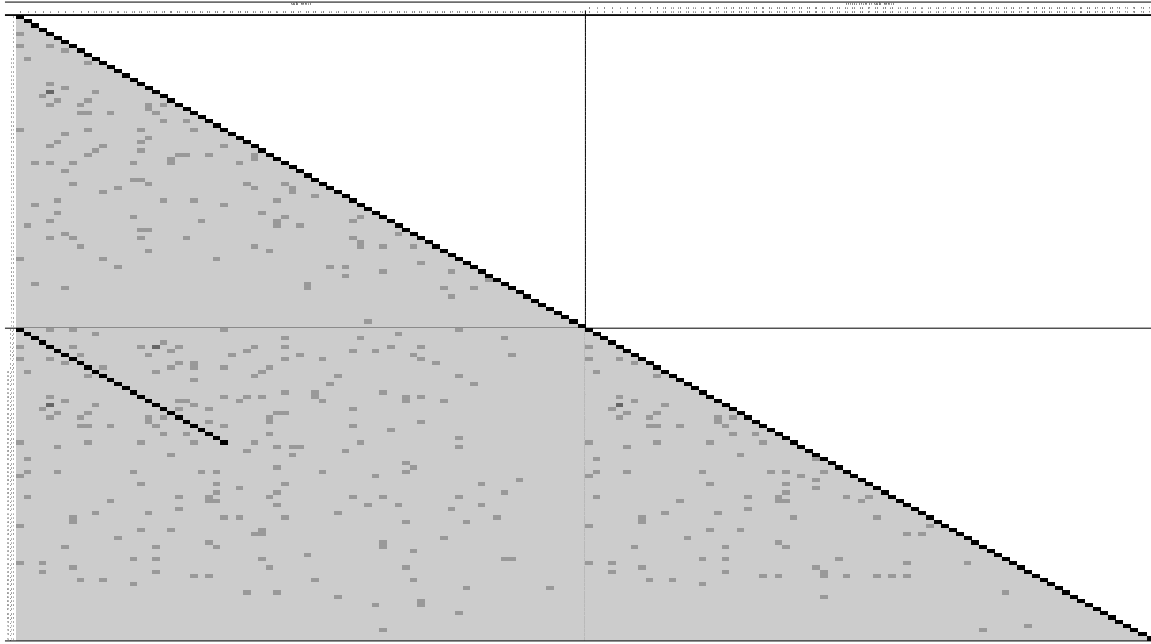
The off-diagonal values of the  $(X'X)$  matrix range from -1.0 to +1.0 [85]. A correlation coefficient of zero means that there is no association between the variables. Values close to -1.0 or +1.0 are an indicator of near-linear dependency between two regressors. A value of +1 indicates a perfect positive linear relationship: as one variable increases in its values, the other variable also increases in its values by an exact linear rule. As a result, an increase in the magnitude of one variable results in an increase in the other. A value of -1 indicates a perfect negative linear relationship: as one variable increases in value, the other variable decreases in value by an exact linear rule.

The presence of correlation has serious effects on the least squares estimates of the regression coefficients. Therefore, a strong correlation between two regressors results in large variances and covariances of the least squares estimators of the corresponding regression coefficients  $\hat{\beta}_j$ , *i.e.*, a poor estimate of the regression coefficient is obtained.

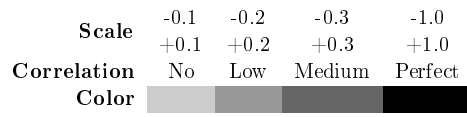
In order to evaluate correlation in the locating array used in Chapter 4, we first scale each value using unit length scaling. *Unit length scaling* allows the units of the different factors to be standardized [85]. After scaling, we construct  $X$  as a  $421 \times 150$  matrix where the first 75 columns of  $X$  correspond to the 75 main effects, and remaining 75 columns of  $X$  correspond to their second order.

Figure 5.1a shows the resulting  $(X'X)$  correlation matrix; the correlation matrix is symmetric about the main diagonal hence only the lower triangle is shown. The colour map in Figure 5.1b shows the degree of correlation. A light colour means no or low correlation, while a dark colour means high correlation.

There is perfect correlation along in the main diagonal, and also along a diagonal corresponding to main effects and their second order for binary factors (*i.e.*, factors 0 to 27). The second order of a binary factor is linearly dependent of the same main effect; hence,



(a) Correlation matrix.



(b) Colour map for correlation matrix.

**Figure 5.1:** Correlation matrix of main effects and second order of main effects for the locating array used in Chapter 4 (see AppendixA.3).

the correlation between them is perfect. However, the second order of factors with more than two levels may not be linearly dependent of its same main effect; here, that correlation between them in the locating array is shown very low.

In the locating array, any correlation between main effects, the second order of main effects, or their combination is low; in the most of the cases they are lower than  $\pm 0.1$  though always lower than 0.3 which means the correlation is not serious.

In general, the correlation of the locating array is very low; this supports the use of the locating array as a design for screening experiments.

### 5.3 Variance inflation factor (VIF) of the Locating Array

Figure 5.2 shows the VIFs of the locating array. The values range between 1.07 and 1.36 and are considered low. Values higher than 5.0 are considered serious correlation [85]. Together, Figures 5.1a and 5.2 support that the locating array is a good design for conducting screening experiments.

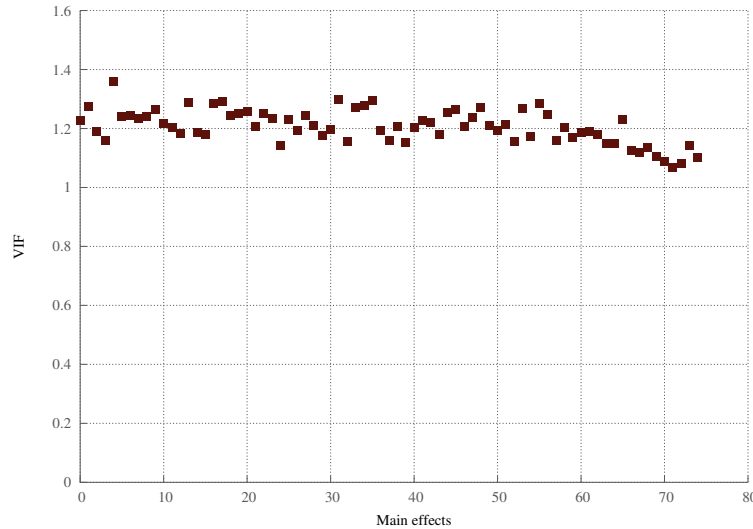
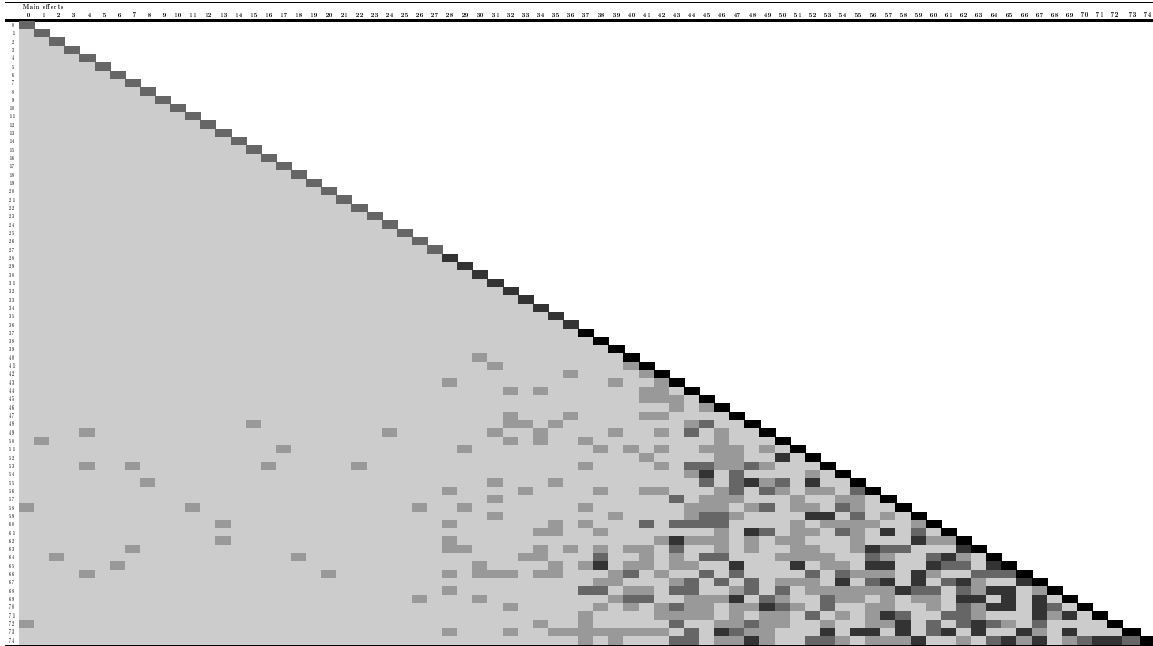


**Figure 5.2:** Variance inflation factors (VIFs) of the locating array used in Chapter 4 (see Appendix A.3).

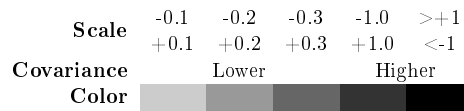
### 5.4 Covariance

Figure 5.3a shows a variance-covariance matrix for the locating array used in Chapter 4. It is symmetric about the main diagonal therefore only the lower triangle is presented. The main diagonal contains the variance of the main effects  $F_i$ . The elements in position  $(i, j)$ ,  $i = 1, \dots, 75, j < i$ , contain the covariance between the factors  $F_i$  and  $F_j$ . The numerical scale and shading shown in Figure 5.3b indicates the severity of covariance; the darker the shading the higher the covariance.

From Figure 5.3a, the factors that are covered fewer times in the locating array (*i.e.*, covariances shown in the lower right part of matrix) have higher variance than those covered



(a) Covariance matrix.



(b) Colour map for covariance matrix.

**Figure 5.3:** Covariance matrix for the main effects in the locating array used in Chapter 4 (see Appendix A.3).

more times (*i.e.*, covariances shown in the upper left part of the matrix). In addition, along the main diagonal the variance is increasing with increasing numbers of levels of the factors. Moreover, the two-factor interactions with the highest number of levels, *i.e.*, 10 levels each, may be covered fewer times compared to the coverage of main effects; therefore, the difference of variance between them may be significantly different.

Knowledge that the variance of a factor is related to its number of levels provides relevant information for when the locating array is utilized for screening. When comparing main effects and/or two-factor interactions where the difference in the number of levels

between them is significant, the analysis must take into account that their variance will be high.

### 5.5 Fraction of Design Space

Utilizing the JMP statistical software, version 11.0 [59], the FDS plot for the locating array used in Chapter 4 is constructed. Figure 5.4 shows the resulting FDS plot. It shows that at 50% of the design space the prediction variance is 1.4 which is very low, and highly desirable [59]. The prediction variance from 0 to 50% and from 50% to 100% of the design space appears constant and uniform. The locating array exhibits good scaled prediction variance for an experimental design.

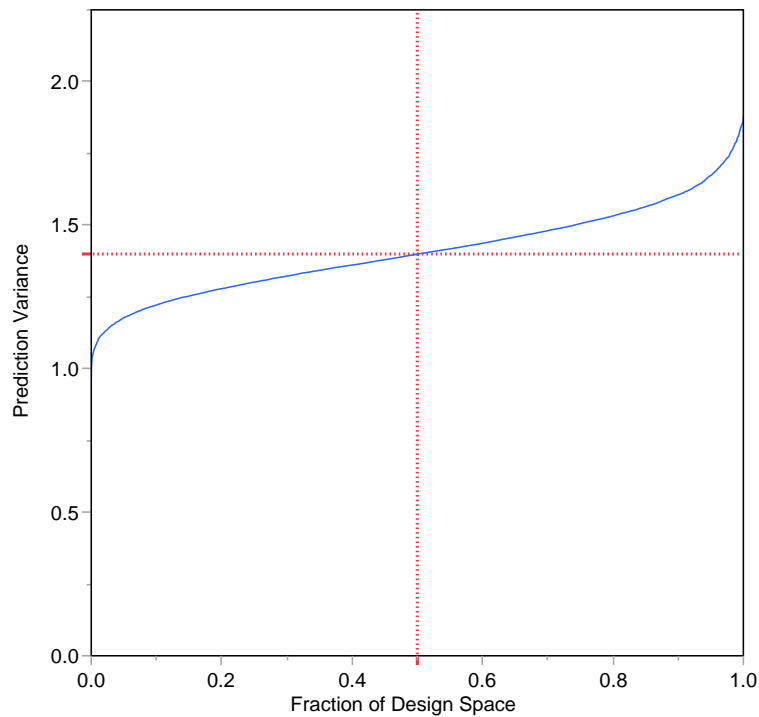


**Figure 5.4:** Fraction of design space for the locating array used in Chapter 4 (see Appendix A.3).

## 5.6 Statistical Properties based on Response

### 5.6.1 Correlation between Main Effects and the Response

One of the goals of an experimental design is to maximize the experimental variance caused by the independent variables on the dependent variable (e.g., of the factors on the response TCP throughput) [140]. For the locating array used in Chapter 4, the correlation between most of the 75 factors and the observed average TCP throughput is high, which is desirable [140].

Figure 5.5 shows the correlation between each of the 75 main effects in the LA and the observed response of average TCP throughput. The  $x$ -axis lists the names of the 75 factors utilized in `ns-2` to simulate the MANET. The  $y$ -axis is the absolute value of the correlation of the factor with the response. The factors on the  $x$ -axis are ordered in descending order of the magnitude of the correlation.

Figure 5.5 illustrates that approximately 60% of the factors have a correlation value greater than or equal to the overall mean of the observed TCP throughput. Moreover, the higher correlation values are approximately 10 times higher than the overall mean. Therefore, the experimental variance on the response caused by the factors in the locating array is high. The correlation between the independent factors forming the locating array and the observed average TCP throughput is strong.

### 5.6.2 Variability on the Response

In order to determine which factors cause the variability on the response, the variance in the average TCP throughput caused by each (factor, level) pair is computed. Figure 5.6 plots the highest variance for each factor over all its levels. The  $x$ -axis of Figure 5.6 gives the main effects grouped according to their number of levels. The  $y$ -axis indicates the mag-



**Figure 5.5:** Correlation between each of the main effects with the mean TCP throughput.

minute of the variance. The factors with more levels correspond to larger variance on the average TCP throughput compared to the factors with fewer levels.

Figure 5.6 also shows the standard deviation of each measure of variance. The standard deviation explains the intra-group variability; the smaller the intra-group variability the better [140]. The figure indicates that the standard deviation of factors with fewer levels is lower (with a few exceptions) than the standard deviation of factors with higher levels. The lower the intra-group variability the better; therefore, the variability shown in Figure 5.6 is expected to be lower.



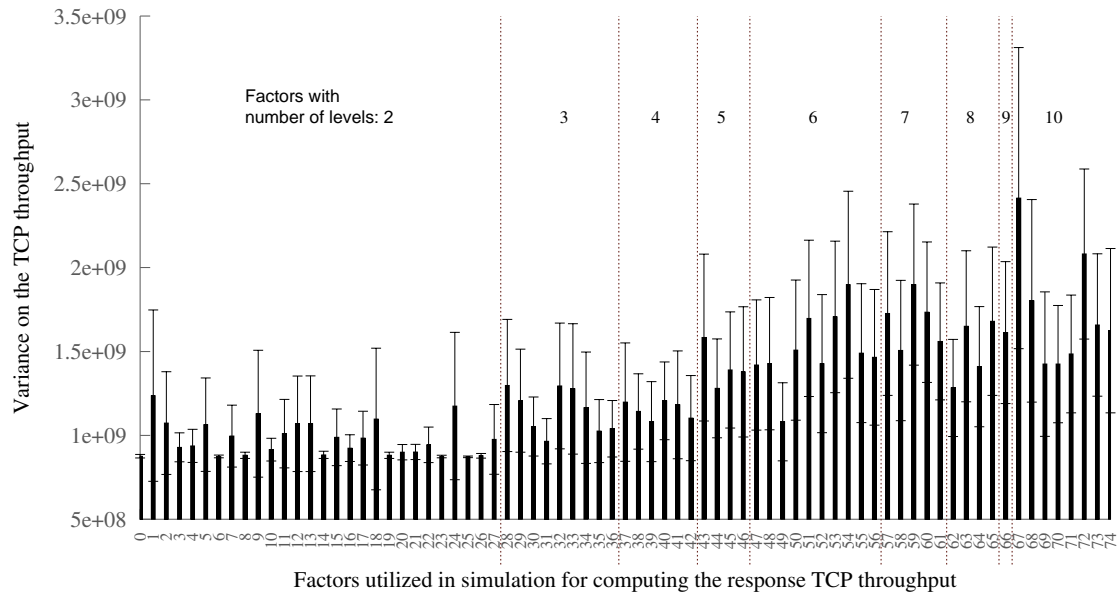


**Figure 5.6:** Variance in the TCP throughput caused per factor.

## 5.7 Aliasing

First, because the locating array is a multi-level design and we need to compare factors of different levels, then we use a method to code each factor using dummy coding [41]; see Section §2.3.2 for details on dummy coding.

We develop an iterative procedure to generate the alias relationships for the locating array in Chapter 4. The interaction between two factors of equal value is 1, otherwise is 0. That is, if the value levels of two factors are 0 and 0, the interaction is 1; if the values are 1 and 1, the interaction is 1; if the value levels of two factors are different, e.g., 0 and 1 or 1 and 0, the interaction is 0.




Then for each main effect, and each two-factor interaction, each row of the locating array is compared. A counter is incremented by 1 each time that the value of the main effect and

the interaction are equal (0 or 1). Then, the counter is divided by the size of the locating array N (e.g., 421) to express the result as a percentage. The result of the comparison gives the percentage of aliasing of the two-factor interaction to the main effect [76]. In the case of computing the aliasing of two-factor interactions with two-factor interactions, the counter is incremented if for each row of the locating array both interactions are equal.

Different factors in the locating array may have equal number of levels. Then, different computations of the percentage of aliasing of two-factor interactions and main effects of equal number of levels is highly similar. Therefore, in order to tabulate the results and to be able of reporting them, an average of the percentage of aliasing of factors of equal number of levels is computed.

A color map is utilized to show different levels of aliasing. In Table 5.1 four different levels of aliasing are described. The percentage 0% indicates zero alias relationship; 100% indicates there is a complete alias relationship; while intermediate values mean a partial alias relationship.

**Table 5.1:** Scale for the color map of the average percentage of alias relationships.

Scale (%)	Color
0	
1, ..., 33	
34, ..., 66	
67, ..., 100	

In this Chapter we are particularly interested in the confounding patterns between main effects and two-factor interactions, also between two two-factor interactions, ignoring interactions of higher order.

Table 5.2 shows the average aliasing relationships of two-factor interactions to main effects in the locating array considering the number of levels of the factors involved. The first two columns label most combinations of the number of levels of the factors involved in the two-way interaction. The remaining columns label the number of levels of the main

effect. The entries give the average aliasing as a percentage between a two-factor interaction and main effects having factors with the given levels.

The highest average alias relationships are shown in the upper left of Table 5.2 (up to 50%) and the lowest average alias relationships are shown in the lower right area of Table 5.2 (as low as 22%). With only one exception, as the number of levels in the main effect increase, the alias percentage decreases.

**Table 5.2:** Average aliasing relationship (as a percentage) of two-factor interactions to main effects considering the number of levels in the factors involved.

Levels of Factors in Two-factor Interaction		Level of Main Effect								
		2	3	4	5	6	7	8	9	10
2	2	49	49	49	49	49	49	49	50	49
2	3	48	48	48	48	47	48	48	48	47
2	4	48	48	48	48	48	48	48	48	48
2	5	48	48	48	48	48	48	48	48	48
2	6	48	48	48	48	48	48	48	48	48
2	7	48	48	48	48	48	48	48	48	48
2	8	48	48	48	48	48	48	48	48	48
2	9	48	48	48	48	48	48	48	48	48
2	10	48	48	48	48	48	48	48	48	48
3	3	48	46	45	45	44	44	44	44	44
3	4	48	45	44	43	43	42	42	42	42
3	5	48	44	43	42	41	41	41	41	40
3	6	48	44	42	41	40	40	40	39	39
3	7	48	44	42	41	40	40	39	39	39
3	8	48	43	42	40	39	39	39	38	38
3	9	47	43	41	40	39	39	38	38	38
3	10	48	43	41	40	39	38	38	38	37
4	4	48	43	42	40	40	39	39	38	38
4	5	48	43	40	39	38	37	37	36	36
4	6	48	42	39	38	37	36	35	35	35
4	7	48	42	39	37	36	35	35	34	34
4	8	47	41	38	36	35	34	34	33	33
4	9	47	41	38	36	35	34	33	32	32
4	10	48	41	38	36	34	34	33	32	32
5	5	47	41	38	37	36	35	34	34	33
5	6	47	41	38	36	34	34	33	32	32
5	7	48	40	37	35	33	32	32	31	31
5	8	47	40	36	34	33	32	31	30	30
5	9	45	37	34	32	30	30	29	28	28
5	10	47	40	36	33	32	31	30	29	29
6	6	48	40	37	34	33	32	31	31	30
6	7	48	40	36	34	32	31	30	30	29
6	8	47	39	35	33	31	30	29	29	28
6	9	47	39	35	32	31	29	28	28	27
6	10	48	39	34	32	30	29	28	27	27
7	7	47	39	35	32	31	30	29	28	28
7	8	47	39	34	32	30	29	28	27	27
7	9	46	37	33	31	29	28	27	26	26
7	10	47	38	34	31	29	27	27	26	25
8	8	47	38	34	31	29	28	27	26	25
8	9	45	36	31	29	27	26	25	24	24
8	10	47	38	33	30	28	27	26	25	24
9	10	47	37	32	29	27	26	25	24	23
10	10	47	37	32	29	26	25	24	23	22

Table 5.3 shows the aliasing relationships of two two-factor interactions in the locating array. However, unlike Table 5.2 where the percentage of aliasing decreases as the number of levels of factors increases the opposite is true in Table 5.3. Overall the percentage range is smaller, from 48-69%. In the locating array, the column corresponding to a factor with high number of levels, e.g., 10 levels, has many zeroes. Then, the interaction of two factors of 10 levels will cause a result with many ones (*i.e.*, interaction 0 and 0 is 1). Therefore, the comparison of two two-factor interactions will count a high number of equal rows. That is, both two-factor interactions will have many ones.



One price we pay for fractioning a full factorial design to construct smaller screening designs is confounding effects or aliasing. Comparing the aliasing of two-factor interaction to main effects of the locating array in Tables 5.2 and 5.3 with the aliasing of the 12-run Plackett Burman shown in [76], the 12-run Plackett Burman formed from 11 binary factors being a popular saturated design for experimentation that just can estimate few main effects and interactions has an aliasing ranging between 33-66%, while, the locating array with 421 runs formed from 75 multi level factors which is able to estimate all main effects and all two-factor interactions has an aliasing ranging between 22-49%.

The overall aliasing percentage from the locating array, despite its high fractionation, suggests that it is a “good” screening design.

## 5.8 Conclusions

In this chapter, several statistical metrics have been considered in an attempt to evaluate the quality of locating arrays when used as screening designs. Specifically, the metrics of correlation, variance inflation factors, covariance, fraction of design space, as well as statistical properties based on the response, and aliasing have been evaluated for the locating array used in Chapter 4. All metrics indicate that the locating array appears to share statistical properties with “good” screening designs.

Of course, such metrics should not have to be computed for a locating array each time one is to be used as a screening design. Instead, it would be most useful to evaluate the metrics using analytic (*e.g.*, linear algebraic) techniques. This would provide a general conclusion about all locating arrays rather than for a specific one. However, such analysis is left for future work.

### CONCLUSIONS AND FUTURE WORK

Complex engineered systems are pervasive in science and engineering. There is great interest in studying their components and the relationships among them to understand, measure and control their overall behaviour. Nowadays, it is possible to partially analyze a complex system and scrutinize in its components (factors). However, when the number of factors is large the size of an experimental design is very large and its statistical analysis is practically infeasible.

In complex engineered networks, such as mobile ad hoc networks (MANETs), the network architecture is organized as a series of layers to reduce design and implementation complexity. This introduces interactions among factors in the same and different layers, further complicating analysis, modelling, and optimization.

The voice over Ip (VoIP) application in MANET in the Chapter 3 emphasizes that the interactions of the factors across layers are important for the outcome of experimentation. Cross-layer factor interactions from PHY/MAC and LLC/Application, occur in the hop-by-hop and the end-to-end communication. The voice is packetized, compressed, and modulated adaptively to optimize network performance and call quality. The adaptive protocol shown in Chapter 3 outperforms standard audio-voice codecs (*e.g.*, G.711, G.729, G.723, GSM) in the number of calls admitted. However, the factors used for experimentation in this chapter are selected a priori by a domain expert.

It is unlikely that a domain expert knows the importance of a particular factor or interaction in the system as a whole. It is imperative not to eliminate factors from experimentation a priori. Instead, an automatic and objective approach to screening is required. In Chapter 4 a screening design and an algorithm is shown to tackle this problem.



The locating arrays are promising screening designs in cases of complex systems with numerous factors, the range of levels is large and the levels among factors is varied.

The algorithm is able to construct a linear regression model to contain the main effects and two-factor interactions most significant for the response in each iteration. The coefficients of the terms forming the model are computed using weighted least squares (WSL) which is appropriate when the variance of the residuals is non constant through the design space. Our results show that using locating arrays for screening appears promising, yielding useful models.

Still exists much work to do in terms of constructing locating arrays and for improvements of the screening algorithm. Even though Chapter 4 cites some approaches in relation to the construction of locating arrays, no general construction methods have been published. That is, constructing locating arrays remains a challenging problem that merits further research.

Certainly further experimentation is needed to assess the merit of screening using LAs, in particular on physical not just simulated complex engineered systems, and draw firm conclusions. What we can conclude is that in a challenging complex systems arising from a MANET, screening using locating arrays is viable and yields useful models.

On the other side, the screening algorithm uses Wilcoxon sum rank non-parametric test for hypothesis testing and the Akaike information criterion ( $AIC_C$ ) for model selection. Other non-parametric hypothesis testing could assess the accuracy of the algorithm. Other model selection criteria could confirm that the factor or interaction selected is the most significant for the response. The screening algorithm terminates when a number of terms have been added to the model. The coefficient of determination  $R^2$  has also been implemented as the criterion for stopping. However, future effort should address the impact of different stopping criteria.

In Chapter 5, the metrics of correlation, variance inflation factors, covariance, fraction of design space, as well as statistical properties based on the response, and aliasing evaluated the quality of the locating array constructed for the case study MANET of Chapter 4. All metrics indicate that the locating array appears to share statistical properties with “good” screening designs.

Such metrics should not have to be computed for a locating array each time one is to be used as a screening design. Instead, it would be most useful to evaluate the metrics using analytic (*e.g.*, linear algebraic) techniques. This would provide a general conclusion about all locating arrays rather than for a specific one.

## REFERENCES

- [1] H. Akaike, “A new look at the statistical model identification”, *IEEE Transactions on Automatic Control*, vol. 19, no. 6, pp. 716–723, 1974.
- [2] J. Angrist and V. Lavy, “Using Maimonides’ rule to estimate the effect of class size on scholastic achievement”, *Quarterly Journal of Economics*, vol. 114, pp. 533–575, May 1999.
- [3] F. Anjum, M. Elaoud, D. Famolari, A. Ghosh, R. Vaidyanathan, A. Dutta, P. Agrawal, T. Kodama, and Y. Katsube, “Voice performance in WLAN networks - an experimental study”, *IEEE Global Telecommunications Conference (Globecom’03)*, vol. 6, pp. 3504–3508, Dec. 2003.
- [4] K. Balachandran, S. R. Kadaba, and S. Nanda, “Channel quality estimation and rate adaptation for cellular mobile radio”, *IEEE Journal on Selected Areas in Communications*, vol. 17, no. 7, pp. 1244–1256, 1999.
- [5] A. Barberis, C. Casetti, J. C. De Martin, and M. Meo, “A simulation study of adaptive voice communications on IP networks”, in *International Symposium on Performance Evaluation of Computer and Telecommunication Systems (SPECTS’00)*, Vancouver, BC, Canada, 2000, pp. 531–542.
- [6] N. Bayer, M. C. de Castro, P. Dely, A. Kassler, Y. Koucheryavy, P. Mitoraj, and D. Staehle, “VoIP service performance optimization in pre-IEEE 802.11s wireless mesh networks”, in *IEEE International Conference on Circuits and Systems for Multimedia Wireless Communications (ICCSC’08)*, Shanghai, China, May 2008, pp. 75–79.
- [7] C. Bormann, C. Burmeister, M. Degermark, H. Fukushima, H. Hannu, L. Jonsson, R. Hakenberg, T. Koren, K. Le, Z. Liu, A. Martensson, A. Miyazaki, K. Svanbro, T. Wiebke, T. Yoshimura, and H. Zheng, “RObust header compression (ROHC): framework and four profiles: RTP, UDP, ESP, and uncompressed”, in *IETF RFC 3095*, 2001.
- [8] G. E. P. Box and J. S. Hunter, “The 2k-p fractional factorial designs”, *Technometrics*, vol. 3, pp. 311–351, 1961.
- [9] R. C. Bryce and C. J. Colbourn, “A density-based greedy algorithm for higher strength covering arrays”, *Software Testing, Verification, and Reliability*, vol. 19, pp. 37–53, 2009.
- [10] R. Burchfield, E. Nourbakhsh, J. Dix, K. Sahu, S. Venkatesan, and R. Prakash, “RF in the jungle: effect of environment assumptions on wireless experiment repeatability”, in *Proceedings of the 2009 IEEE International Conference on Communications (ICC’09)*, 2009, pp. 4993–4998.

- [11] T. Camp, J. Boleng, and V. Davies, “A survey of mobility models for ad hoc network research”, *Wireless Communication and Mobile Computing (WCMC): Special issue on Mobile Ad hoc Networking: Research trends and applications*, vol. 2, no. 5, pp. 483–502, 2002.
- [12] D. Cavin, Y. Sasson, and A. Schiper, “On the accuracy of MANET simulators”, in *Proceedings of the Second ACM International Workshop on Principles of Mobile Computing (POMC '02)*, 2002, pp. 38–43.
- [13] J. N. Cawse, “Experimental design for combinatorial and high throughput materials development”, *GE Global Research Technical Report*, vol. 29, no. 9, pp. 769–781, 2002.
- [14] T. Chen, M. Kazantzidis, M. Gerla, and I. Slain, “Experiments on QoS adaptation for improving end user speech perception over multihop wireless networks”, in *IEEE International Conference on Communications (ICC'99), Vancouver, BC, Canada*, 1999, pp. 708–715.
- [15] C. J. Colbourn, “Combinatorial aspects of covering arrays”, *Le Matematiche (Catania)*, vol. 58, pp. 121–167, 2004.
- [16] ———, “Covering arrays and hash families”, in *Information Security and Related Combinatorics*, ser. NATO Peace and Information Security, IOS Press, 2011, pp. 99–136.
- [17] C. J. Colbourn, S. S. Martirosyan, G. L. Mullen, D. E. Shasha, G. B. Sherwood, and J. L. Yucas, “Products of mixed covering arrays of strength two”, *Journal of Combinatorial Designs*, vol. 14, no. 2, pp. 124–138, 2006.
- [18] C. J. Colbourn and D. W. McClary, “Locating and detecting arrays for interaction faults”, *Journal of Combinatorial Optimization*, vol. 15, pp. 17–48, 2008.
- [19] C. Colbourn, D. Horsley, and V. Syrotiuk, “Frameproof codes and compressive sensing”, in *Communication, Control, and Computing (Allerton), 2010 48th Annual Allerton Conference on*, Sep. 2010, pp. 985–990.
- [20] S. R. Dalal, A. Jain, N. Karunanithi, J. M. Leaton, C. M. Lott, G. C. Patton, and B. M. Horowitz, “Model-based testing in practice”, in *Proceedings of the 21st International Conference on Software Engineering*, ser. ICSE '99, ACM, 1999, pp. 285–294.
- [21] P. Damaschke, “Adaptive versus nonadaptive attribute-efficient learning”, *Machine Learning*, vol. 41, pp. 197–215, 2000.
- [22] H. Dong, I. D. Chakares, C. H. Lin, A. Gersho, E. Belding-Royer, U. Madhow, and J. D. Gibson, “Selective bit-error checking at the MAC layer for voice over mobile ad hoc networks with IEEE 802.11”, in *IEEE Wireless Communications and Networking Conference (WCNC'04), Atlanta, GA*, 2004, pp. 1240–1245.

- [23] ———, “Speech coding for mobile ad hoc networks”, in *Asilomar Conference on Signals, Systems, and Computers (ACSSC’03)*, Pacific Grove, CA, vol. 1, 2003, pp. 280–284.
- [24] S. Dunietz, W. K. Ehrlich, B. D. Szablak, C. L. Mallows, and A. Iannino, “Applying design of experiments to software testing”, in *Proc. Intl. Conf. on Software Engineering (ICSE ’97)*, Los Alamitos, CA: IEEE, 1997, pp. 205–215.
- [25] M. M. El Saoud, “MANET reference configurations and evaluation of service location protocol for MANET”, Masters Thesis, Carleton University, 2005.
- [26] ETSI European Telecommunications Standards Institute, *Enhanced full rate (EFR) speech transcoding(GSM 06.60 version 8.0.1)*, ETSI Digital cellular telecommunications system (Phase2+), 1999.
- [27] ———, *Full rate speech, transcoding (GSM 06.10 version 8.2.0)*, ETSI Digital cellular telecommunications system (Phase2+), 2005-2006.
- [28] E. Fasolo, F. Maguolo, A. Zanella, M. Zorzi, S. Ruffino, and P. Stupar, “VoIP communications in wireless ad-hoc network with gateways”, in *Computers and Communications, 2007. ISCC 2007. 12th IEEE Symposium on*, Jul. 2007, pp. 69–74.
- [29] M. Fay and M. Proschan, “Wilcoxon-Mann-Whitney or t-test? On assumptions for hypothesis tests and multiple interpretations of decision rules”, *Statistics Surveys*, vol. 4, pp. 1–39, 2010.
- [30] S. Floyd, M. Handley, J. Padhye, and J. Widmer, “Equation-based congestion control for unicast applications: The extended version”, *SIGCOMM Computing Communications Review*, vol. 30, pp. 43–56, 2000.
- [31] M. Forbes, J. Lawrence, Y. Lei, R. N. Kacker, and D. R. Kuhn, “Refining the in-parameter-order strategy for constructing covering arrays”, *Journal of Research of the National Institute of Standards and Technology*, vol. 113, pp. 287–297, 2008.
- [32] C. Fraleigh, F. Tobagi, and C. Diot, “Provisioning IP backbone networks to support latency sensitive traffic”, in *IEEE Conference on Computer Communications (Infocom’03)*, San Francisco, CA, 2003, pp. 375–385.
- [33] S. Garg and M. Kappes, “Can I add a VoIP call?”, in *Communications, 2003. ICC ’03. IEEE International Conference on*, vol. 2, May 2003, pp. 779–783.
- [34] M. S. Gast, *802.11 Wireless Networks: The Definitive Guide*, 2nd ed. O’Reilly Media, Inc., 2005.
- [35] D. van Geyn, H. Hassanein, and M. El-Hennawey, “Voice call quality using 802.11e on a wireless mesh network”, in *Local Computer Networks, 2009. LCN 2009. IEEE 34th Conference on*, Oct. 2009, pp. 792–799.

- [36] S. Ghosh and C. Burns, “Comparison of four new general classes of search designs”, *Australian & New Zealand Journal of Statistics*, vol. 44, pp. 357–366, 2002.
- [37] S. Gilmour, “Factor screening via supersaturated designs”, in *Screening: Methods for Experimentation in Industry, Drug Discovery and Genetics*, A. Dean and S. Lewis, Eds., Springer New York, 2006, pp. 169–190.
- [38] A. Goldsmith, *Wireless Communications*. Cambridge University Press, 2005.
- [39] A. Goldsmith and S. B. Wicker, “Design challenges for energy-constrained ad hoc wireless networks”, *IEEE Wireless Communications Magazine*, vol. 9, no. 4, pp. 8–27, 2002.
- [40] G. Grinnemo and A. Brunstrom, “A simulation based performance analysis of a TCP extension for best-effort multimedia applications”, in *Proceedings 35th Annual Simulation Symposium (ANSS-35 2002), San Diego, California, USA, 14-18 April 2002*, 2002, pp. 327–336.
- [41] M. A. Hardy, “Regression with dummy variables”, in *Regression with Dummy Variables*, ser. Quantitative Applications in the Social Sciences 93. Newbury Park, CA: SAGE Publications, Inc., 1993.
- [42] A. Hartman, “Software and hardware testing using combinatorial covering suites”, in *Interdisciplinary Applications of Graph Theory, Combinatorics, and Algorithms*, M. C. Golumbic and I. B.-A. Hartman, Eds., Norwell, MA: Springer, 2005, pp. 237–266.
- [43] J. Hasegawa, H. Yomo, Y. Kondo, P. Davis, R. Suzuki, S. Obana, and K. Sakakibara, “Bidirectional packet aggregation and coding for VoIP transmission in wireless multi-hop networks”, in *Communications, 2009. ICC '09. IEEE International Conference on*, Jun. 2009, pp. 1–6.
- [44] A. S. Hedayat, N. J. A. Sloane, and J. Stufken, *Orthogonal Arrays*. New York: Springer-Verlag, 1999.
- [45] D. Hole and F. A. Tobagi, “Capacity of an IEEE 802.11b wireless LAN supporting VoIP”, in *Proceedings of IEEE International Conference on Communications (ICC'04)*, vol. 1, 2004, pp. 196–201.
- [46] D. S. Hoskins, C. J. Colbourn, and M. Kulahci, “Truncated D-optimal designs for screening experiments”, *American Journal of Mathematical and Management Sciences*, vol. 28, pp. 359–383, 2008.
- [47] D. S. Hoskins, C. J. Colbourn, and D. C. Montgomery, “D-optimal designs with interaction coverage”, *Journal of Statistical Theory and Practice*, vol. 3, pp. 817–830, 2009.

- [48] C. Hoxby, “The effects of class size on student achievement: new evidence from population variation”, *Quarterly Journal of Economics*, vol. 115, no. 4, pp. 1239–1285, Nov. 2000.
- [49] *IEEE standard 802.11: W-LAN medium access control & physical layer specifications*, Dec. 1999.
- [50] ITU-T Recommendation G.114, *One-way transmission time*, International Telecommunication Union, Geneva, 1996.
- [51] ITU-T Recommendation G.711.1, *Wideband embedded extension for G.711 pulse code modulation*, International Telecommunication Union, Telecommunication Standardization Sector, 2008.
- [52] ITU-T Recommendation G.723.1, *Dual rate speech coder for multimedia communications transmitting at 5.3 and 6.3 kbit/s*, International Telecommunication Union, Telecommunication Standardization Sector, 2006.
- [53] ITU-T Recommendation G.728, *Implementors guide for ITU-T recommendation G.728: coding of speech at 16 kbits/sec using low-delay code excited linear prediction*, International Telecommunication Union, Geneva, 1992.
- [54] ITU-T Recommendation G.729, *Coding of speech at 8 kbit/s using conjugate-structure algebraic-code-excited linear prediction (CS-ACELP)*, International Telecommunication Union, Telecommunication Standardization Sector, 2007.
- [55] ITU-T Recommendation P.800, *Methods for subjective determination of transmission quality*, International Telecommunication Union, Geneva, 1996.
- [56] ITU-T Recommendation P.830, *Subjective performance assessment of telephone-band and wideband digital codecs*, International Telecommunication Union, Telecommunication Standardization Sector, 1996.
- [57] ITU-T Recommendation P.862, *Perceptual evaluation of speech quality (PESQ): An objective method for end-to-end speech quality assessment of narrow-band telephone networks and speech codecs*, International Telecommunication Union, Geneva, 2001.
- [58] R. Jain, S. Munir, and J. Iyer, “Performance of VBR voice over ATM: Effect of scheduling and drop policies”, in *ATM Forum/97-0608*, 1997.
- [59] *JMP statistical software from SAS*, <http://www.jmp.com>, 2014.
- [60] B. Jones and C. J. Nachtsheim, “A class of three-level designs for definitive screening in the presence of second-order effects”, *Journal of Quality Technology*, vol. 43, no. 1, pp. 1–14, 2011.

- [61] V. Kawadia and P. R. Kumar, “A cautionary perspective on cross layer design”, *IEEE Wireless Communications Magazine*, vol. 12, no. 1, pp. 3–11, 2005.
- [62] K. Kim and S. Hong, “VoMESH: voice over wireless mesh networks”, in *Wireless Communications and Networking Conference, (WCNC) 2006. IEEE*, vol. 1, Apr. 2006, pp. 193–198.
- [63] S. Kim, M. Ji, and J. Ma, “Voice call capacity model for hybrid multi-channel protocol over multi-hop multi-channel multi-radio wireless mesh networks”, in *Advanced Communication Technology (ICACT), 2011 13th International Conference on*, Feb. 2011, pp. 1239–1244.
- [64] J. P. C. Kleijnen, “An overview of the design and analysis of simulation experiments for sensitivity analysis”, *European Journal of Operational Research*, vol. 164, pp. 287–300, 2005.
- [65] J. P. C. Kleijnen, B. Bettonvil, and F. Persson, “Screening for the important factors in large discrete-even simulation models: Sequential bifurcation and its applications”, in *Screening: Methods for Experimentation in Industry, Drug Discovery and Genetics*, A. M. Dean and S. M. Lewis, Eds., Springer-Verlag, 2006, ch. 13, pp. 287–307.
- [66] D. Kotz, C. Newport, R. S. Gray, J. Liu, Y. Yuan, and C. Elliott, “Experimental evaluation of wireless simulation assumptions”, in *Proceedings of the 7th ACM International Symposium on Modeling, Analysis and Simulation of Wireless and Mobile Systems (MSWiM '04)*, 2004, pp. 78–82.
- [67] D. Kuhn and M. Reilly, “An investigation of the applicability of design of experiments to software testing”, in *Proc. 27th Annual NASA Goddard/IEEE Software Engineering Workshop*, Los Alamitos, CA: IEEE, 2002, pp. 91–95.
- [68] D. R. Kuhn, D. R. Wallace, and A. M. Gallo Jr., “Software fault interactions and implications for software testing”, *IEEE Transactions on Software Engineering*, vol. 30, no. 6, pp. 418–421, Jun. 2004.
- [69] V. Kulkarni and M. Devetsikiotis, “Cross-layer response surface methodology applied to wireless mesh network voip call capacity”, in *Simulation Symposium, 2008. ANSS 2008. 41st Annual*, Apr. 2008, pp. 15–22.
- [70] S. Kurkowski, T. Camp, and M. Colagrosso, “MANET simulation studies: the incredible”, *SIGMOBILE Mobile Computing Communications Review*, vol. 9, no. 4, pp. 50–61, Oct. 2005.
- [71] R. Y. W. Lam, V. C. M. Leung, and H. C. B. Chan, “Polling-based protocols for packet voice transport over IEEE 802.11 wireless local area networks”, *IEEE Wireless Communications*, vol. 13, no. 1, pp. 22–29, 2006.



- [72] S. B. Lee and A. T. Campbell, “INSIGNIA: an IP-based quality of service framework for mobile ad hoc networks”, *Journal of Parallel and Distributed Computing*, vol. 60, no. 4, pp. 374–406, 2000.
- [73] R. Li and D. K. J. Lin, “Analysis methods for supersaturated designs: Some comparisons”, *Journal of Data Science*, pp. 249–260, 2003.
- [74] R. Li and D. K. J. Lin, “Analysis methods for supersaturated designs: Some comparisons.”, *Journal of Data Science*, pp. 249–260, 2003.
- [75] D. K. J. Lin, “Generating systematic supersaturated designs”, *Technometrics*, vol. 37, pp. 213–225, 1995.
- [76] D. K. J. Lin and N. R. Draper, “Generating alias relationships for two-level Plackett and Burman designs”, *Computational Statistics & Data Analysis*, vol. 15, no. 2, pp. 147–157, Feb. 1993.
- [77] W. Liwlompaisan and A. Phonphoem, “Call capacity improvement techniques for VoIP over wireless mesh networks”, in *Electrical Engineering/Electronics, Computer, Telecommunications and Information Technology, 2009. ECTI-CON 2009. 6th International Conference on*, vol. 2, May 2009, pp. 902–905.
- [78] H. B. Mann and D. R. Whitney, “On a test of whether one of two random variables is stochastically larger than the other”, *Annals of Mathematical Statistics*, vol. 18, pp. 50–60, 1947.
- [79] W. Mansouri, F. Zarai, K. Mnif, and L. Kamoun, “New scheduling algorithm for wireless mesh networks”, in *Multimedia Computing and Systems (ICMCS), 2011 International Conference on*, Apr. 2011, pp. 1–6.
- [80] C. Martínez, L. Moura, D. Panario, and B. Stevens, “Locating errors using ELAs, covering arrays, and adaptive testing algorithms”, *SIAM Journal on Discrete Mathematics*, vol. 23, no. 4, pp. 1776–1799, 2009.
- [81] M. Mathis, J. Semke, J. Mahdavi, and T. Ott, “The macroscopic behavior of the TCP congestion avoidance algorithm”, *SIGCOMM Computer Communication Review*, vol. 27, pp. 67–82, 1997.
- [82] D. E. McDysan and D. Spohn, *ATM Theory and Applications*. McGraw-Hill, 1999.
- [83] D. Miras, *A survey of network QoS needs of advanced Internet applications*, Internet2 QoS Working Group, Working Document, Dec. 2002.
- [84] D. C. Montgomery, *Design and Analysis of Experiments*, 8th ed. John Wiley & Sons, Inc. New York, 2012.
- [85] D. C. Montgomery, E. A. Peck, and C. G. Vining, *Introduction to Linear Regression Analysis*, 4th ed. John Wiley & Sons, Inc. New York, 2006.

- [86] A. Munjal, T. Camp, and W. Navidi, “Constructing rigorous MANET simulation scenarios with realistic mobility”, in *European Wireless Conference (EW)*, 2010, pp. 817–824.
- [87] R. H. Myers, D. C. Montgomery, and C. M. Anderson-Cook, *Response Surface Methodology, Process and Product Optimization Using Designed Experiments*, 3rd ed. John Wiley and Sons, Inc. New York, 2009.
- [88] R. H. Myers, G. Vining, A. Giovannitti-Jensen, and S. L. Myers, “Variance dispersion properties of second order response surface designs”, *Journal of Quality Technology*, vol. 24, no. 1, pp. 1–11, 1992.
- [89] P. Nayeri, C. J. Colbourn, and G. Konjevod, “Randomized postoptimization of covering arrays”, *European Journal of Combinatorics*, vol. 34, pp. 91–103, 2013.
- [90] C. Nie and H. Leung, “A survey of combinatorial testing”, *ACM Computing Surveys*, vol. 43, pp. 1–29, Feb. 2011.
- [91] NIST, *NIST/SEMATECH e-Handbook of Statistical Methods*, C. Croarkin, P. Tobias, J. J. Filliben, B. Hembree, W. Guthrie, L. Trutna, and J. Prins, Eds. NIST/SEMATECH, Apr. 2012. [Online]. Available: <http://www.itl.nist.gov/div898/handbook/>.
- [92] NITRD, *Networking and information technology research and development (NITRD) large scale networking (LSN) workshop report on complex engineered networks*, 2012.
- [93] Ns2, *The network simulator - ns-2*, [Online; accessed Jan-2015], 2012. [Online]. Available: <http://www.isi.edu/nsnam/ns>.
- [94] K. Nurmela, “Upper bounds for covering arrays by tabu search”, *Discrete Applied Mathematics*, vol. 138, no. 9, pp. 143–152, 2004.
- [95] S. A. Obeidat and V. R. Syrotiuk, “An opportunistic cross-layer architecture for voice in multi-hop wireless LANs”, *International Journal of Communications Systems*, vol. 22, no. 4, pp. 419–439, Apr. 2009.
- [96] S. A. Obeidat, “Cross-layer opportunistic adaptation for voice over wireless ad hoc networks”, PhD thesis, Arizona State University, Tempe, AZ, May 2008.
- [97] J. Okech, Y. Hamam, and A. Kurien, “A cross-layer adaptation for VoIP over infrastructure mesh network”, in *Broadband Communications, Information Technology Biomedical Applications, 2008 Third International Conference on*, Nov. 2008, pp. 97–102.
- [98] A. B. de Oliveira, S. Fischmeister, A. Diwan, M. Hauswirth, and P. F. Sweeney, “Why you should care about quantile regression”, *SIGARCH Comput. Archit. News*, pp. 207–218, Mar. 2013.

- [99] J. Padhye, V. Firoiu, D. Towsley, and J. Kurose, “Modeling TCP throughput: A simple model and its empirical validation”, *SIGCOMM Computing Communications Review*, vol. 28, pp. 303–314, 1998.
- [100] J. Padhye, V. Firoiu, D. F. Towsley, and J. F. Kurose, “Modeling TCP Reno performance: A simple model and its empirical validation”, *IEEE/ACM Transactions on Networking*, vol. 8, pp. 133–145, 2000.
- [101] S. Panwar, *Testbeds and the evolving research paradigm*, Panel on Network Testbeds at the 26th IEEE Computer Communications Workshop (CCW 2012), Nov. 2012.
- [102] N. Parvez, A. Mahanti, and C. Williamson, “An analytic throughput model for TCP New Reno”, *IEEE/ACM Transactions on Networking*, vol. 18, no. 2, pp. 448–461, Apr. 2010.
- [103] C. Perkins, O. Hodson, and V. Hardman, “A survey of packet loss recovery techniques for streaming audio”, in *IEEE Network*, 1998, pp. 40–48.
- [104] C. E. Perkins and E. M. Royer, “Ad hoc on-demand distance vector routing”, in *Proc. Second IEEE Workshop on Mobile Computing Systems and Applications*, 1999, pp. 90–100.
- [105] S. Poljak, A. Pultr, and V. Rödl, “On qualitatively independent partitions and related problems”, *Discrete Applied Mathematics*, vol. 6, no. 2, pp. 193–205, Jul. 1983.
- [106] R. Punnoose, P. Nikitin, and D. Stancil, “Efficient simulation of Ricean fading within a packet simulator”, in *IEEE Vehicular Technology Conference (VTC’00), Boston, MA*, 2000, pp. 764–767.
- [107] B. Raman, P. Bhagwat, and S. Seshan, “Arguments for cross-layer optimizations in bluetooth scatternets”, in *IEEE 2001 Symposium on Applications and the Internet*, 2001, pp. 176–184.
- [108] S. A. Ramprashad, D. Li, U. Kozat, and C. Pepin, “An analysis of joint aggregation, bursting, routing, and rate adaptation for increasing VoIP capacity in multi-hop 802.11 networks”, *Wireless Communications, IEEE Transactions on*, vol. 7, no. 8, pp. 3128–3139, Aug. 2008.
- [109] S. Rein, F. Fitzek, and M. Reisslein, “Voice quality evaluation for wireless packet voice: A tutorial and performance results for ROHC”, *IEEE Wireless Communications*, vol. 12, pp. 60–76, Feb. 2005.
- [110] A. H. Ronneseth and C. J. Colbourn, “Merging covering arrays and compressing multiple sequence alignments”, *Discrete Applied Mathematics*, vol. 157, no. 9, pp. 2177–2190, May 2009.

- [111] B. Sadeghi, V. Kanodia, A. Sabharwal, and E. Knightly, “Opportunistic media access for multirate ad hoc networks”, in *International Conference on Mobile Computing and Networking (MobiCom’02)*, Atlanta, GA, 2002, pp. 24–35.
- [112] B. Schwartz and A. Grant, “Too much of a good thing: the challenge and opportunity of the inverted U”, *Perspectives on Psychological Science*, vol. 6, no. 1, pp. 61–76, Jan. 2011.
- [113] P. Seeling, M. Reisslein, F. H. P. Fitzek, and S. Hendrata, “Video quality evaluation for wireless transmission with robust header compression”, in *Fourth International Conference on Information, Communications and Signal Processing (ICICS’03)*, vol. 3, Dec. 2003, pp. 1346–1350.
- [114] G. Seroussi and N. H. Bshouty, “Vector sets for exhaustive testing of logic circuits”, *IEEE Transactions on Information Theory*, vol. 34, no. 3, pp. 513–522, May 1988.
- [115] D. E. Shasha, A. Y. Kouranov, L. V. Lejay, M. F. Chou, and G. M. Coruzzi, “Using combinatorial design to study regulation by multiple input signals: A tool for parsimony in the post-genomics era”, *Plant Physiology*, vol. 127, pp. 1590–1594, 2001.
- [116] S. Shenker, “Fundamental design issues for the future Internet”, *IEEE Journal on Selected Areas in Communications*, vol. 13, no. 7, pp. 1176–1188, Sep. 1995.
- [117] T. Shirakura, T. Takahashi, and J. N. Srivastava, “Searching probabilities for nonzero effects in search designs for the noisy case”, *The Annals of Statistics*, vol. 24, no. 6, pp. 2560–2568, 1996.
- [118] M. Siddique and J. Kamruzzaman, “VoIP call capacity over wireless mesh networks”, in *Global Telecommunications Conference, 2008. IEEE GLOBECOM 2008. IEEE*, Nov. 2008, pp. 1–6.
- [119] M. Siekkinen, G. Urvoy-Keller, and E. W. Biersack, “On the interaction between Internet applications and TCP”, in *International Teletraffic Congress*, L. Mason, T. Drwiega, and J. Yan, Eds., ser. Lecture Notes in Computer Science, vol. 4516, Springer, 2007, pp. 962–973.
- [120] S. Singh, P. A. Acharya, U. Madhow, and E. M. Belding-Royer, “Sticky CSMA/CA: Implicit synchronization and real-time QoS in mesh networks”, *Ad Hoc Networks*, vol. 5, no. 6, pp. 744–768, 2007.
- [121] P. L. Smith, “Splines as a useful and convenient statistical tool”, *The American Statistician*, vol. 33, no. 2, pp. 57–62, 1979.
- [122] Speex, *Speex: A free codec for free speech*, [Online; accessed July-2009], 2009. [Online]. Available: <http://www.speex.org>.

- [123] K. Sriram and M. H. Sherif, “Voice packetization and compression in broadband ATM networks”, *IEEE Journal on Selected Areas in Communications*, vol. 9, no. 3, pp. 294–304, 1991.
- [124] J. N. Srivastava, “Designs for searching non-negligible effects”, in *A Survey of Statistical Design and Linear Models*, J. N. Srivastava, Ed., North-Holland, Amsterdam, 1975, pp. 507–519.
- [125] V. Srivastava and M. Motani, “Cross-layer design: A survey and the road ahead”, *IEEE Communications Magazine*, vol. 43, no. 12, pp. 112–119, 2005.
- [126] W. Stallings, *High Speed Networks: TCP/IP and ATM Design Principles*. Prentice Hall, 1998.
- [127] D. T. Tang and C. L. Chen, “Iterative exhaustive pattern generation for logic testing”, *IBM Journal Research and Development*, vol. 28, no. 2, pp. 212–219, 1984.
- [128] Y. Tang, C. J. Colbourn, and J. Yin, “Optimality and constructions of locating arrays”, *J. Stat. Theory Pract.*, vol. 6, no. 1, pp. 20–29, 2012.
- [129] The Monarch Group, *The Monarch project: Wireless and mobility extensions to ns-2*, <http://www.monarch.cs.rice.edu/cmu-ns.html>, [Online; accessed March-2014], 2014.
- [130] J. Torres-Jimenez and E. Rodriguez-Tello, “New upper bounds for binary covering arrays using simulated annealing”, *Information Sciences*, vol. 185, no. 1, pp. 137–152, Feb. 2012.
- [131] T. Ue, S. Sampei, N. Morinaga, and K. Hamaguchi, “Symbol rate and modulation level-controlled adaptive modulation/TDMA/TDD system for high-bit-rate wireless data transmission”, *IEEE Transactions on Vehicular Technology*, vol. 47, no. 4, pp. 1134–1147, 1999.
- [132] K. K. Vadde and V. R. Syrotiuk, “Factor interaction on service delivery in mobile ad hoc networks”, *IEEE Journal on Selected Areas in Communications*, vol. 22, no. 7, pp. 1335–1346, 2004.
- [133] M. A. Visser and M. El Zarki, “Voice and data transmission over an 802.11 wireless network”, in *IEEE International Symposium on personal, indoor, and mobile radio communications (PIMRC'95), Toronto, Canada*, 1995, pp. 648–652.
- [134] W. Wang, S. C. Liew, and V. O. K. Li, “Solutions to performance problems in VoIP over a 802.11 wireless LAN”, *IEEE Transactions on Vehicular Technology*, vol. 54, no. 1, pp. 366–384, 2005.
- [135] P. J. Werbos, “Beyond regression: new tools for prediction and analysis in the behavioral sciences”, PhD thesis, Harvard University, 1974.

- [136] F. Wilcoxon, “Individual comparisons by ranking methods”, *Biometrics Bulletin*, vol. 1, pp. 80–83, 1945.
- [137] C. Wu and M. Hamada, *Experiments: Planning, Analysis and Parameter Design Optimization*, English, ser. Wiley Series in Probability and Statistics. John Wiley and Sons, Inc. New York, 2011.
- [138] I. Yeom and A. L. N. Reddy, “Modeling TCP behavior in a differentiated services network”, *IEEE/ACM Transactions on Networking*, vol. 9, no. 1, pp. 31–46, Feb. 1999.
- [139] C. Yilmaz, M. B. Cohen, and A. Porter, “Covering arrays for efficient fault characterization in complex configuration spaces”, *IEEE Transactions on Software Engineering*, vol. 29, no. 4, pp. 45–54, Jul. 2004.
- [140] C.-h. Yu, “Experimental design as variance control”, *Design of experiments*, 2009. [Online]. Available: <http://www.creative-wisdom.com/teaching/WBI/>.
- [141] B. Zhou, C. P. Fu, D.-M. Chiu, C. T. Lau, and L. H. Ngoh, “A simple throughput model for TCP Reno”, in *Proceedings of the IEEE International Communications Conference (ICC’06)*, 2006.
- [142] E. Ziouva and T. Antonakopoulos, “CBR packetized voice transmission in IEEE 802.11 networks”, in *IEEE Symposium on Computers and Communications, Hammamet, Tunisia*, 2001, pp. 392–398.
- [143] M. Zorzi, A. Chockalingam, and R. R. Rao, “Throughput analysis of TCP on channels with memory”, *IEEE Journal on Selected Areas in Communications*, vol. 18, pp. 1289–1300, 2000.

## APPENDIX A

### LOCATING ARRAYS FOR SCREENING ENGINEERED SYSTEMS

## A.1 Factors and Levels used in the MANET Case Study

Table A.1 gives the 75 controllable factors in the ns-2 simulator identified for experimentation. The column labelled “LA” gives the column  $j$  in which the factor  $F_j$  occurs in the locating array (LA),  $1 \leq j \leq 75$ . They are grouped (more or less) by Application down the protocol stack. The column labelled “ $l_j$ ” is the number of levels for the factor  $F_j$ . The column labelled “Factor” is the variable name utilized in ns-2. Finally, the columns under “Levels” give the levels  $L_j = \{v_{j,1}, \dots, v_{j,l_j}\}$  for factor  $F_j$ . The levels in bold are the default values in the ns-2 simulator.

Table A.1: Factors and levels in the MANET.

LA	$l_j$	Factor	Levels															
		<b>Application</b>																
67	10	APP_flows_	1	2	4	6	8	10	12	14	16	18						
		<b>Transport (TCP)</b>																
47	6	TCP_window_	1	5	10	15	<b>20</b>	40										
0	2	TCP_windowInit_	<b>2</b>	5														
68	10	TCP_packetSize_	64	128	256	512	768	1024	1280	1536	1792	2048						
1	2	TCP_tcpip_base_hdr_size_	20	<b>40</b>														
2	2	TCP_overhead_	<b>0</b>	0.01														
29	3	TCP_maxburst_	<b>0</b>	3	4													
		<b>TCP timer mechanism</b>																
4	2	TCP_srtt_init_	<b>0</b>	1														
5	2	TCP_rttvar_init_	0	<b>12</b>														
6	2	TCP_rtxcur_init_	3	6														
7	2	TCP_T_SRTT_BITS_	1	<b>3</b>														
8	2	TCP_T_RTTVAR_BITS_	2	4														
9	2	TCP_RTTvar_exp_	2	4														
10	2	TCP_tcpTick_	<b>0.01</b>	0.1														
49	6	TCP_min_RTO_	0.1	<b>0.2</b>	10	20	30	40										
11	2	TCP_ts_resetRTO_	<b>false</b>	true														
12	2	TCP_updated_rttvar_	false	<b>true</b>														
		<b>TCP congestion control mechanism</b>																

Continued on next page



Table A.1 – continued from previous page

LA	#L	Factor name	Levels									
3	2	TCP_control_increase_	0	1								
13	2	TCP_precisionReduce_	false	true								
28	3	TCP_numdupacks_	2	3	4							
14	2	TCP_numdupacksFrac_	-1	10								
30	3	TCP_decrease_num_	0.5	1.0	2.0							
31	3	TCP_increase_num_	0.5	1.0	2.0							
48	6	TCP_maxcwnd_	0	1	4	8	16	32				
15	2	TCP_noFastRetrans_	false	true								
16	2	TCP_slow_start_restart_	false	true								
		<b>Random Waypoint (RWP) mobility Model</b>										
62	8	RWP_Nodes_	36	51	66	81	96	111	126	141		
43	5	RWP_Area_	8	16	24	32	40					
69	10	RWP_Node_speed_	4	8	10	12	14	16	18	20	22	
57	7	RWP_Node_pause_time_	0	1	5	10	15	20	30			
37	4	RWP_Scenario_Ratio_	1	2	3	4						
		<b>Ad hoc on-demand distance vector (AODV)</b>										
70	10	AODV_ACTIVE_ROUTE_TIMEOUT_	1	2	3	4	5	8	10	12	14	
50	6	AODV_MY_ROUTE_TIMEOUT_	2	4	6	8	10	12				
71	10	AODV_RREQ_RETRIES_	1	2	3	4	5	6	7	8	9	
63	8	AODV_NETWORK_DIAMETER_	3	5	7	10	15	20	30	35		
38	4	AODV_HELLO_INTERVAL_	0.1	0.5	1	10						
66	9	AODV_ALLOWED_HELLO_LOSS_	0	1	2	3	4	5	6	7	8	
44	5	AODV_NODE_TRAVERSAL_TIME_	0.01	0.02	0.03	0.04	0.05					
17	2	AODV_TTL_START_	1	5								
36	3	AODV_TTL_INCREMENT_	1	2	3							
32	3	AODV_TTL_THRESHOLD_	3	7	15							
		<b>Link</b>										
46	5	LL_delay_	2us	10us	25us	50us	100us					
		<b>Queue</b>										
72	10	Queue_ifqlen_	5	10	15	20	25	50	75	100	150	
19	2	Queue_interleave_	false	true								

Continued on next page

Table A.1 – continued from previous page

LA	#L	Factor name	Levels																	
20	2	Queue_acksfirst_	false	true																
21	2	Queue_ackfromfront_	false	true																
22	2	Queue_DT_drop_front_	false	true																
23	2	Queue_DT_summarystats_	false	true																
24	2	Queue_DT_queue_in_bytes_	false	true																
<b>IEEE 802.11b DCF MAC layer</b>																				
52	6	MAC_BeaconInterval_	0.01	0.05	<b>0.1</b>	0.2	0.5	1												
25	2	MAC_ScanType_	<b>PASSIVE</b>	ACTIVE																
53	6	MAC_ProbeDelay_	0.00001	0.00005	<b>0.0001</b>	0.0002	0.0005	0.001												
39	4	MAC_Min_Max_ChannelTime_	1	2	3	4														
54	6	MAC_ChannelTime_	0.012	0.06	<b>0.12</b>	0.24	0.6	1.2												
33	3	MAC_RTSThreshold_	0	1500	3000															
<b>IEEE 802.11b DSSS PHY layer</b>																				
73	10	DSSS_CWMin_CWMax_	0	1	2	3	4	5	6	7	8	9								
26	2	PLPC_Preamble_	72	<b>144</b>																
51	6	MAC_802_11_SlotTime_	0.000005	0.000010	0.000015	<b>0.000020</b>	0.000025	0.000030												
<b>PHY/WirelessPhy</b>																				
40	4	PHY_Wir_bandwidth_	1e6	<b>2e6</b>	5.5e6	11e6														
74	10	PHY_Wir_RXThresh_m_	25	50	75	100	125	150	175	200	225	<b>250</b>								
41	4	PHY_Wir_CPThresh_	1.59	5.98	6.99	<b>10.0</b>														
45	5	PHY_Wir_freq_	868e+06	<b>914e+06</b>	2412e+06	2437e+06	2462e+06													
59	7	PHY_Wir_L_	<b>1.0</b>	1.5	2.0	2.5	3.0	3.5	4.0											
<b>Radio propagation model</b>																				
35	3	Propagation_	<b>TwoRayGround</b>	FreeSpace	Shadowing															
<b>Energy Model</b>																				
64	8	ENER_initialEnergy_	4	7	10	13	16	20	25	50										
60	7	ENER_txPower_	0.01	<b>0.02</b>	0.03	0.04	0.05	0.06	0.07											
61	7	ENER_rxPower_	0.10	0.25	0.40	0.55	0.70	0.85	1.0											
42	4	ENER_idlePower_	0.0001	0.001	0.0055	0.01														
58	7	ENER_sleepPower_	0.001	0.002	0.003	0.004	0.005	0.010	0.015											
65	8	ENER_transitionPower_	0.001	0.005	0.01	0.05	0.1	0.15	0.2	0.3										

Continued on next page

Table A.1 – continued from previous page

LA #L	Factor name	Levels									
55	6	ENER_transitionTime_	0.0001	0.0005	0.001	0.005	0.01	0.05			
		<b>Error Model</b>									
18	2	ErrorModel_ranvar_	Uniform	Exponential							
34	5	ErrorModel_rate_	1.0E-07	1.0E-06	1.0E-05						
56	6	ErrorModel_FECstrength_	1	2	3	4	5	6			
27	2	ErrorModel_unit_	pkt	bit							

## A.2 Description of Factors and Levels used in the MANET Case Study

Table A.2 provides a brief description of each factor. For referencing, they are listed in the same order appearing in Table A.1.

Table A.2: Description of the factors.

Factor name	Unit	Description
<b>Application FTP</b>		
APP_flows_	flows	Number of flows
<b>Transport</b>		
TCP_window_	bytes	Upper bound on window size, RFC 1323, in 16 bits 65534
TCP_windowInit_	bytes	Initial value of window size
TCP_packetSize_	bytes	TCP packet size in bytes
TCP_tcpip_base_hdr_size_	bytes	TCP basic header size in bytes
TCP_overhead_	sec	The range of a uniform random variable used to delay each output packet
TCP_maxburst_	bytes	Maximum number of bytes that a TCP sender can transmit in one transmission
<b>Variables related to TCP timer mechanism</b>		
TCP_srtt_init_	tcpTick	Initial value of t_srtt_
TCP_rttvar_init_	tcpTick	Initial value of t_rttvar_
TCP_rtxcur_init_	tcpTick	Initial value of t_rtxcur_
TCP_T_SRTT_BITS_	bits	Multiplicative factor for smoothed RTT, (alpha)
TCP_T_RTTVAR_BITS_	bits	Multiplicative factor for RTT deviation (beta)
TCP_RTTvar_exp_	unit	Multiplicative factor for RTO computation
TCP_tcpTick_	secs	Timer granularity in seconds, simulation time unit
TCP_min_RTO_	secs	Lower bound on RTO
TCP_ts_resetRTO_	boolean	Set to true to un-back-off RTO after any valid RTT measurement.
TCP_updated_rttvar_	boolean	Update rttvar
<b>TCP congestion control mechanism</b>		
TCP_control_increase_	boolean	If set to 1, do not open the congestion window when the network is limited
TCP_precisionReduce_	boolean	Precision
TCP_numdupacks_	unit	Number of duplicated ACKs which triggers Fast Retransmit
TCP_numdupacksFrac_	boolean	If set 1, sender will transmit new packets upon receiving first few duplicated ACK packets
TCP_decrease_num_	unit	Window decreasing factor
TCP_increase_num_	unit	Window increasing factor

Continued on next page

Table A.2 – continued from previous page

<b>Factor name</b>	<b>Unit</b>	<b>Description</b>
TCP_maxcwnd_	unit	Upper bound on cwnd_
TCP_noFastRetrans_	boolean	Fast retransmit
TCP_slow_start_restart_	boolean	Slow start restart
<b>Random Waypoint Mobility Model</b>		
RWP_Nodes_	unit	Number of nodes
RWP_Area_	unit	X, Y sides. Modified by scenario ratio and transmission threshold
RWP_Node_speed_	m/sec	Speed of node movement (m/secs)
RWP_Node_pause_time_	sec	Time stopped at destination (secs)
RWP_Scenario_Ratio_	unit	1x1, 1x2, 1x3, 1x4
<b>AODV</b>		
AODV_ACTIVE_ROUTE_TIMEOUT_	sec	Static parameter that defines how long a route is kept in the routing table.
AODV_MY_ROUTE_TIMEOUT_	sec	[1..10]
AODV_RREQ_RETRIES_	unit	Number of times AODV will repeat expanded ring search for a destination.
AODV_NETWORK_DIAMETER_	hops	Maximum possible number of hops between two nodes in the network.
AODV_HELLO_INTERVAL_	sec	1,000 Milliseconds <a href="http://tools.ietf.org/html/rfc3561">http://tools.ietf.org/html/rfc3561</a>
AODV_ALLOWED_HELLO_LOSS_	packets	<a href="http://tools.ietf.org/html/rfc3561">http://tools.ietf.org/html/rfc3561</a>
AODV_NODE_TRAVERSAL_TIME_	sec	Estimate of the average one hop traversal time
AODV_TTL_START_	sec	[1..10]
AODV_TTL_INCREMENT_	sec	[1..20]
AODV_TTL_THRESHOLD_	sec	[1..10]
<b>Link</b>		
LL_delay_	us	Time needed to deliver an entire packet
<b>Queue</b>		
Queue_ifqlen_	packets	Interface Queue Length, max packet in ifq
Queue_interleave_	boolean	Interleave
Queue_acksfirst_	boolean	ACK first
Queue_ackfromfront_	boolean	ACK from front
<b>Drop Tail</b>		
Queue_DT_drop_front_	boolean	Use of drop front queue or not (Queue/DropTail)
Queue_DT_summarystats_	boolean	Summary of statistics
Queue_DT_queue_in_bytes_	boolean	Default false, meaning packets.
<b>IEEE 802.11b DCF MAC layer</b>		

Continued on next page

Table A.2 – continued from previous page

<b>Factor name</b>	<b>Unit</b>	<b>Description</b>
MAC_BeaconInterval_	sec	Packet broadcast by the router to synchronize the wireless network
MAC_ScanType_	unit	Active, Passive scanning
MAC_ProbeDelay_	sec	Ensures that an empty or lightly loaded channel does not completely block the scan
MAC_Min_Max_ChannelTime_	sec	Default Min 5ms Max 11 ms
MAC_ChannelTime_	sec	120 ms default value in ns2
MAC_RTSThreshold_	bytes	ON = 0, OFF= 3000 bytes. Reduce frame collisions introduced
<b>IEEE 802.11b DSSS PHY layer</b>		
DSSS_CWMin_CWMax_	unit	[Minimum, Maximum] Contention Window
PLPC_Preamble_	unit	Preamble Length & Header, Short 72+48, Long 144+48 (96usecs, 192usecs respectively)
MAC_802_11_SlotTime_	secs	If channel busy during the DIFS interval, the station should defer its transmission
<b>PHY/WirelessPhy</b>		
PHY_Wir_bandwidth_	Mbps	Bandwidth
PHY_Wir_RXThresh_m_	watts	Receive power threshold (W)
PHY_Wir_CPTthresh_	dB	Capture threshold (db): Initialize the SharedMedia interface
PHY_Wir_freq_	Mhz	A device working frequency band, the number of channels supported are 11.
PHY_Wir_L_	unit	System-loss factor
<b>Radio propagation model</b>		
Propagation_	type	Radio propagation
<b>Energy Model</b>		
ENER_initialEnergy_	joules	Energy the node has at the beginning of the simulation
ENER_txPower_	watts	Power consumption for transmission, Energy usage for every packet it transmits
ENER_rxPower_	watts	Power consumption for reception, Energy usage for every packet it receives
ENER_idlePower_	watts	Idle power consumption (W)
ENER_sleepPower_	watts	Power consumption (Watt) in sleep state
ENER_transitionPower_	watts	power consumption (Watts) in state transition from sleep to idle (active)
ENER_transitionTime_	sec	time (sec) used in state transition from sleep to idle (active)
<b>Error Model</b>		
ErrorModel_ranvar_	unit	Data distribution to compare error rate
ErrorModel_rate_	%	Error probability rate
ErrorModel_FECstrength_	bits	Number of bits that can be corrected/recovered per packet
ErrorModel_unit_	unit	Unit of data in errors

### A.3 The Locating Array

Table A.3 gives the  $421 \times 75$   $(\bar{1}, \bar{2})$ -locating array  $A = (a_{ij})$  used for screening, *i.e.*, it has 421 design points for the 75 factors. Entry  $a_{ij}$  contains the number of the level assigned to factor  $F_j$  in design point  $i$ ,  $1 \leq i \leq 421, 1 \leq j \leq 75$ , *i.e.*,  $a_{ij} \in \{0, 1, \dots, \ell_j - 1\}$ . The first column is not part of the array; it is simply the number of the design point. The first row is also not part of the array; it is the number of levels  $\ell_j$  for factor  $F_j$  (in column  $1 \leq j \leq 75$ ).

While the order of the columns is not important, the columns are ordered left-to-right by factors with increasing number of levels; *i.e.*, the first 28 columns of the LA are the binary factors, whereas the last 8 columns are for factors with 10 levels.

Table A.3: The  $(\bar{1}, \bar{2})$ -locating array used in experimentation.

$i$	Index $k, k \in \{0, \dots, \ell_j - 1\}$ of level in $L_j$ of factor $F_j$ in design point $i$
1	011100011001001110110011110112220012032002233102140525311230445012345811182
2	100011111101101100111101100011222111220122344443112043545016406405394107117
3	11011111001110000000000001010220110013311200420100522133235514111014217224
4	111001011110100101011111011021222110220012021033033515353120036241725476817
5	010010111011011010011101000111110022200322211433444213012230412621317734381
6	010111011001100010100010000022112201203103111433003015350133602517555241962
7	100001111000000011101010111112220222132231244132035210405625646042760166869
8	101011101111100111110010100011220100110310224213442305312454114012451552166
9	11011111111100101101110111000222201233202040043520151031125140001133235939
10	000001100111000011101001001121201021120201044240333405043260517165556501815
11	100011110000011100101011000010220012122021220141213030213121010412127182397
12	101110101001000110111100001120210121230200321420001432355154063112112108592
13	010001001001001111010000001020020110133203202114330133145056232306691637652
14	101111001101010011010110011120001120201010041241055005250503304513604791243
15	010100100001111111010010011110211110033310324114344341405623340544239957866
16	111000010100011101100111100011202120120032014112302033100503231541278299417
17	011110100101001100101101000012020021112022013244351201402233651545363189461
18	000111101100100111010010111020120021013203001434201253441162537244148068981
19	100011111110101110010010111121220111221103040000140132230525330612577323259
20	110101101110001100001011011011011120112111103322242041231004050376452375917

Continued on next page

Table A.3 – continued from previous page

$i$	Index $k, k \in \{0, \dots, \ell_j - 1\}$ of level in $L_j$ of factor $F_j$ in design point $i$
21	011101101011000000001010000120201121123333022334221140052261603416031493385
22	11101000100100110100110011111111220110213202323345504110532457710832877139
23	011011110000001110101011010110000110001202140312314534524453310144727703649
24	101001101110100011011101101021112120212210114115425011453164631571302582129
25	110111110000011011111011111102210122110233302415451342425240327101085304548
26	010110101111101001101100110012000010103101343203250223423110666322074293572
27	101101100001110111010001110000112122013112321114024414122611125621259179052
28	011111010011001000010000111110201212102013310041241503513120044107157698034
29	110111101001110110111100101011222122002231200232131400050132266474446584004
30	00110001101011101101001001002221102210012311134112023554533247335637463514
31	000111010101000000100001010121211102113313233412524250120156261170825982204
32	111100011111000000010011110000022211021323133304332514002643464230512877406
33	011100010000111010000100100012022110231101140440442530002052320260874566332
34	000111011111110010010000000100200121112122233124150531313352630445003175968
35	110011010010001100000000000112112202121213020205431114411210217305498061968
36	000101101100001110011101101112111111013213210101431452502250543007776929498
37	000110011101101100101110011011120122113333033334240054354605235535861469320
38	001001111010101000110011101001202202112223302142552154122155407715669215830
39	111000011001100011000001000111001222030330302402004020504503023607725054473
40	110111000111010111010001001100001210203302212113414504330311651222260533765
41	110010000111000101101000001002212001103022033230534422231466463062548451937
42	000011010000110111100001011021201222203201102201143405500634523721483347937
43	110101010001000100101101011121200021031222034021435145103124505517608226497
44	110000011110011000000100010001012212020221322405413143554403413100263790294
45	010101111011000000010111001102000121111100321300510245044560627323218652283
46	001100001111100100011100010000000102130330240025021310402133152617883535764
47	0101100000000000001110101011001201210021120213432523115302611542277036319458
48	101001000001011010101001010022012000210110013444403252404300516124781285456
49	011111110101110110111111101022022112031130343245454552254432357414566184938
50	101000101111000101000000111010211010131232131205413330450662555745489078621
51	101011110111000110110111100010111202222133112031320354501416543322254964621
52	111110000100111011101101100000122120131301213301104320155263164622179666183

Continued on next page



Table A.3 – continued from previous page

$i$	Index $k, k \in \{0, \dots, \ell_j - 1\}$ of level in $L_j$ of factor $F_j$ in design point $i$
53	101011101111000001001110010111212112020123314022224400143635055723816627803
54	011000010010111000111010011110101201033031002042402415104031666457396513805
55	000110000010011010001010101111020020020230201200423405024442356576139641780
56	001101010110010101100001001100101022113020241000115401515166252222394286079
57	110111110011001010010111011020002200003301140443351345334041201420149172019
58	110000001110010110001010111011200221111310130244221110055412541416654052559
59	001001101111110000101001011011222221211233102325433122324566563623887936112
60	010000101000100100001001001000000001212311332000040230141160145055672821146
61	010110001110110101110111100010010211030202243025015055053516642406431709622
62	001011010101000111111101111101112001033231213401043003231643240551300795356
63	010111000101101001110101010021101220133000311001512301243524465753050480741
64	000000001111110100000001110111111100202001043201223131011042024116580369886
65	101110111000111011011110000111211202103313234311043034135236212357409080310
66	000011010010101101110111111002020002203332033132050223154564460063707039591
67	101110010000010010110111110120101021201312004124240321544123551323592918572
68	000011110000011011111100110101022021012210234003144105011203125315488442763
69	011010100000101000101001100022022202032021024105531001300411037406834738763
70	101000111010101000101111100001010202103310031105052022412664227661635674393
71	101000110010110001100100001102000201223010300140343050025556103033346279786
72	000000110000111110001100010002012200212201320414425201335614565236534125889
73	111101100100001011011001010101120112203021031124200255222366044527618044066
74	111100000000000011101111100100100000130103300410235130554146426607477942331
75	110101010101110001000100001012100112210110011000304110214110060035688834635
76	001000001000011011100010001100100021113300304332451314332162441622748727114
77	001100100110101101000001010000221211222112031223300111524142222205536784160
78	110000111111000111001010101121210111112132301300035543434315003762322670160
79	000100000001011100100000110022122000200223010023442420410635325724408559640
80	101011100000111100100010101100012001201002023303511554102331243322800596794
81	001000000001100011001010010100011200200011103203345543453332644521692402794
82	010001010100000100001010011020220220031032021214555131525134017027471381274
83	110000110011111100000000100100102012201113041133123021111321305230763958224
84	001000100001110101100100100101000010011020002301541511143334537735557244219

Continued on next page

Table A.3 – continued from previous page

$i$	Index $k, k \in \{0, \dots, \ell_j - 1\}$ of level in $L_j$ of factor $F_j$ in design point $i$
85	011000001101111001000101101010110102210011041032500030245010210175335123799
86	000010000110111111010000101001110001020000310015211312150325312575621122842
87	101110111001011010110110111002221110022000131234401551554502143434430935845
88	000100000110111101010110011002122000210303032034145002104231224204392902313
89	010010110101011000011101100120020110210101130000541513000536051132191021378
90	100011001010101110000000010112002022232102312341020510551413434571381917378
91	001000001010100000100010100121001012101012104340230121005364615321103192858
92	101000101000010110011100101100002011203301141101543504010102344731155863902
93	001001010110001000000110110020010000110202330040402143201350406706230759902
94	001101011100111111100000010100110001202311024035044130212101607120026638482
95	100101010010010000011010010100100201003131320403114001522165510742610605427
96	011100101101111011010111110000011200010103041021322244221606602430100591427
97	010000100000101010000000101110101000031310221013103240341215111027880470907
98	010001011100010000001100000122000101021022040021402510023230327333289437051
99	000100010100110010011000101022011022222232111233515301422140127332393614197
100	111001100000000101000000000000102000020012010315100525334166134266855207501
101	001000000011001001011011100001002011132210204211225032204332456304223398121
102	110111010001111100101110001011102222033000102025015043133615112140538462125
103	100110010010110010110010110112121120033123220033050021242011440561353867605
104	110110101000100010010110000100021201200232121125200422435240265547438225096
105	101101001010110001110010011101112120220220002001141520302346247044224111396
106	100110001000111111110111001000101100222213134025104315545452036346008090272
107	011101100011000010011011111020200110202320011133410041102100560243835140370
108	100011110111100001111110101011112201000230203113323535342061362040650036974
109	000011100111111011011100101121220111200001301110312030053054234520435811451
110	011011111000010001100100000112120202101330310104330023242645525171192964857
111	000110001110100011110111001122111101232010003212355324500050202615887450857
112	000001100100100011010010010122210010211300122343033045404431441437062239337
113	000110111000010110100010110112201212130210101005104525423031451466510789732
114	010010000001010100001011000100121010020123124224514422223425266131305175736
115	1111101101000110000001000100020122001033321211202221024552025241333380354212
116	000000000101011101000111000020112211031013201412312450434421157245747603618

Continued on next page

Table A.3 – continued from previous page

$i$	Index $k, k \in \{0, \dots, \ell_j - 1\}$ of level in $L_j$ of factor $F_j$ in design point $i$
117	111010101010100100001000010110222012120010132012555451225344321042132599688
118	11000000110111111101010011022002201003110032304512034502245212537417448198
119	001001101111100100001001001010111000012020120121022512120535532615474118503
120	001001111101001101101000000101022002201101023013020130235366414242019304507
121	110000110110111001011011010021000222200102112213032231410353465333744885383
122	101100110011010001011000010012121022021010112445002420223320223745601332489
123	101101000110000000001010010022122122002122132205453053242235245652496068489
124	001101011011000010110110011101212000001230103203433402134133516434271407969
125	11001111110101000011010101102202122222131313221055312242024613262629453364
126	101110110001001110010110100000111010010332133212225413004015225414714143364
127	111010100010111111110101111012200000110232130122432413224460426336599622294
128	0111000000000000110010100110022000201001231113231224513530332324542356271240
129	001000000011100001100101010101111000211001001314211034313463656747541167240
130	110100110010111100111101100000202010011131122324021551241451037232826840720
131	010110001000010000100001111011022011101111233331411251013626435315216913874
132	100111110111001000001001111022021100221323122215453431531625167752201899079
133	110111000011100110111101100001221111102022104133140521524010400542786728354
134	001110010001001010111010110110022111210202130343031543022053334266805258347
135	100001001001010110001110010102212212021113142315003410523212650050590154347
136	100010011011111110010000010102111000001203223300452113120521247643575083827
137	010010011010001011010110110122210101021111314333040453441665102437431386671
138	01111110110001010110011101011011020112220020301425454213231156554585891043
139	000100000000000011011100000121001000020122141325300443552526533746860210163
140	100011001001110101100100011102221001132300040330551254341323203557484680010
141	000100000111101110100011010122001211222122123310334215410644055151379528916
142	011010011110111011101100001122020122130203232423300231011065040044154427490
143	101111100001010000000000101001020002221023224111244443035661561452379810158
144	110111010011110110000010001122211002001300323024100545220510057257164706156
145	110111111100000011111000101102001212032330040435003252552442337141899820616
146	111001100000001101110101101121110200220330341341050350533410527554163027492
147	00100101011001101110100001001120022202221004420414025450650366453858913492
148	011001101101110111001111100100202210111331311430351242312354554244663882972

Continued on next page

Table A.3 – continued from previous page

$i$	Index $k, k \in \{0, \dots, \ell_j - 1\}$ of level in $L_j$ of factor $F_j$ in design point $i$
149	011000000100010110010111101111100111222121004322000530541242307653058114729
150	111010111110100111110111111122201021232333134431414445541600521400713000723
151	010110000111011011000001001012200221232301344331332225032263242340528989209
152	110000001100001100101011100000012112111112002234125051045655641716842321065
153	011101101001100110001100100002121120202003214441030435452212123610637197065
154	010001100101111000000111001001122011023020244430230232104351104441412196545
155	100000011100010001101101011122212212013112334041005012552512033357647549201
156	101110101011101011000000101010020010021223041343403105552042420451422405201
157	111111100100110110110100101122200210132330330020303532314055141241207314783
158	101010111011100010000001000021120102032031034023104214110655623010421706538
159	011101101100100100111111110010011200230102003041251443202302112055216682538
160	001110010100111110101110101100122211220001204411440225311054243547091571018
161	111111101100111000010100110020102120103233200314052340512234136066859720443
162	011010110000011001010010111100112111003021142445112104510240046163644616526
163	00101000001000111110110000011212011203310110110520511102440305155342959593
164	000110011111010001110111010011001121132000104032441053323245557665362490708
165	001101000011100010001000000101121101113221300425305113154420405062157386718
166	1110111111101000101101111101011102011002113303015050100253666606651832265288
167	101011100000001111111101010010011121133202044022114152145524153261214871395
168	111001111101001111111010100122020211200000141320135502341145035375409769395
169	111000111000111000010110011011100212023001243105305004235310611750284648875
170	101001100110111001011011011121010201103022032023402302011405010364776156682
171	01010101010101100000001001100021020012130210310332124311434442102251461043082
172	000101100000100100010111001021111000220213140220121004002230620351045920560
173	100110100100000110100011111121201022100203003405043102553260554465128533570
174	110101001001001011111000001100122102200201330010100043130501446321813419670
175	010100111111110000111111010011202220000131310030352024302022120051798308150
176	111111001111011001111111111002020012102311322434500023415552665763480916267
177	010011101111010101110100110122200111212201141022011051333414303461275802267
178	00111010010100110101101101101200222211331032003211122021340423250750787747
179	011000111010001011111011111122101112221023021315402252143004166673731202954
180	11110011010110111111101000000002210220301022044030043245164523577526199954

Continued on next page

Table A.3 – continued from previous page

$i$	Index $k, k \in \{0, \dots, \ell_j - 1\}$ of level in $L_j$ of factor $F_j$ in design point $i$
181	000110000110011011100110000122222000201301343144430042441536641155011076084
182	101011001111100101101001000002111020130123101124013003023214625712093681549
183	101101010000111110110000010101200100001320210211321055435031547656788576541
184	101110010000101111101001111020210200011002124101235204212456364457563454021
185	111110101111111000111000010102020001002310113140430402443523354561245065139
186	101010110011100100111010100120010121011211012410155114110103017361030999149
187	110110000001100110100011100110002022112101014440321111022126326254715830619
188	01110110011000100100101110100200002222121221013155520311543251421507345820
189	000101100110011001011101100002112022111210210132525434241441352421392283896
190	100011001011000111010110010022110101201202110143214122123435025106167314306
191	000011111010001001000011001122111001012312121000515144545466637070391548562
192	000010111010100111000011101110110212110003032415252524134654331144186464462
193	110000111100110000100100001101021100222103034120314100111633512564861313042
194	010111111100100110111100100101120011123223134125401443310306665374820673259
195	010100100010110101000011101111221210222003304224143302213453504072615569459
196	000001101110101111011100010100000021221010213142215250030044425661490448639
197	001000011111010100001101100100101112103023334441552144411313425270549036307
198	010101000001001011110001110121202221233033103030024323505301203365334022007
199	110000111011111101010100010000011202112030200005230352544115230563119901587
200	000010000100010000101100110010011200112311102212021511510054256370268009945
201	010001111001011010000011011121221011211320324100222100340333112276753695645
202	001001101101011001001101001002100211202020200222521124523222063566738574624
203	010100111111010110110010111110101112003303220004114351010424006475687261191
204	110110110101000110111111011010111022230031101020103453312646462372772557093
205	001001000111111101100100100011212200220130142015235000205155010562557036973
206	100001011011010010101111001111112222023220103300003315131246613401200824131
207	100001001011100001001100100111111220002000241111012101503253045402591710731
208	10001101100100001101000101100220222000033301111121221133015624263276699311
209	101110010110111011110011101112200201012310012110035244103010406672415397680
210	000010011000010101010000101112212012023120321004221342312530110570002283683
211	101000010011010000001101000021001020120130301122303531120306131403085162663
212	000011011110101011110100101021210022032320241303340015331102055776394950428

Continued on next page

Table A.3 – continued from previous page

$i$	Index $k, k \in \{0, \dots, \ell_j - 1\}$ of level in $L_j$ of factor $F_j$ in design point $i$
213	010101000001000010011110011010212100023312213030301300000054622673829846528
214	110111000000100111101111001002212122133100012144213031435603317443604728904
215	001100110000111000010010000012212021102010021313555223411126021672753412276
216	011111010010011111001000100012020010013320121011532302031331413435648308076
217	110001101110011000001110111020002011032031201220004111430652251165623287356
218	01111110010110110110110110122110200020330130311322223120451133773672085114
219	110110010011111111011111011011011022023031203313051534023163535700467971652
220	001111100010001011001101110000021111003032311222134521223060007370242850694
221	010000010000011110000001011012212121100031114303231315222651216006024365791
222	101000111010100000010001000020020021223122142044152241430162462741019251711
223	111110000000001010110011111121000020231111122222341232311321142662196130201
224	100011111101100100110010001000020000103032340434501451511164201173297856400
225	101000011001011110110001110112022100131002040114235250430006653030082742410
226	001100100110000100100001100001021000003000311243100141132045634620767621920
227	010111011011001111100110101110120002023022343445214014532011037226473451749
228	101110110101001110101101100020111121002122204124154541555126615133268497819
229	010000010101110010110000001110101002033000301043300221003252102763043376399
230	100010111010011101000111110102020012200101221315053232444531227336650247108
231	101001100000101111100111011121201200233002020345215150524640407524445133108
232	011011101111010100110101101000201120103031120223341024030661150767220012688
233	01100001100111101100110110012212220223330210342344512314025360421836092517
234	111110101100010000100101101101002200021020334222030450153630001326621988517
235	001001101010100000110110000102121100200101230402515200454366052716406867087
236	110000100000001000110000011121210121100032220242450414135564264554012738926
237	111100010110001100111011010121000020121001310232312445541511536421107624936
238	110010011101100000111110011122022102233131310344221123055542122263583503476
239	101110100111100101011101111012012200003301242313025021325536550607109483235
240	111100001011000111100011110120201112100231043443113231353544532504894379245
241	101010000101100011001111010021221111101213314404550405533523603304679258705
242	100111100101000010101001100000202112033310340240431441530002005766705433851
243	101010101110110111111100000000211020032323042133451412144350141156606343171
244	010110000101111111100011000112002011233112123422530032020313530053021622831

Continued on next page

Table A.3 – continued from previous page

$i$	Index $k, k \in \{0, \dots, \ell_j - 1\}$ of level in $L_j$ of factor $F_j$ in design point $i$
245	00011111101111000100100010112212102222120202313512230421030420575777777777
246	001000101111100011011010011102202102030220024341342244305534063604562663777
247	110000011101100000010000111002011220033303303025423231111622254444247542257
248	100111000000111101011000110021111012130101303314555353300160155416327014985
249	001001011100101100001010010022122120021202144131215121200142437315112900985
250	111101001010110011000010001111202020030203324215245010301531314153897889465
251	011110100110000111001000100112201210101223022212544133244133465713233555516
252	110001101011100011010110010000112211113000102332210344255242414304678545410
253	001011001110011110110011001100012221122100104222420540121565453602123249015
254	100110000111001100111111100012221110220222244123154244100044520057340288062
255	000001000110011100101111011022000222200002042023213015111056162013139770272
256	0111111000100100011001110100222201111013124222014401023205424077007073172
257	110100000101011101000100100011110210033110344200312452443403044302186745309
258	111100111000010001001110110012201202130232330301222345254365453107871631309
259	110111011001001001101101000122022002100222023340500114105611633437656560889
260	000011101010001000010010111120202010212332010114425344025104504071366436281
261	010001110000110110011001011020012002200332042341301105223261433470349791866
262	100011111000010110101010011110012121111110124422143555352105664550143381833
263	000001101101001110011010110102100002210212111430345122232020434140861974413
264	111001111001100011001000111120000201120132121041012033235042022127126963043
265	100001010111111011011110100112201221202121330410130114440201367137341749593
266	100110000011011000000101000021102111213110232221314211301516230463462659173
267	110110000101100111101100010120112000010032231441521110115013613664297745273
268	000101101001010000001011000101221000131113231000552233023326412021124249925
269	100000000100011000011011010101122112102310214124515154441001364635894107256
270	100101001111001100100110110122010211012122303340422333144256531372684993236
271	010101000000000001111101011110122100022122330011533501015261127572464972716
272	11111001110110110000011001110110212001111104334422223100006636514251340697
273	01010010100000101011011011012022220130103222104151100232541113601546176697
274	001001100000111011110100101100111211101313203400332555125240316501721155177
275	01110111100001110100011100111112111033101021414002414141326360070643938740
276	000010101110100001101101110012112102022203111244125232050401252074458894750

Continued on next page

Table A.3 – continued from previous page

$i$	Index $k, k \in \{0, \dots, \ell_j - 1\}$ of level in $L_j$ of factor $F_j$ in design point $i$
277	001001111100000011010100101001111201100210113413353322301460133046213793230
278	10101110111100110101100011020221221230212223001243451210103526616748610312
279	111111001000111000110001111011122002011130210110253315430545000722533506362
280	010101001100010000010010110120001202232211311445533435342362251302318485822
281	011110001011100111000111100111000211033100130324224323413644656035099996990
282	001111010101000001011000101120012002231202002423441440353036227431784882990
283	001010001100011101000100110102021221212103124212204531445225500311065761474
284	110000111011010010011110000010010212131032200242003322330002630750754039866
285	000101000111001101000000000121221101110130131332300234523414312007049945853
286	001101010111011101000100000002122210101200221122405415514524661667324804340
287	011010011111111011100001011120120111110303043101303444251345216507160831584
288	101101011100010111011100011102200211113323122432233052023020650004555727524
289	111010011101101001110101101021111202212313334310043521334550351064030606005
290	010000100110111000110101101010001012131210042223524443204564131224308967511
291	11110100110001110011111111012122121022221141322114501101163103130193853581
292	101000100101011100100011001002120201022131314205200051112042354711878732091
293	11000001111110011110011001100222020120233300342222030352521103424688888888
294	111000110011011001101000110112000211223311142000143220542023016460673774888
295	101100010000010001011110010011000010211202034204510040443525364135458653368
296	010001000000001101110100110012100110010001222312124542405142630435095655155
297	101011110100010010010010101010110101113213032230242333410456227700566805585
298	101010000000011000010001110001201011232202132340155211043005346771627580035
299	110001011010111101011000110121221000113320232144120334155500410103719562048
300	01100000100110001100001101102102000011302001330500152500132162460504458048
301	001101000111001010100001101102021200022321301311014441242161315744589337528
302	011111110010100100110111001020112110011310344114155452002266207505170325542
303	000010011110111111000001110022112211100013044034411435221400021162865212941
304	110110110110110010001110100001200211021231110203451243125403212612740191421
305	111101111100100001011111110010222200100221242444325300235202557013761350600
306	111011000001111011100011111022012122232330244030131302020260234725533260030
307	000110011010101100111111110110202121021031122323403413044022546525764765538
308	000000111001110110001010011111202221100232034104414455113333330516505056050

Continued on next page



Table A.3 – continued from previous page

$i$	Index $k, k \in \{0, \dots, \ell_j - 1\}$ of level in $L_j$ of factor $F_j$ in design point $i$
309	1010101111000000111111111001011022122011203220200042124040532344247369842271
310	100101000000111000111000000121200202230322320334120540205410364354722331235
311	10111111111010000000111011010101212202131133223425540205351244142760385129684
312	000101001101001110111011000101012102021320322131014022324650034765170215614
313	000100001110001101011011001110202020130012234231112020425300205475855994334
314	101100100100010000101101001120001111210303203111223144250224341122437753939
315	111100110010001000000011001101120101123232000404111354251451305035730942175
316	10101010110101100011101101000101102022221221243545115313460106247775026835
317	011000000000110000000010001002002111211302144024030135444243125174620001630
318	011010000110111010001010011002022201011333311443522123501451401324306697666
319	011010111110001101101101010102001211102013331322412311013012600100500816110
320	100100111110001010110110000121111200203312002431421451142541412322055762555
321	011010011010001110011000000020021010222202120221032315155033513222840059555
322	000100111010010111010100101112100112231121243313313104541601041017525368015
323	101111111010111100101101101022120121013110013211553323104345663350265081656
324	111011011000110111000100000021020010132233201301152215322342122323067808849
325	010011001011011011000110010101210122231032004145042234330315557352705955035
326	001001000001110000111011010120210201221003010005210120421662026712265568253
327	011101011101011100001110110122120222210212330204044223442434641303204130841
328	100000110001111101000011110010120210113122213045134042245314032117004517032
329	011100100010000100000111000010100222001113333443140123231460060671180032143
330	10101001011111001110111110001222122032121122301342020550601360307017057946
331	111100011001110011001110010001122221001202320135454342530530102760795963026
332	010100111000110000001000001010102120210230133011232354143411351363380878434
333	000001010111010110001001100120011122132111213012052312052623362204002646444
334	101011010001110010000110111121022122200321241032524151415652043700373619929
335	110001111010110110101011001010011002133313024100020105000060303332444474444
336	101010011010000101100111101022210000010003230235114053320253450231239330426
337	100000101011101110100011011112001021123121331241515213203301447373138716240
338	100101001010001101111100111000222120103003032325312301452341644734123097323
339	100110110000111101101001111101111001210122110125533452021501446563151855961
340	000000100011111110001000101122220012123021232001200205021646054036200203260

Continued on next page

Table A.3 – continued from previous page

$i$	Index $k, k \in \{0, \dots, \ell_j - 1\}$ of level in $L_j$ of factor $F_j$ in design point $i$
341	000010010100011001110101011000011022022211330132504300254456066707252178350
342	101110110010100111110000101022121002113313223232153525031162602253698199333
343	01000000100101001000001100020101200133310023324314202024320366646779929969
344	000111010111100110011011001101210202131221110241342352424005514166440860872
345	001000100111101101011100011012021011121320021122155441330546014166127130434
346	001010010111001000010101010002002211130332324010435524445316652536477466526
347	000011100001110011101010110012200112203203303340113134332203416120392431524
348	10001101010101011101011011012022220012131142114325022055632036646826421136
349	010101100111010011100111110111111202021311231003503502524302165575682510435
350	001010000011100011111100001111220021220323110411051032251600414526584940699
351	110001111001001000111110111001211121212031100230234021300561546604669584679
352	101000110010110011110110001011100020021321232233132512111150622227883721608
353	001110010110101101010110111110002201021110023425424105315013154163782244055
354	000011001111111111011111000111010122011022114101433335112314316764483029180
355	111010111010110100100110110121221010031122203444555311141202042574070424553
356	010110111110100100111000001122012012132013100012525010200564644643736991005
357	000100100100110001010111001101102102012103134435531041314034224033073715645
358	101010110001111010000110100020212022102223044401551440550306363713115226148
359	000110101010110111111110110002001221011030003023210053532023315630000815006
360	110111011101100001111001101022021020111320232105325253415612212236145270590
361	000100001010010101010100100111202110212112212014021030104364305350578170596
362	0000010000010000000000001111020121000222122343111411350402342010660111394195
363	110011010110001011001001101000222202033113023424243530231554535542070700080
364	111011100100111100100011001000021100123013002320520410354206625210511660751
365	001001101110001101000001000101100111032220111321105434224422266410196275675
366	011000101011100011110110000101100211103012300241530140512206233250339380944
367	111010010101110011110001001120010001020030341433211201541504460056812019824
368	100000100111011100000011110000001211012302233212013215515223447753566262693
369	010011100110100010111001101101200111201223213221104423423115240301541447445
370	110100111101011000110101001122001002011223314405214500133125111205895541986
371	100101001111010100001001011121100020212011243305434504324451010525739445341
372	011011111000101110111111110121211221111230140410253452141256011433028537755

Continued on next page

Table A.3 – continued from previous page

$i$	Index $k, k \in \{0, \dots, \ell_j - 1\}$ of level in $L_j$ of factor $F_j$ in design point $i$
373	111011100111010110101000010010202120030130333345534424503141620036813124079
374	10111100001110011101011111111110100033211332341350132000311541632801101814
375	110110010000001001110011110120101121110122044335531310104654462406309103413
376	111111010101011011110100101022100020203111133134241230402424443245742425752
377	011110010100110111100101100100000011122210301403431224421321505754639414603
378	110101101111001110100001001000220110023111312222452202502626251763357466033
379	11101011000011001010101001011111000200313031034334425320131153520022922222
380	010001110111001101001111100102001210110331042234020525310545316625012518222
381	010000101010001010100000011000220111210123203201130351054634261737792094702
382	100010000111000100101010110000022111103030222015030152054303103377295713020
383	000100111000101010111101110002212011201033003102501533153405646244089609039
384	010101100101011110001001001121110212133113314122044521033116146667208587508
385	000011011011111110011000000112222022102120033134340234434043121426676352320
386	101100000010110000010100110110111220122331004025532043413616330275441234800
387	010100110101100101011001100010110210001201023042033000134652526644090752894
388	110111011111000101110100101111012222132003122114444301011031031204136648896
389	000100010011110101010000000012110111121303341232214120323630547470810527371
390	011101000010110001000010101110101121010230042213305435122130433705318046253
391	101110111111000111001101011012020120222023213403525103150235327415203902952
392	101000000111001010010000111020211212111303232140315120304665400725088811793
393	011011111010010010000010101011212121233131233200331415200205114504496210315
394	100100111101111101111011000102021022232323144212252044202552534377281126725
395	111111011101100000111110011020202222110220234043122243225516555170036005291
396	011010101111101011100000101111000121222010314011342035141021612344064523187
397	011101000000000101001001111011112021030203110230503414231263537110759419187
398	100011110111010110011101010020221101203203330234401330030502244171534398667
399	010110110010001011111001001100012110223110141244535345454653431511675634298
400	000111001100000001011000010012101122030212230130532202304125150216660526298
401	101101101101100110000010110011111120100232310232203340312213004503145409778
402	001111001011101101010101011020110021222031234404134353352240305617846543923
403	000011000000011000111000010021211210001212031122005510303633140015631873323
404	001111001001101000111100001101221112122030231120023030040453667645316352403

Continued on next page

Table A.3 – continued from previous page

$i$	Index $k, k \in \{0, \dots, \ell_j - 1\}$ of level in $L_j$ of factor $F_j$ in design point $i$
405	110111111010001110010111000020200202223132214030521213102120406711181053746
406	101001011110110101101000111112011020101313300343533002305001510112276940746
407	010001101101101010100010101021220110100000233002141441053253511152451828216
408	000101001010111010110010110112110211031011320320443523214503464217117120169
409	111110011101000111110111101000000220032002103003154325311210216212402316569
410	010110101100110000111111011110220122111221020021043300531535302001887295949
411	010000000001101110010001100111021101030331341444141541125025006217352905381
412	111011111101001011000110010110110212220320344430410553455604344014347892380
413	01111101010000000101110011102202122213333113435112330053136602534222776861
414	101000110101111110000111100101022100110033012340205215510140052516298372104
415	010011100000011101011001011012220020211112304230201345312216563442333966804
416	111110011001000000100001100020011000102032140400441015503523660005568147684
417	100111010101000100101111010002120202113122044141000024055510166415023849917
418	110001011110111101011001001011010010002122041103301202031411516611318735017
419	100111101010011010011011110102100202123231342132351443031446112631634508533
420	11111010111111101010010010020210211230120320402322403145120304600562570018
421	100010101100100011111001011001120012001023044342443435432302150772634970618

## A.4 Grouping of Factors

The locating array is designed for 75 factors of mixed levels, *i.e.*, the number of levels of factors is unequal. As a result, the locating array covers (factor, level) combinations (main effects) and pairs of (factor, level) combinations (two-way interactions) different numbers of times. This resulted in the sets  $S$  and  $\bar{S}$  in the screening algorithm having high variance making direct comparison impossible. As a consequence, we decided to group factors and two-way interactions into groups covered about the same number of times.

The factors with  $i$  levels are expected to be covered about  $\lfloor 421/i \rfloor$  times in the locating array,  $2 \leq i \leq 10$ . Figure A.1 shows the coverage for (factor, level) combinations. The  $x$ -axis gives the number of times each (factor, level) combination is covered, and the  $y$ -axis gives the frequency of such coverage. On the left side of the figure are the (factor, level) combinations for factors with the largest number of levels (*i.e.*, 10 levels); on the right side are the (factor, level) combinations for factors with the lowest number of levels (*i.e.*, 2 levels). We choose the midpoint  $\lfloor \frac{421(\frac{1}{i} + \frac{1}{i+1})}{2} \rfloor$ , and midpoint minus one, to define the lower bound on the range of group  $G_i$ , and the upper bound on the range of group  $G_{i+1}$ , for  $2 \leq i \leq 9$ . The extremes are special cases. For group  $G_2$  the upper bound on the range is simply the largest number of times a (factor, level) combination is covered. For group  $G_{10}$  the lower bound on the range is the smallest number of times one is covered. The groups  $G_2, \dots, G_{10}$  formed in this way are indicated in Figure A.1. Table A.4 summarizes the resulting ranges of coverage for main effects.

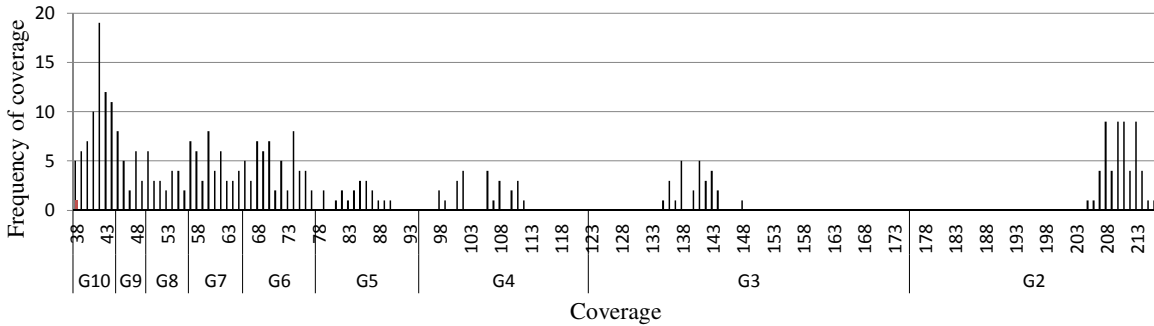


**Figure A.1:** Coverage of main effects and groups constructed.

**Table A.4:** Range [low, high] of coverage for groups of main effects.

Group	$G_2$	$G_3$	$G_4$	$G_5$	$G_6$	$G_7$	$G_8$	$G_9$	$G_{10}$
<b>Low</b>	176	123	95	78	66	57	50	45	41
<b>High</b>	216	175	122	94	77	65	56	49	44

For pairs of (factor, level) combinations, *i.e.*, two-way interactions, we group differently. (There are a many more two-way interactions than main effects!) While a few of the two-way interactions are covered the same number of times as main effects, most are covered fewer times (some as few as three times). We form an additional seven groups by dividing the coverage into about equal sizes. As Figure A.2 extends Figure A.1, adding coverage for the two-way interactions. Table A.5 summarizes the resulting ranges of coverage for two-way interactions.

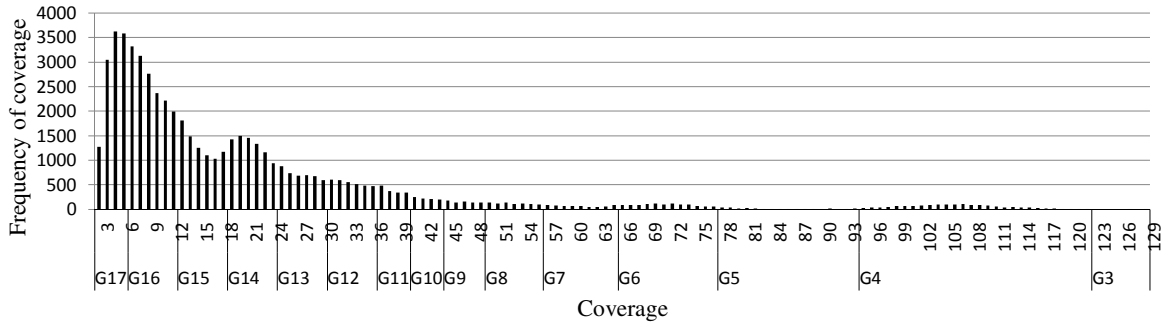


**Figure A.2:** Set size of 2-way factor interactions and groups constructed.

**Table A.5:** Groups added to account for two-way interactions.

<b>Group</b>	$G_{11}$	$G_{12}$	$G_{13}$	$G_{14}$	$G_{15}$	$G_{16}$	$G_{17}$
<b>Low</b>	37	31	25	19	13	7	1
<b>High</b>	40	36	30	24	18	12	6

## A.5 The Screening Algorithm

---

**Algorithm A.1 Screening algorithm** builds a multiple linear regression model

---

**Input:**

- $N$  // number of rows in the locating array
- $k$  // number of columns (factors) in the locating array
- $LA[]$  //  $N \times k$  locating array
- $L[]$  //  $1 \times k$  array of number of levels per factor; each  $L_i = \{\ell_{i1}, \dots, \ell_{il_i}\}$

1: ·  $obsTH[]$  //  $N \times 1$  observed average TCP throughput

- $avgTH$  // average TCP throughput; the initial intercept value
- $maxTerms$  // stopping condition; the number maximum of terms to add
- $G[]$  // group IDs and ranges [min,max]

**Output:**

- $MODEL[]$  // linear regression model containing  $maxTerms$

2: // get all main effects and interactions and determine its group

3:  $MAIN\_INTERACTIONS[] \leftarrow$  CategorizeMain( $N, k, LA[], L[], G[]$ )

4:  $MAIN\_INTERACTIONS[] \leftarrow$  CategorizeInteractions( $N, k, LA[], L[], G[]$ )

5:  $m \leftarrow 0$

6: **repeat**

7:    $termsInModel, MODEL[m] \leftarrow$  ReadModel( $m$ ) // read last model constructed

8:    $resTH[] \leftarrow$  UpdateFittedResiduals( $termsInModel, MODEL[m], N, k, LA[], L[]$ )

9:   **for**  $i = 0 \rightarrow$  size of( $G[]$ ) **do**

10:      $group, min_i, max_i \leftarrow G[i]$

11:      $INSAMEGROUP[] \leftarrow$  FindSameGroup( $MAIN\_INTERACTIONS[], group$ )

12:      $hTest \leftarrow 0$

13:     **for**  $set_1 = 0 \rightarrow$  size of( $INSAMEGROUP[]$ ) **do**

14:       **for**  $set_2 = set_1 + 1 \rightarrow$  size of( $INSAMEGROUP[]$ ) **do**

15:          $s_1, s_2, W\_Array[] \leftarrow$  LoadWArray( $resTH[], INSAMEGROUP[set_1],$   
 $INSAMEGROUP[set_2], LA[], N$ )

16:          $W\_Array[] \leftarrow$  QuickSort( $W\_Array[], INSAMEGROUP[], set_1, set_2, s_1,$   
 $s_2$ )

17:          $R_{set_1}, R_{set_2} \leftarrow$  Rank( $W\_Array[], INSAMEGROUP[], set_1, set_2, s_1, s_2$ )

18:          $U_{set_1}, U_{set_2} \leftarrow$  U'Test( $set_1, set_2, s_1, s_2, R_{set_1}, R_{set_2}$ )

19:          $Z_{set_1}, Z_{set_2} \leftarrow$  Z'Test( $set_1, set_2, s_1, s_2, U_{set_1}, U_{set_2}$ )

20:         **if** ( $min_i \leq 30 \leq max_i$ ) **OR** ( $max_i \leq 30$ ) **then**

21:           **if** ( $abs(U_{set_1} - U_{set_2}) \geq abs(hTest)$ ) **then**

22:              $hSet_1 \leftarrow set_1$   $hSet_2 \leftarrow set_2$

23:              $hTest \leftarrow U_{set_1} - U_{set_2}$

24:           **end if**

25:         **else**

▷ Continued on next page

---



---

**Algorithm A.1** Screening algorithm (continued)

---

```
26:           if (  $\text{abs}(Z_{set_1}) \geq \text{abs}(hTest)$  ) then
27:              $hSet_1 \leftarrow set_1$    $hSet_2 \leftarrow set_2$ 
28:              $hTest \leftarrow Z_{set_1}$ 
29:           end if
30:         end if
31:       end for
32:     end for
33:     CANDIDATES_PERGROUP[ $i * 2$ ]  $\leftarrow$  INSAMEGROUP[ $hSet_1$ ]
34:     CANDIDATES_PERGROUP[ $i * 2 + 1$ ]  $\leftarrow$  INSAMEGROUP[ $hSet_2$ ]
35:   end for
36:    $F_A, L_A, F_B, L_B \leftarrow \text{AkaikeICc}(\text{MODEL}[m], \text{CANDIDATES\_PERGROUP}[])$ 
37:   // compute intercept and coefficients for all terms
38:    $\text{MODEL}[m+1] \leftarrow \text{WeightedLeastSquares}(\text{MODEL}[m], F_A, L_A, F_B, L_B,$ 
     $\text{obsTH}[], N)$ 
39:    $m \leftarrow m + 1$  // number of terms in MODEL
40: until ( $m == \text{maxTerms}$ )
41: return MODEL[]
```

---

## A.6 Predictive Model produced in JMP

Table A.6 repeats the nine unique factors present in the twelve terms in the screening model.

**Table A.6:** Unique factors from the screening model in Table 4.6.

Factor	Level	
	Minimum	Maximum
TCP_RTTvar_exp_	2	4
ErrorModel_ranvar_	<i>Uniform</i>	<i>Exponential</i>
ErrorModel_unit_	<i>pkt</i>	<i>bit</i>
MAC_RTSThreshold_	0	3000
ErrorModel_rate_	1.0E-07	1.0E-05
RWP_Area_	8	40
TCP_min_max_RTO_	0.1	40
APP_flows_	1	18
TCP_packetSize_	64	2048

Table A.7 show the model constructed by JMP 11.0 using the  $2^9$  full-factorial design in Table A.6. The model contains only the main effects and two-factor interactions from screening for TCP throughput. The  $R^2$  of the model in JMP is 0.96, and the adjusted  $R^2$  is 0.95. The F-test statistic of the model is 328.6 on 35 and 476 df with a p-Value  $< 0.0001^*$ .

Table A.7: Partial model of the  $2^9$  full-factorial screening experiment using JMP 11.0 on the nine factors in Table A.6.

Term	Estimate	Prob >  t
Intercept	8.700	< .0001*
ErrorModel_ranvar_ <i>[Uniform]*</i> ErrorModel_unit_ <i>[pkt]</i>	-1.279	< .0001*
ErrorModel_ranvar_ <i>[Uniform]</i>	1.267	< .0001*
ErrorModel_unit_ <i>[pkt]</i>	1.052	< .0001*
TCP_packetSize_ <i>[64]</i>	-0.712	< .0001*
APP_flows_ <i>[1]</i>	0.590	< .0001*
TCP_min_max_rto_ <i>[0.1]</i>	0.411	< .0001*
RWP_Area_ <i>[8]</i>	0.395	< .0001*
MAC_RTSThreshold_ <i>[0]</i>	-0.392	< .0001*
ErrorModel_unit_ <i>[pkt]*</i> TCP_packetSize_ <i>[64]</i>	0.304	< .0001*
ErrorModel_rate_ <i>[1.0E-07]</i>	0.234	< .0001*
ErrorModel_ranvar_ <i>[Uniform]*</i> MAC_RTSThreshold_ <i>[0]</i>	0.228	< .0001*
APP_flows_ <i>[1]*</i> RWP_Area_ <i>[8]</i>	0.228	< .0001*
ErrorModel_unit_ <i>[pkt]*</i> ErrorModel_rate_ <i>[1.0E-07]</i>	0.220	< .0001*
TCP_packetSize_ <i>[64]*</i> ErrorModel_rate_ <i>[1.0E-07]</i>	-0.209	< .0001*
ErrorModel_unit_ <i>[pkt]*</i> MAC_RTSThreshold_ <i>[0]</i>	0.188	< .0001*
ErrorModel_ranvar_ <i>[Uniform]*</i> APP_flows_ <i>[1]</i>	0.178	< .0001*
APP_flows_ <i>[1]*</i> TCP_min_max_rto_ <i>[0.1]</i>	0.169	< .0001*
ErrorModel_unit_ <i>[pkt]*</i> APP_flows_ <i>[1]</i>	0.134	< .0001*
ErrorModel_ranvar_ <i>[Uniform]*</i> TCP_min_max_rto_ <i>[0.1]</i>	-0.094	< .0001*

Continued on next page

Table A.7 – continued from previous page

<b>Term</b>	<b>Estimate</b>	<b>Prob&gt;  t </b>
ErrorModel_ranvar_ <i>[Uniform]</i> *TCP_packetSize_[64]	0.093	< .0001*
TCP_packetSize_[64]*APP_flows_[1]	0.083	0.0004
TCP_min_max_rto_[0.1]*RWP_Area_[8]	-0.071	0.0025
ErrorModel_ranvar_ <i>[Uniform]</i> *RWP_Area_[8]	-0.066	0.0049
MAC_RTSThreshold_[0]*ErrorModel_rate_[1.0E-07]	0.055	0.0173
TCP_min_max_rto_[0.1]*ErrorModel_rate_[1.0E-07]	-0.055	0.0191
TCP_min_max_rto_[0.1]*TCP_rttvar_exp_[2]	0.047	0.0413
ErrorModel_unit_ <i>[pkt]</i> *TCP_min_max_rto_[0.1]	-0.047	0.0426
APP_flows_[1]*ErrorModel_rate_[1.0E-07]	0.044	0.0614
RWP_Area_[8]*MAC_RTSThreshold_[0]	0.041	0.0771
ErrorModel_unit_ <i>[pkt]</i> *RWP_Area_[8]	-0.040	0.0861
TCP_rttvar_exp_[2]	0.039	0.0909
TCP_packetSize_[64]*RWP_Area_[8]	-0.037	0.1158
APP_flows_[1]*MAC_RTSThreshold_[0]	-0.028	0.2266
RWP_Area_[8]*ErrorModel_rate_[1.0E-07]	-0.023	0.3237
ErrorModel_ranvar_ <i>[Uniform]</i> *TCP_rttvar_exp_[2]	-0.022	0.3416

A.7 The  $2^9$  full-factorial design utilized for JMP

Table A.8 gives the  $2^9$  full factorial design for the nine factors in Table A.6. The last column, TCP\_throughput, contains the average TCP throughput for 10 replicates of the design point run in the ns-2 simulator. All remaining  $75 - 9 = 66$  factors are set to their default values.

Table A.8:  $2^9$  full-factorial design and TCP throughput.

Design Point	TCP_rttvar_exp_	ErrorModel_ranvar_	ErrorModel_unit_	MAC_RTSThreshold_	ErrorModel_rate_	RWP_Area_	TCP_min_max_rto_	APP_flows_	TCP_packetSize_	TCP_throughput
1	2	Uniform	pkt	0	1.0E-07	8	0.1	1	64	11.0316843713
2	4	Uniform	pkt	0	1.0E-07	8	0.1	1	64	10.9371238911
3	2	Exponential	pkt	0	1.0E-07	8	0.1	1	64	10.9998658477
4	4	Exponential	pkt	0	1.0E-07	8	0.1	1	64	10.9348292358
5	2	Uniform	bit	0	1.0E-07	8	0.1	1	64	10.9987728128
6	4	Uniform	bit	0	1.0E-07	8	0.1	1	64	11.008528301
7	2	Exponential	bit	0	1.0E-07	8	0.1	1	64	4.3090257418
8	4	Exponential	bit	0	1.0E-07	8	0.1	1	64	3.8331529433
9	2	Uniform	pkt	3000	1.0E-07	8	0.1	1	64	11.3542864108
10	4	Uniform	pkt	3000	1.0E-07	8	0.1	1	64	11.313459377
11	2	Exponential	pkt	3000	1.0E-07	8	0.1	1	64	11.2389970426
12	4	Exponential	pkt	3000	1.0E-07	8	0.1	1	64	11.3191688565
13	2	Uniform	bit	3000	1.0E-07	8	0.1	1	64	11.3858949529
14	4	Uniform	bit	3000	1.0E-07	8	0.1	1	64	11.2640881376
15	2	Exponential	bit	3000	1.0E-07	8	0.1	1	64	7.6993205321
16	4	Exponential	bit	3000	1.0E-07	8	0.1	1	64	6.5746182743
17	2	Uniform	pkt	0	1.0E-05	8	0.1	1	64	10.9736058835
18	4	Uniform	pkt	0	1.0E-05	8	0.1	1	64	10.9843887551
19	2	Exponential	pkt	0	1.0E-05	8	0.1	1	64	10.9565556033
20	4	Exponential	pkt	0	1.0E-05	8	0.1	1	64	10.9357048423
21	2	Uniform	bit	0	1.0E-05	8	0.1	1	64	10.9800082763
22	4	Uniform	bit	0	1.0E-05	8	0.1	1	64	10.9799535797
23	2	Exponential	bit	0	1.0E-05	8	0.1	1	64	4.4041794393
24	4	Exponential	bit	0	1.0E-05	8	0.1	1	64	4.4181656813
25	2	Uniform	pkt	3000	1.0E-05	8	0.1	1	64	11.2885860739
26	4	Uniform	pkt	3000	1.0E-05	8	0.1	1	64	11.3329423319
27	2	Exponential	pkt	3000	1.0E-05	8	0.1	1	64	11.2718003347
28	4	Exponential	pkt	3000	1.0E-05	8	0.1	1	64	11.2894213487
29	2	Uniform	bit	3000	1.0E-05	8	0.1	1	64	11.3093397806
30	4	Uniform	bit	3000	1.0E-05	8	0.1	1	64	11.2840067696

Continued on next page

Table A.8 – continued from previous page

Design Point	TCP_rttvar_exp_	ErrorModel_ranvar_	ErrorModel_unit_	MAC_RTSThreshold_	ErrorModel_rate_	RWP_Area_	TCP_min_max_rto_	APP_flows_	TCP_packetSize_	TCP_throughput
31	2	Exponential	bit	3000	1.0E-05	8	0.1	1	64	7.8350824843
32	4	Exponential	bit	3000	1.0E-05	8	0.1	1	64	6.5670886582
33	2	Uniform	pkt	0	1.0E-07	40	0.1	1	64	10.026109086
34	4	Uniform	pkt	0	1.0E-07	40	0.1	1	64	9.8032544249
35	2	Exponential	pkt	0	1.0E-07	40	0.1	1	64	9.9745525424
36	4	Exponential	pkt	0	1.0E-07	40	0.1	1	64	9.9163386227
37	2	Uniform	bit	0	1.0E-07	40	0.1	1	64	10.0189973397
38	4	Uniform	bit	0	1.0E-07	40	0.1	1	64	10.0331622677
39	2	Exponential	bit	0	1.0E-07	40	0.1	1	64	3.787819402
40	4	Exponential	bit	0	1.0E-07	40	0.1	1	64	3.3055671506
41	2	Uniform	pkt	3000	1.0E-07	40	0.1	1	64	10.3900176149
42	4	Uniform	pkt	3000	1.0E-07	40	0.1	1	64	10.335190745
43	2	Exponential	pkt	3000	1.0E-07	40	0.1	1	64	10.3511308551
44	4	Exponential	pkt	3000	1.0E-07	40	0.1	1	64	10.3816658033
45	2	Uniform	bit	3000	1.0E-07	40	0.1	1	64	10.3962816816
46	4	Uniform	bit	3000	1.0E-07	40	0.1	1	64	10.2093013718
47	2	Exponential	bit	3000	1.0E-07	40	0.1	1	64	6.4225194262
48	4	Exponential	bit	3000	1.0E-07	40	0.1	1	64	5.1528753229
49	2	Uniform	pkt	0	1.0E-05	40	0.1	1	64	10.0437363329
50	4	Uniform	pkt	0	1.0E-05	40	0.1	1	64	9.7760614844
51	2	Exponential	pkt	0	1.0E-05	40	0.1	1	64	9.8327152416
52	4	Exponential	pkt	0	1.0E-05	40	0.1	1	64	9.9355074016
53	2	Uniform	bit	0	1.0E-05	40	0.1	1	64	10.0218544177
54	4	Uniform	bit	0	1.0E-05	40	0.1	1	64	9.7794798085
55	2	Exponential	bit	0	1.0E-05	40	0.1	1	64	3.0622687974
56	4	Exponential	bit	0	1.0E-05	40	0.1	1	64	2.0874097113
57	2	Uniform	pkt	3000	1.0E-05	40	0.1	1	64	10.3465804391
58	4	Uniform	pkt	3000	1.0E-05	40	0.1	1	64	10.1378293686
59	2	Exponential	pkt	3000	1.0E-05	40	0.1	1	64	10.3335028241
60	4	Exponential	pkt	3000	1.0E-05	40	0.1	1	64	10.3077272435
61	2	Uniform	bit	3000	1.0E-05	40	0.1	1	64	10.3692785712
62	4	Uniform	bit	3000	1.0E-05	40	0.1	1	64	10.1782355898
63	2	Exponential	bit	3000	1.0E-05	40	0.1	1	64	5.3062855362
64	4	Exponential	bit	3000	1.0E-05	40	0.1	1	64	5.5496673498
65	2	Uniform	pkt	0	1.0E-07	8	40	1	64	10.1427792184
66	4	Uniform	pkt	0	1.0E-07	8	40	1	64	10.1925731396
67	2	Exponential	pkt	0	1.0E-07	8	40	1	64	10.3657613837
68	4	Exponential	pkt	0	1.0E-07	8	40	1	64	10.2859272658
69	2	Uniform	bit	0	1.0E-07	8	40	1	64	10.2539141159

Continued on next page

Table A.8 – continued from previous page

Design Point	TCP_rttvar_exp_	ErrorModel_ranvar_	ErrorModel_unit_	MAC_RTSThreshold_	ErrorModel_rate_	RWP_Area_	TCP_min_max_rto_	APP_flows_	TCP_packetSize_	TCP_throughput
70	4	Uniform	bit	0	1.0E-07	8	40	1	64	10.2498627356
71	2	Exponential	bit	0	1.0E-07	8	40	1	64	2.4768744781
72	4	Exponential	bit	0	1.0E-07	8	40	1	64	2.9615548218
73	2	Uniform	pkt	3000	1.0E-07	8	40	1	64	10.5061215045
74	4	Uniform	pkt	3000	1.0E-07	8	40	1	64	10.7354975758
75	2	Exponential	pkt	3000	1.0E-07	8	40	1	64	10.6415990165
76	4	Exponential	pkt	3000	1.0E-07	8	40	1	64	10.5935677848
77	2	Uniform	bit	3000	1.0E-07	8	40	1	64	10.4972546324
78	4	Uniform	bit	3000	1.0E-07	8	40	1	64	10.6585982229
79	2	Exponential	bit	3000	1.0E-07	8	40	1	64	4.1054823066
80	4	Exponential	bit	3000	1.0E-07	8	40	1	64	4.5179551519
81	2	Uniform	pkt	0	1.0E-05	8	40	1	64	10.3006065956
82	4	Uniform	pkt	0	1.0E-05	8	40	1	64	10.2121946666
83	2	Exponential	pkt	0	1.0E-05	8	40	1	64	10.2255529356
84	4	Exponential	pkt	0	1.0E-05	8	40	1	64	10.2642652188
85	2	Uniform	bit	0	1.0E-05	8	40	1	64	10.2684462413
86	4	Uniform	bit	0	1.0E-05	8	40	1	64	10.1618808663
87	2	Exponential	bit	0	1.0E-05	8	40	1	64	2.9681555058
88	4	Exponential	bit	0	1.0E-05	8	40	1	64	2.9001020425
89	2	Uniform	pkt	3000	1.0E-05	8	40	1	64	10.4873836032
90	4	Uniform	pkt	3000	1.0E-05	8	40	1	64	10.496108624
91	2	Exponential	pkt	3000	1.0E-05	8	40	1	64	10.5305528883
92	4	Exponential	pkt	3000	1.0E-05	8	40	1	64	10.520993201
93	2	Uniform	bit	3000	1.0E-05	8	40	1	64	10.6327426739
94	4	Uniform	bit	3000	1.0E-05	8	40	1	64	10.5683242464
95	2	Exponential	bit	3000	1.0E-05	8	40	1	64	4.1747564325
96	4	Exponential	bit	3000	1.0E-05	8	40	1	64	4.4824148087
97	2	Uniform	pkt	0	1.0E-07	40	40	1	64	8.8162851232
98	4	Uniform	pkt	0	1.0E-07	40	40	1	64	9.2427676775
99	2	Exponential	pkt	0	1.0E-07	40	40	1	64	9.1154424872
100	4	Exponential	pkt	0	1.0E-07	40	40	1	64	9.0759251603
101	2	Uniform	bit	0	1.0E-07	40	40	1	64	8.5632329099
102	4	Uniform	bit	0	1.0E-07	40	40	1	64	9.3392284511
103	2	Exponential	bit	0	1.0E-07	40	40	1	64	2.1186622548
104	4	Exponential	bit	0	1.0E-07	40	40	1	64	1.7054751006
105	2	Uniform	pkt	3000	1.0E-07	40	40	1	64	9.7171544804
106	4	Uniform	pkt	3000	1.0E-07	40	40	1	64	9.6284532916
107	2	Exponential	pkt	3000	1.0E-07	40	40	1	64	9.3263290877
108	4	Exponential	pkt	3000	1.0E-07	40	40	1	64	9.0204294487

Continued on next page

Table A.8 – continued from previous page

Design Point	TCP_rttvar_exp_	ErrorModel_ranvar_	ErrorModel_unit_	MAC_RTSThreshold_	ErrorModel_rate_	RWP_Area_	TCP_min_max_rto_	APP_flows_	TCP_packetSize_	TCP_throughput
109	2	Uniform	bit	3000	1.0E-07	40	40	1	64	9.4342696945
110	4	Uniform	bit	3000	1.0E-07	40	40	1	64	9.1659129273
111	2	Exponential	bit	3000	1.0E-07	40	40	1	64	3.3603753871
112	4	Exponential	bit	3000	1.0E-07	40	40	1	64	3.3149130131
113	2	Uniform	pkt	0	1.0E-05	40	40	1	64	8.83669016
114	4	Uniform	pkt	0	1.0E-05	40	40	1	64	8.6168061012
115	2	Exponential	pkt	0	1.0E-05	40	40	1	64	9.0124746278
116	4	Exponential	pkt	0	1.0E-05	40	40	1	64	8.7380162926
117	2	Uniform	bit	0	1.0E-05	40	40	1	64	8.9131626919
118	4	Uniform	bit	0	1.0E-05	40	40	1	64	8.7233357616
119	2	Exponential	bit	0	1.0E-05	40	40	1	64	1.8761006177
120	4	Exponential	bit	0	1.0E-05	40	40	1	64	1.8154759958
121	2	Uniform	pkt	3000	1.0E-05	40	40	1	64	9.0276931622
122	4	Uniform	pkt	3000	1.0E-05	40	40	1	64	9.1299176421
123	2	Exponential	pkt	3000	1.0E-05	40	40	1	64	9.2334936541
124	4	Exponential	pkt	3000	1.0E-05	40	40	1	64	9.2825253965
125	2	Uniform	bit	3000	1.0E-05	40	40	1	64	9.0726265308
126	4	Uniform	bit	3000	1.0E-05	40	40	1	64	9.536852312
127	2	Exponential	bit	3000	1.0E-05	40	40	1	64	3.2069651738
128	4	Exponential	bit	3000	1.0E-05	40	40	1	64	3.504956616
129	2	Uniform	pkt	0	1.0E-07	8	0.1	18	64	8.2658037889
130	4	Uniform	pkt	0	1.0E-07	8	0.1	18	64	8.3323999158
131	2	Exponential	pkt	0	1.0E-07	8	0.1	18	64	8.263291648
132	4	Exponential	pkt	0	1.0E-07	8	0.1	18	64	8.3406091701
133	2	Uniform	bit	0	1.0E-07	8	0.1	18	64	8.2608852879
134	4	Uniform	bit	0	1.0E-07	8	0.1	18	64	8.3335421112
135	2	Exponential	bit	0	1.0E-07	8	0.1	18	64	4.1203732286
136	4	Exponential	bit	0	1.0E-07	8	0.1	18	64	3.7979132151
137	2	Uniform	pkt	3000	1.0E-07	8	0.1	18	64	8.5861817755
138	4	Uniform	pkt	3000	1.0E-07	8	0.1	18	64	8.6525891142
139	2	Exponential	pkt	3000	1.0E-07	8	0.1	18	64	8.5962959087
140	4	Exponential	pkt	3000	1.0E-07	8	0.1	18	64	8.6385743485
141	2	Uniform	bit	3000	1.0E-07	8	0.1	18	64	8.5831027306
142	4	Uniform	bit	3000	1.0E-07	8	0.1	18	64	8.6456062438
143	2	Exponential	bit	3000	1.0E-07	8	0.1	18	64	5.7809081113
144	4	Exponential	bit	3000	1.0E-07	8	0.1	18	64	5.8748008847
145	2	Uniform	pkt	0	1.0E-05	8	0.1	18	64	8.2269863344
146	4	Uniform	pkt	0	1.0E-05	8	0.1	18	64	8.2972799725
147	2	Exponential	pkt	0	1.0E-05	8	0.1	18	64	8.2122783281

Continued on next page

Table A.8 – continued from previous page

Design Point	TCP_rttvar_exp_	ErrorModel_ranvar_	ErrorModel_unit_	MAC_RTSThreshold_	ErrorModel_rate_	RWP_Area_	TCP_min_max_rto_	APP_flows_	TCP_packetSize_	TCP_throughput
148	4	Exponential	pkt	0	1.0E-05	8	0.1	18	64	8.3041988511
149	2	Uniform	bit	0	1.0E-05	8	0.1	18	64	8.2778028168
150	4	Uniform	bit	0	1.0E-05	8	0.1	18	64	8.3356793883
151	2	Exponential	bit	0	1.0E-05	8	0.1	18	64	4.0944038197
152	4	Exponential	bit	0	1.0E-05	8	0.1	18	64	3.8493340321
153	2	Uniform	pkt	3000	1.0E-05	8	0.1	18	64	8.4975947459
154	4	Uniform	pkt	3000	1.0E-05	8	0.1	18	64	8.6001935926
155	2	Exponential	pkt	3000	1.0E-05	8	0.1	18	64	8.5182223505
156	4	Exponential	pkt	3000	1.0E-05	8	0.1	18	64	8.5983844495
157	2	Uniform	bit	3000	1.0E-05	8	0.1	18	64	8.5634469352
158	4	Uniform	bit	3000	1.0E-05	8	0.1	18	64	8.6468975369
159	2	Exponential	bit	3000	1.0E-05	8	0.1	18	64	5.8979057217
160	4	Exponential	bit	3000	1.0E-05	8	0.1	18	64	5.8328386834
161	2	Uniform	pkt	0	1.0E-07	40	0.1	18	64	8.506963917
162	4	Uniform	pkt	0	1.0E-07	40	0.1	18	64	8.5364847077
163	2	Exponential	pkt	0	1.0E-07	40	0.1	18	64	8.5266488565
164	4	Exponential	pkt	0	1.0E-07	40	0.1	18	64	8.4633910918
165	2	Uniform	bit	0	1.0E-07	40	0.1	18	64	8.5182721869
166	4	Uniform	bit	0	1.0E-07	40	0.1	18	64	8.5685774906
167	2	Exponential	bit	0	1.0E-07	40	0.1	18	64	2.8312768297
168	4	Exponential	bit	0	1.0E-07	40	0.1	18	64	2.4852029022
169	2	Uniform	pkt	3000	1.0E-07	40	0.1	18	64	8.9581586534
170	4	Uniform	pkt	3000	1.0E-07	40	0.1	18	64	8.9497330698
171	2	Exponential	pkt	3000	1.0E-07	40	0.1	18	64	8.8999594636
172	4	Exponential	pkt	3000	1.0E-07	40	0.1	18	64	8.885119705
173	2	Uniform	bit	3000	1.0E-07	40	0.1	18	64	8.9116711838
174	4	Uniform	bit	3000	1.0E-07	40	0.1	18	64	8.8810170498
175	2	Exponential	bit	3000	1.0E-07	40	0.1	18	64	5.7798102958
176	4	Exponential	bit	3000	1.0E-07	40	0.1	18	64	5.0169324623
177	2	Uniform	pkt	0	1.0E-05	40	0.1	18	64	8.5156403642
178	4	Uniform	pkt	0	1.0E-05	40	0.1	18	64	8.5002788809
179	2	Exponential	pkt	0	1.0E-05	40	0.1	18	64	8.5422284228
180	4	Exponential	pkt	0	1.0E-05	40	0.1	18	64	8.4960765745
181	2	Uniform	bit	0	1.0E-05	40	0.1	18	64	8.5228798583
182	4	Uniform	bit	0	1.0E-05	40	0.1	18	64	8.4690273057
183	2	Exponential	bit	0	1.0E-05	40	0.1	18	64	2.9489667251
184	4	Exponential	bit	0	1.0E-05	40	0.1	18	64	2.4581823451
185	2	Uniform	pkt	3000	1.0E-05	40	0.1	18	64	8.8978466047
186	4	Uniform	pkt	3000	1.0E-05	40	0.1	18	64	8.917154053

Continued on next page



Table A.8 – continued from previous page

Design Point	TCP_rttvar_exp_	ErrorModel_ranvar_	ErrorModel_unit_	MAC_RTSThreshold_	ErrorModel_rate_	RWP_Area_	TCP_min_max_rto_	APP_flows_	TCP_packetSize_	TCP_throughput
187	2	Exponential	pkt	3000	1.0E-05	40	0.1	18	64	8.9087428907
188	4	Exponential	pkt	3000	1.0E-05	40	0.1	18	64	8.8947823276
189	2	Uniform	bit	3000	1.0E-05	40	0.1	18	64	8.9329697093
190	4	Uniform	bit	3000	1.0E-05	40	0.1	18	64	8.9104735063
191	2	Exponential	bit	3000	1.0E-05	40	0.1	18	64	5.9651844529
192	4	Exponential	bit	3000	1.0E-05	40	0.1	18	64	5.1657455134
193	2	Uniform	pkt	0	1.0E-07	8	40	18	64	8.4050008735
194	4	Uniform	pkt	0	1.0E-07	8	40	18	64	8.4315319571
195	2	Exponential	pkt	0	1.0E-07	8	40	18	64	8.3921260913
196	4	Exponential	pkt	0	1.0E-07	8	40	18	64	8.4443621063
197	2	Uniform	bit	0	1.0E-07	8	40	18	64	8.4277193426
198	4	Uniform	bit	0	1.0E-07	8	40	18	64	8.4316821913
199	2	Exponential	bit	0	1.0E-07	8	40	18	64	2.8614132693
200	4	Exponential	bit	0	1.0E-07	8	40	18	64	2.9063423124
201	2	Uniform	pkt	3000	1.0E-07	8	40	18	64	8.7720477559
202	4	Uniform	pkt	3000	1.0E-07	8	40	18	64	8.7837328975
203	2	Exponential	pkt	3000	1.0E-07	8	40	18	64	8.7647885372
204	4	Exponential	pkt	3000	1.0E-07	8	40	18	64	8.7579959504
205	2	Uniform	bit	3000	1.0E-07	8	40	18	64	8.7619932497
206	4	Uniform	bit	3000	1.0E-07	8	40	18	64	8.7529708179
207	2	Exponential	bit	3000	1.0E-07	8	40	18	64	4.3326496317
208	4	Exponential	bit	3000	1.0E-07	8	40	18	64	4.3708533341
209	2	Uniform	pkt	0	1.0E-05	8	40	18	64	8.4102456393
210	4	Uniform	pkt	0	1.0E-05	8	40	18	64	8.405843865
211	2	Exponential	pkt	0	1.0E-05	8	40	18	64	8.4072877707
212	4	Exponential	pkt	0	1.0E-05	8	40	18	64	8.3760775554
213	2	Uniform	bit	0	1.0E-05	8	40	18	64	8.4121479594
214	4	Uniform	bit	0	1.0E-05	8	40	18	64	8.4171244275
215	2	Exponential	bit	0	1.0E-05	8	40	18	64	2.9710752159
216	4	Exponential	bit	0	1.0E-05	8	40	18	64	2.8358764615
217	2	Uniform	pkt	3000	1.0E-05	8	40	18	64	8.7456223051
218	4	Uniform	pkt	3000	1.0E-05	8	40	18	64	8.7315576972
219	2	Exponential	pkt	3000	1.0E-05	8	40	18	64	8.7293465624
220	4	Exponential	pkt	3000	1.0E-05	8	40	18	64	8.7414418208
221	2	Uniform	bit	3000	1.0E-05	8	40	18	64	8.7416943452
222	4	Uniform	bit	3000	1.0E-05	8	40	18	64	8.7819618792
223	2	Exponential	bit	3000	1.0E-05	8	40	18	64	4.3768577434
224	4	Exponential	bit	3000	1.0E-05	8	40	18	64	4.3752481571
225	2	Uniform	pkt	0	1.0E-07	40	40	18	64	8.0215335728

Continued on next page

Table A.8 – continued from previous page

Design Point	TCP_rttvar_exp_	ErrorModel_ranvar_	ErrorModel_unit_	MAC_RTSThreshold_	ErrorModel_rate_	RWP_Area_	TCP_min_max_rto_	APP_flows_	TCP_packetSize_	TCP_throughput
226	4	Uniform	pkt	0	1.0E-07	40	40	18	64	7.9846289876
227	2	Exponential	pkt	0	1.0E-07	40	40	18	64	8.0382131455
228	4	Exponential	pkt	0	1.0E-07	40	40	18	64	8.1114787189
229	2	Uniform	bit	0	1.0E-07	40	40	18	64	8.0124244101
230	4	Uniform	bit	0	1.0E-07	40	40	18	64	8.0275949239
231	2	Exponential	bit	0	1.0E-07	40	40	18	64	1.7015916006
232	4	Exponential	bit	0	1.0E-07	40	40	18	64	1.562672364
233	2	Uniform	pkt	3000	1.0E-07	40	40	18	64	8.4885513464
234	4	Uniform	pkt	3000	1.0E-07	40	40	18	64	8.5377758194
235	2	Exponential	pkt	3000	1.0E-07	40	40	18	64	8.4709597527
236	4	Exponential	pkt	3000	1.0E-07	40	40	18	64	8.5496009843
237	2	Uniform	bit	3000	1.0E-07	40	40	18	64	8.5819167996
238	4	Uniform	bit	3000	1.0E-07	40	40	18	64	8.5063599229
239	2	Exponential	bit	3000	1.0E-07	40	40	18	64	3.3187814898
240	4	Exponential	bit	3000	1.0E-07	40	40	18	64	3.4088127554
241	2	Uniform	pkt	0	1.0E-05	40	40	18	64	7.9519473623
242	4	Uniform	pkt	0	1.0E-05	40	40	18	64	8.0330959026
243	2	Exponential	pkt	0	1.0E-05	40	40	18	64	8.0345187994
244	4	Exponential	pkt	0	1.0E-05	40	40	18	64	7.9516745045
245	2	Uniform	bit	0	1.0E-05	40	40	18	64	7.945279915
246	4	Uniform	bit	0	1.0E-05	40	40	18	64	8.0820877501
247	2	Exponential	bit	0	1.0E-05	40	40	18	64	1.4738981552
248	4	Exponential	bit	0	1.0E-05	40	40	18	64	1.4948497677
249	2	Uniform	pkt	3000	1.0E-05	40	40	18	64	8.3502197277
250	4	Uniform	pkt	3000	1.0E-05	40	40	18	64	8.4724851839
251	2	Exponential	pkt	3000	1.0E-05	40	40	18	64	8.4804917236
252	4	Exponential	pkt	3000	1.0E-05	40	40	18	64	8.3672307841
253	2	Uniform	bit	3000	1.0E-05	40	40	18	64	8.4972408382
254	4	Uniform	bit	3000	1.0E-05	40	40	18	64	8.4745041077
255	2	Exponential	bit	3000	1.0E-05	40	40	18	64	3.3376499741
256	4	Exponential	bit	3000	1.0E-05	40	40	18	64	3.346451741
257	2	Uniform	pkt	0	1.0E-07	8	0.1	1	2048	12.9653254
258	4	Uniform	pkt	0	1.0E-07	8	0.1	1	2048	12.8360049619
259	2	Exponential	pkt	0	1.0E-07	8	0.1	1	2048	12.8920441423
260	4	Exponential	pkt	0	1.0E-07	8	0.1	1	2048	12.8751945158
261	2	Uniform	bit	0	1.0E-07	8	0.1	1	2048	12.9337379127
262	4	Uniform	bit	0	1.0E-07	8	0.1	1	2048	12.7743086014
263	2	Exponential	bit	0	1.0E-07	8	0.1	1	2048	6.5219986761
264	4	Exponential	bit	0	1.0E-07	8	0.1	1	2048	6.2462927947

Continued on next page

Table A.8 – continued from previous page

Design Point	TCP_rttvar_exp_	ErrorModel_ranvar_	ErrorModel_unit_	MAC_RTSThreshold_	ErrorModel_rate_	RWP_Area_	TCP_min_max_rto_	APP_flows_	TCP_packetSize_	TCP_throughput
265	2	Uniform	pkt	3000	1.0E-07	8	0.1	1	2048	12.9006295819
266	4	Uniform	pkt	3000	1.0E-07	8	0.1	1	2048	12.8361463646
267	2	Exponential	pkt	3000	1.0E-07	8	0.1	1	2048	12.8518485673
268	4	Exponential	pkt	3000	1.0E-07	8	0.1	1	2048	12.8629424371
269	2	Uniform	bit	3000	1.0E-07	8	0.1	1	2048	12.8885311552
270	4	Uniform	bit	3000	1.0E-07	8	0.1	1	2048	12.885577187
271	2	Exponential	bit	3000	1.0E-07	8	0.1	1	2048	9.1025816496
272	4	Exponential	bit	3000	1.0E-07	8	0.1	1	2048	8.2965425303
273	2	Uniform	pkt	0	1.0E-05	8	0.1	1	2048	11.3315837879
274	4	Uniform	pkt	0	1.0E-05	8	0.1	1	2048	10.5858634303
275	2	Exponential	pkt	0	1.0E-05	8	0.1	1	2048	11.5507024441
276	4	Exponential	pkt	0	1.0E-05	8	0.1	1	2048	10.9020656709
277	2	Uniform	bit	0	1.0E-05	8	0.1	1	2048	12.8349572669
278	4	Uniform	bit	0	1.0E-05	8	0.1	1	2048	12.7708448307
279	2	Exponential	bit	0	1.0E-05	8	0.1	1	2048	5.7004703289
280	4	Exponential	bit	0	1.0E-05	8	0.1	1	2048	6.3372645729
281	2	Uniform	pkt	3000	1.0E-05	8	0.1	1	2048	11.8807701841
282	4	Uniform	pkt	3000	1.0E-05	8	0.1	1	2048	11.4452276117
283	2	Exponential	pkt	3000	1.0E-05	8	0.1	1	2048	12.1172922502
284	4	Exponential	pkt	3000	1.0E-05	8	0.1	1	2048	11.580736158
285	2	Uniform	bit	3000	1.0E-05	8	0.1	1	2048	13.0057785486
286	4	Uniform	bit	3000	1.0E-05	8	0.1	1	2048	12.9219458721
287	2	Exponential	bit	3000	1.0E-05	8	0.1	1	2048	9.2060676569
288	4	Exponential	bit	3000	1.0E-05	8	0.1	1	2048	8.7770870223
289	2	Uniform	pkt	0	1.0E-07	40	0.1	1	2048	11.8693066258
290	4	Uniform	pkt	0	1.0E-07	40	0.1	1	2048	11.4954045665
291	2	Exponential	pkt	0	1.0E-07	40	0.1	1	2048	11.8271909467
292	4	Exponential	pkt	0	1.0E-07	40	0.1	1	2048	11.4915184614
293	2	Uniform	bit	0	1.0E-07	40	0.1	1	2048	12.0333117991
294	4	Uniform	bit	0	1.0E-07	40	0.1	1	2048	11.5584426598
295	2	Exponential	bit	0	1.0E-07	40	0.1	1	2048	5.417344073
296	4	Exponential	bit	0	1.0E-07	40	0.1	1	2048	3.8949175375
297	2	Uniform	pkt	3000	1.0E-07	40	0.1	1	2048	11.9475596554
298	4	Uniform	pkt	3000	1.0E-07	40	0.1	1	2048	11.6730950519
299	2	Exponential	pkt	3000	1.0E-07	40	0.1	1	2048	11.7053374418
300	4	Exponential	pkt	3000	1.0E-07	40	0.1	1	2048	11.6318782162
301	2	Uniform	bit	3000	1.0E-07	40	0.1	1	2048	11.8814513088
302	4	Uniform	bit	3000	1.0E-07	40	0.1	1	2048	11.7899811266
303	2	Exponential	bit	3000	1.0E-07	40	0.1	1	2048	6.6517579028

Continued on next page

Table A.8 – continued from previous page

Design Point	TCP_rttvar_exp_	ErrorModel_ranvar_	ErrorModel_unit_	MAC_RTSThreshold_	ErrorModel_rate_	RWP_Area_	TCP_min_max_rto_	APP_flows_	TCP_packetSize_	TCP_throughput
304	4	Exponential	bit	3000	1.0E-07	40	0.1	1	2048	7.2679440422
305	2	Uniform	pkt	0	1.0E-05	40	0.1	1	2048	9.3907188756
306	4	Uniform	pkt	0	1.0E-05	40	0.1	1	2048	8.8898744678
307	2	Exponential	pkt	0	1.0E-05	40	0.1	1	2048	9.6970359129
308	4	Exponential	pkt	0	1.0E-05	40	0.1	1	2048	9.1911491937
309	2	Uniform	bit	0	1.0E-05	40	0.1	1	2048	11.8503424694
310	4	Uniform	bit	0	1.0E-05	40	0.1	1	2048	11.3206729591
311	2	Exponential	bit	0	1.0E-05	40	0.1	1	2048	5.2812118986
312	4	Exponential	bit	0	1.0E-05	40	0.1	1	2048	5.0735725339
313	2	Uniform	pkt	3000	1.0E-05	40	0.1	1	2048	10.5365347736
314	4	Uniform	pkt	3000	1.0E-05	40	0.1	1	2048	10.1381129346
315	2	Exponential	pkt	3000	1.0E-05	40	0.1	1	2048	10.5740978241
316	4	Exponential	pkt	3000	1.0E-05	40	0.1	1	2048	9.9440615803
317	2	Uniform	bit	3000	1.0E-05	40	0.1	1	2048	11.7986674817
318	4	Uniform	bit	3000	1.0E-05	40	0.1	1	2048	11.250133319
319	2	Exponential	bit	3000	1.0E-05	40	0.1	1	2048	7.939429726
320	4	Exponential	bit	3000	1.0E-05	40	0.1	1	2048	8.0044243475
321	2	Uniform	pkt	0	1.0E-07	8	40	1	2048	11.7959853968
322	4	Uniform	pkt	0	1.0E-07	8	40	1	2048	11.8655145532
323	2	Exponential	pkt	0	1.0E-07	8	40	1	2048	12.0614656297
324	4	Exponential	pkt	0	1.0E-07	8	40	1	2048	12.2817168941
325	2	Uniform	bit	0	1.0E-07	8	40	1	2048	12.0266439005
326	4	Uniform	bit	0	1.0E-07	8	40	1	2048	11.8749977769
327	2	Exponential	bit	0	1.0E-07	8	40	1	2048	5.7140759809
328	4	Exponential	bit	0	1.0E-07	8	40	1	2048	5.864358184
329	2	Uniform	pkt	3000	1.0E-07	8	40	1	2048	12.0708399207
330	4	Uniform	pkt	3000	1.0E-07	8	40	1	2048	12.1027054752
331	2	Exponential	pkt	3000	1.0E-07	8	40	1	2048	12.1268479282
332	4	Exponential	pkt	3000	1.0E-07	8	40	1	2048	11.9494927145
333	2	Uniform	bit	3000	1.0E-07	8	40	1	2048	12.0206474775
334	4	Uniform	bit	3000	1.0E-07	8	40	1	2048	12.106061408
335	2	Exponential	bit	3000	1.0E-07	8	40	1	2048	7.241893365
336	4	Exponential	bit	3000	1.0E-07	8	40	1	2048	7.575428742
337	2	Uniform	pkt	0	1.0E-05	8	40	1	2048	8.7777191519
338	4	Uniform	pkt	0	1.0E-05	8	40	1	2048	8.403943863
339	2	Exponential	pkt	0	1.0E-05	8	40	1	2048	8.8618339744
340	4	Exponential	pkt	0	1.0E-05	8	40	1	2048	8.9638225075
341	2	Uniform	bit	0	1.0E-05	8	40	1	2048	11.950789739
342	4	Uniform	bit	0	1.0E-05	8	40	1	2048	11.844832583

Continued on next page

Table A.8 – continued from previous page

Design Point	TCP_rttvar_exp_	ErrorModel_ranvar_	ErrorModel_unit_	MAC_RTSThreshold_	ErrorModel_rate_	RWP_Area_	TCP_min_max_rto_	APP_flows_	TCP_packetSize_	TCP_throughput
343	2	Exponential	bit	0	1.0E-05	8	40	1	2048	5.5996656298
344	4	Exponential	bit	0	1.0E-05	8	40	1	2048	5.2386522842
345	2	Uniform	pkt	3000	1.0E-05	8	40	1	2048	10.0480051255
346	4	Uniform	pkt	3000	1.0E-05	8	40	1	2048	10.1153416167
347	2	Exponential	pkt	3000	1.0E-05	8	40	1	2048	10.1682657473
348	4	Exponential	pkt	3000	1.0E-05	8	40	1	2048	10.2352770565
349	2	Uniform	bit	3000	1.0E-05	8	40	1	2048	12.0755652475
350	4	Uniform	bit	3000	1.0E-05	8	40	1	2048	12.1440354202
351	2	Exponential	bit	3000	1.0E-05	8	40	1	2048	7.3475470928
352	4	Exponential	bit	3000	1.0E-05	8	40	1	2048	7.4138979548
353	2	Uniform	pkt	0	1.0E-07	40	40	1	2048	10.5876214351
354	4	Uniform	pkt	0	1.0E-07	40	40	1	2048	10.9734703677
355	2	Exponential	pkt	0	1.0E-07	40	40	1	2048	10.5463816869
356	4	Exponential	pkt	0	1.0E-07	40	40	1	2048	10.3064618278
357	2	Uniform	bit	0	1.0E-07	40	40	1	2048	10.3632627998
358	4	Uniform	bit	0	1.0E-07	40	40	1	2048	10.4676654895
359	2	Exponential	bit	0	1.0E-07	40	40	1	2048	4.6288867126
360	4	Exponential	bit	0	1.0E-07	40	40	1	2048	3.6072354651
361	2	Uniform	pkt	3000	1.0E-07	40	40	1	2048	10.5831682659
362	4	Uniform	pkt	3000	1.0E-07	40	40	1	2048	10.4288273147
363	2	Exponential	pkt	3000	1.0E-07	40	40	1	2048	10.5087491377
364	4	Exponential	pkt	3000	1.0E-07	40	40	1	2048	10.6256383327
365	2	Uniform	bit	3000	1.0E-07	40	40	1	2048	10.7776116362
366	4	Uniform	bit	3000	1.0E-07	40	40	1	2048	11.0178512997
367	2	Exponential	bit	3000	1.0E-07	40	40	1	2048	5.7667197144
368	4	Exponential	bit	3000	1.0E-07	40	40	1	2048	7.015812954
369	2	Uniform	pkt	0	1.0E-05	40	40	1	2048	7.6385218913
370	4	Uniform	pkt	0	1.0E-05	40	40	1	2048	7.6084896042
371	2	Exponential	pkt	0	1.0E-05	40	40	1	2048	7.2707971112
372	4	Exponential	pkt	0	1.0E-05	40	40	1	2048	7.6246189862
373	2	Uniform	bit	0	1.0E-05	40	40	1	2048	10.8187105946
374	4	Uniform	bit	0	1.0E-05	40	40	1	2048	10.967621744
375	2	Exponential	bit	0	1.0E-05	40	40	1	2048	4.18259961
376	4	Exponential	bit	0	1.0E-05	40	40	1	2048	3.3559210368
377	2	Uniform	pkt	3000	1.0E-05	40	40	1	2048	8.7643744678
378	4	Uniform	pkt	3000	1.0E-05	40	40	1	2048	8.9133005184
379	2	Exponential	pkt	3000	1.0E-05	40	40	1	2048	9.1388677857
380	4	Exponential	pkt	3000	1.0E-05	40	40	1	2048	8.6606463996
381	2	Uniform	bit	3000	1.0E-05	40	40	1	2048	10.5014551598

Continued on next page

Table A.8 – continued from previous page

Design Point	TCP_rttvar_exp_	ErrorModel_ranvar_	ErrorModel_unit_	MAC_RTSThreshold_	ErrorModel_rate_	RWP_Area_	TCP_min_max_rto_	APP_flows_	TCP_packetSize_	TCP_throughput
382	4	Uniform	bit	3000	1.0E-05	40	40	1	2048	10.7315342207
383	2	Exponential	bit	3000	1.0E-05	40	40	1	2048	6.3936175094
384	4	Exponential	bit	3000	1.0E-05	40	40	1	2048	6.4004434745
385	2	Uniform	pkt	0	1.0E-07	8	0.1	18	2048	10.2997862214
386	4	Uniform	pkt	0	1.0E-07	8	0.1	18	2048	10.3650072041
387	2	Exponential	pkt	0	1.0E-07	8	0.1	18	2048	10.2993958244
388	4	Exponential	pkt	0	1.0E-07	8	0.1	18	2048	10.3460094602
389	2	Uniform	bit	0	1.0E-07	8	0.1	18	2048	10.3200417012
390	4	Uniform	bit	0	1.0E-07	8	0.1	18	2048	10.3633707607
391	2	Exponential	bit	0	1.0E-07	8	0.1	18	2048	6.1993527698
392	4	Exponential	bit	0	1.0E-07	8	0.1	18	2048	5.9892933028
393	2	Uniform	pkt	3000	1.0E-07	8	0.1	18	2048	10.2245723809
394	4	Uniform	pkt	3000	1.0E-07	8	0.1	18	2048	10.2795027565
395	2	Exponential	pkt	3000	1.0E-07	8	0.1	18	2048	10.2190775305
396	4	Exponential	pkt	3000	1.0E-07	8	0.1	18	2048	10.2909209208
397	2	Uniform	bit	3000	1.0E-07	8	0.1	18	2048	10.2700684171
398	4	Uniform	bit	3000	1.0E-07	8	0.1	18	2048	10.3354432043
399	2	Exponential	bit	3000	1.0E-07	8	0.1	18	2048	7.9335732736
400	4	Exponential	bit	3000	1.0E-07	8	0.1	18	2048	7.8185396788
401	2	Uniform	pkt	0	1.0E-05	8	0.1	18	2048	9.3561173279
402	4	Uniform	pkt	0	1.0E-05	8	0.1	18	2048	9.2021764712
403	2	Exponential	pkt	0	1.0E-05	8	0.1	18	2048	9.4326343447
404	4	Exponential	pkt	0	1.0E-05	8	0.1	18	2048	9.3104621996
405	2	Uniform	bit	0	1.0E-05	8	0.1	18	2048	10.2574985736
406	4	Uniform	bit	0	1.0E-05	8	0.1	18	2048	10.319666477
407	2	Exponential	bit	0	1.0E-05	8	0.1	18	2048	6.2131207707
408	4	Exponential	bit	0	1.0E-05	8	0.1	18	2048	6.1515556429
409	2	Uniform	pkt	3000	1.0E-05	8	0.1	18	2048	9.2704102046
410	4	Uniform	pkt	3000	1.0E-05	8	0.1	18	2048	9.2929543966
411	2	Exponential	pkt	3000	1.0E-05	8	0.1	18	2048	9.329750784
412	4	Exponential	pkt	3000	1.0E-05	8	0.1	18	2048	9.4282154202
413	2	Uniform	bit	3000	1.0E-05	8	0.1	18	2048	10.1128719324
414	4	Uniform	bit	3000	1.0E-05	8	0.1	18	2048	10.1932027194
415	2	Exponential	bit	3000	1.0E-05	8	0.1	18	2048	7.976370758
416	4	Exponential	bit	3000	1.0E-05	8	0.1	18	2048	7.8254714833
417	2	Uniform	pkt	0	1.0E-07	40	0.1	18	2048	10.4340683515
418	4	Uniform	pkt	0	1.0E-07	40	0.1	18	2048	10.3098171461
419	2	Exponential	pkt	0	1.0E-07	40	0.1	18	2048	10.4563476067
420	4	Exponential	pkt	0	1.0E-07	40	0.1	18	2048	10.2676920823

Continued on next page

Table A.8 – continued from previous page

Design Point	TCP_rttvar_exp_	ErrorModel_ranvar_	ErrorModel_unit_	MAC_RTSThreshold_	ErrorModel_rate_	RWP_Area_	TCP_min_max_rto_	APP_flows_	TCP_packetSize_	TCP_throughput
421	2	Uniform	bit	0	1.0E-07	40	0.1	18	2048	10.4722442695
422	4	Uniform	bit	0	1.0E-07	40	0.1	18	2048	10.3161631837
423	2	Exponential	bit	0	1.0E-07	40	0.1	18	2048	5.2386522842
424	4	Exponential	bit	0	1.0E-07	40	0.1	18	2048	4.9748376932
425	2	Uniform	pkt	3000	1.0E-07	40	0.1	18	2048	10.4946871799
426	4	Uniform	pkt	3000	1.0E-07	40	0.1	18	2048	10.4981335304
427	2	Exponential	pkt	3000	1.0E-07	40	0.1	18	2048	10.4309985087
428	4	Exponential	pkt	3000	1.0E-07	40	0.1	18	2048	10.3809090113
429	2	Uniform	bit	3000	1.0E-07	40	0.1	18	2048	10.506778325
430	4	Uniform	bit	3000	1.0E-07	40	0.1	18	2048	10.4939817494
431	2	Exponential	bit	3000	1.0E-07	40	0.1	18	2048	7.6437677518
432	4	Exponential	bit	3000	1.0E-07	40	0.1	18	2048	7.2572521666
433	2	Uniform	pkt	0	1.0E-05	40	0.1	18	2048	9.0046436114
434	4	Uniform	pkt	0	1.0E-05	40	0.1	18	2048	8.6615136747
435	2	Exponential	pkt	0	1.0E-05	40	0.1	18	2048	9.2633134686
436	4	Exponential	pkt	0	1.0E-05	40	0.1	18	2048	8.7792614292
437	2	Uniform	bit	0	1.0E-05	40	0.1	18	2048	10.3523337175
438	4	Uniform	bit	0	1.0E-05	40	0.1	18	2048	10.2978400324
439	2	Exponential	bit	0	1.0E-05	40	0.1	18	2048	4.9811073062
440	4	Exponential	bit	0	1.0E-05	40	0.1	18	2048	4.9115562432
441	2	Uniform	pkt	3000	1.0E-05	40	0.1	18	2048	9.6090166958
442	4	Uniform	pkt	3000	1.0E-05	40	0.1	18	2048	9.342392866
443	2	Exponential	pkt	3000	1.0E-05	40	0.1	18	2048	9.7347512765
444	4	Exponential	pkt	3000	1.0E-05	40	0.1	18	2048	9.3170900124
445	2	Uniform	bit	3000	1.0E-05	40	0.1	18	2048	10.4675302668
446	4	Uniform	bit	3000	1.0E-05	40	0.1	18	2048	10.4438662957
447	2	Exponential	bit	3000	1.0E-05	40	0.1	18	2048	7.7087559651
448	4	Exponential	bit	3000	1.0E-05	40	0.1	18	2048	7.1544375633
449	2	Uniform	pkt	0	1.0E-07	8	40	18	2048	10.3783080101
450	4	Uniform	pkt	0	1.0E-07	8	40	18	2048	10.3493660063
451	2	Exponential	pkt	0	1.0E-07	8	40	18	2048	10.3633062093
452	4	Exponential	pkt	0	1.0E-07	8	40	18	2048	10.376551245
453	2	Uniform	bit	0	1.0E-07	8	40	18	2048	10.3644692556
454	4	Uniform	bit	0	1.0E-07	8	40	18	2048	10.3798848342
455	2	Exponential	bit	0	1.0E-07	8	40	18	2048	5.5353515503
456	4	Exponential	bit	0	1.0E-07	8	40	18	2048	5.5912124941
457	2	Uniform	pkt	3000	1.0E-07	8	40	18	2048	10.3764308152
458	4	Uniform	pkt	3000	1.0E-07	8	40	18	2048	10.3933043959
459	2	Exponential	pkt	3000	1.0E-07	8	40	18	2048	10.3809229939

Continued on next page

Table A.8 – continued from previous page

Design Point	TCP_rttvar_exp_	ErrorModel_ranvar_	ErrorModel_unit_	MAC_RTSThreshold_	ErrorModel_rate_	RWP_Area_	TCP_min_max_rto_	APP_flows_	TCP_packetSize_	TCP_throughput
460	4	Exponential	pkt	3000	1.0E-07	8	40	18	2048	10.3615516994
461	2	Uniform	bit	3000	1.0E-07	8	40	18	2048	10.4006393509
462	4	Uniform	bit	3000	1.0E-07	8	40	18	2048	10.4036521254
463	2	Exponential	bit	3000	1.0E-07	8	40	18	2048	7.2269566901
464	4	Exponential	bit	3000	1.0E-07	8	40	18	2048	7.2677852995
465	2	Uniform	pkt	0	1.0E-05	8	40	18	2048	8.3144830325
466	4	Uniform	pkt	0	1.0E-05	8	40	18	2048	8.3536159243
467	2	Exponential	pkt	0	1.0E-05	8	40	18	2048	8.5766197939
468	4	Exponential	pkt	0	1.0E-05	8	40	18	2048	8.5088454681
469	2	Uniform	bit	0	1.0E-05	8	40	18	2048	10.3031411733
470	4	Uniform	bit	0	1.0E-05	8	40	18	2048	10.3368088096
471	2	Exponential	bit	0	1.0E-05	8	40	18	2048	5.5671563512
472	4	Exponential	bit	0	1.0E-05	8	40	18	2048	5.5154052861
473	2	Uniform	pkt	3000	1.0E-05	8	40	18	2048	9.1275104224
474	4	Uniform	pkt	3000	1.0E-05	8	40	18	2048	9.1765925786
475	2	Exponential	pkt	3000	1.0E-05	8	40	18	2048	9.2775633285
476	4	Exponential	pkt	3000	1.0E-05	8	40	18	2048	9.2858055521
477	2	Uniform	bit	3000	1.0E-05	8	40	18	2048	10.2518525667
478	4	Uniform	bit	3000	1.0E-05	8	40	18	2048	10.2444207568
479	2	Exponential	bit	3000	1.0E-05	8	40	18	2048	7.2226477673
480	4	Exponential	bit	3000	1.0E-05	8	40	18	2048	7.0877155316
481	2	Uniform	pkt	0	1.0E-07	40	40	18	2048	9.9340030329
482	4	Uniform	pkt	0	1.0E-07	40	40	18	2048	9.8403138714
483	2	Exponential	pkt	0	1.0E-07	40	40	18	2048	9.842420693
484	4	Exponential	pkt	0	1.0E-07	40	40	18	2048	9.8045592257
485	2	Uniform	bit	0	1.0E-07	40	40	18	2048	9.8095459686
486	4	Uniform	bit	0	1.0E-07	40	40	18	2048	10.0190032098
487	2	Exponential	bit	0	1.0E-07	40	40	18	2048	4.2848302326
488	4	Exponential	bit	0	1.0E-07	40	40	18	2048	4.4571753349
489	2	Uniform	pkt	3000	1.0E-07	40	40	18	2048	10.3154627867
490	4	Uniform	pkt	3000	1.0E-07	40	40	18	2048	10.1710559868
491	2	Exponential	pkt	3000	1.0E-07	40	40	18	2048	10.0670146032
492	4	Exponential	pkt	3000	1.0E-07	40	40	18	2048	10.2001361346
493	2	Uniform	bit	3000	1.0E-07	40	40	18	2048	10.2123662598
494	4	Uniform	bit	3000	1.0E-07	40	40	18	2048	10.1572217748
495	2	Exponential	bit	3000	1.0E-07	40	40	18	2048	6.3061909363
496	4	Exponential	bit	3000	1.0E-07	40	40	18	2048	6.3388735837
497	2	Uniform	pkt	0	1.0E-05	40	40	18	2048	7.4437630215
498	4	Uniform	pkt	0	1.0E-05	40	40	18	2048	7.3794286246

Continued on next page



Table A.8 – continued from previous page

Design Point	TCP_rttvar_exp_	ErrorModel_ranvar_	ErrorModel_unit_	MAC_RTSThreshold_	ErrorModel_rate_	RWP_Area_	TCP_min_max_rto_	APP_flows_	TCP_packetSize_	TCP_throughput
499	2	Exponential	pkt	0	1.0E-05	40	40	18	2048	7.5553879911
500	4	Exponential	pkt	0	1.0E-05	40	40	18	2048	7.6451838501
501	2	Uniform	bit	0	1.0E-05	40	40	18	2048	9.8562569009
502	4	Uniform	bit	0	1.0E-05	40	40	18	2048	9.8523009367
503	2	Exponential	bit	0	1.0E-05	40	40	18	2048	4.2753813434
504	4	Exponential	bit	0	1.0E-05	40	40	18	2048	4.2722117687
505	2	Uniform	pkt	3000	1.0E-05	40	40	18	2048	8.5133330172
506	4	Uniform	pkt	3000	1.0E-05	40	40	18	2048	8.60089633
507	2	Exponential	pkt	3000	1.0E-05	40	40	18	2048	8.6670917772
508	4	Exponential	pkt	3000	1.0E-05	40	40	18	2048	8.5889376043
509	2	Uniform	bit	3000	1.0E-05	40	40	18	2048	10.0833908729
510	4	Uniform	bit	3000	1.0E-05	40	40	18	2048	9.9792798606
511	2	Exponential	bit	3000	1.0E-05	40	40	18	2048	6.2915493863
512	4	Exponential	bit	3000	1.0E-05	40	40	18	2048	6.2813841145